



**Rice Husk as Bioadsorbent for Dyes Removal and Recovery from
Aqueous Solutions**

Ph.D. Thesis

By

Hadid Sukmana

Supervisor

Prof. Dr. Cecilia Hodúr

Doctoral School of Environmental Sciences

Department of Biosystems Engineering

Faculty of Science and Informatics

University of Szeged

Szeged, 2024

Table of Contents

Acknowledgment	4
List of figures	5
List of tables	7
1 Introduction	8
2 Literature review	11
2.1 Dyes.....	11
2.1.1 Categorization of dyes	13
2.1.2 Hazardous dyes	15
2.1.3 Methylene blue (MB) and Basic red 9 (BR9).....	16
2.2 Wastewater treatment.....	18
2.2.1 Adsorption.....	19
2.2.2 Adsorption mechanism	20
2.2.3 Adsorption modelling	21
2.2.4 Adsorbent.....	23
2.3 Application of rice husk	25
2.3.1 Rice husk and its modification as a bioadsorbent for dyes removal.....	27
2.4 Implementing color evaluation from reusing of dyes for cotton fabrics.....	29
3 Aims	31
4 Materials and Methods	33
4.1 Dyes preparation	33
4.1.1 Single and binary dye solutions	33
4.1.2 Methylene blue model wastewater stock solution	33
4.2 Bioadsorbent preparation	33
4.3 Hydrochar preparation.....	34
4.4 Characterization of RH.....	34
4.4.1 Chemical content analysis.....	34
4.4.2 Zeta potential	35
4.4.3 Fourier Transform Infrared Spectroscopy (FT-IR) analysis.....	35
4.4.4 Scanning Electron Microscopic (SEM) analysis	35
4.4.5 Batch adsorption studies	35
4.4.6 Isotherm and kinetic studies.....	37
4.5 Desorption and regeneration of adsorbent	38
4.6 Application dyes for textile cotton fabric.....	39
5 Results and Discussion	40
5.1 Characterization of RH.....	40
5.1.1 Chemical content	40

5.1.2	Zeta potential values	41
5.1.3	Fourier Transform Infrared Spectroscopy (FT-IR) analysis.....	41
5.1.4	Scanning Electro Microscopic (SEM) analysis	44
5.2	Adsorption of cationic dyes using RH from aqueous solution.....	45
5.2.1	Effect of pH.....	45
5.2.2	Effect of initial dye concentration.....	47
5.2.3	Effect of adsorbent dose.....	48
5.2.4	Effect of contact time	49
5.2.5	Effect of temperature	50
5.2.6	Adsorption isotherm modelling in single solution.....	51
5.2.7	Adsorption kinetic modelling in single solution.....	55
5.3	Binary adsorption of cationic dyes using RH from aqueous solution.....	57
5.3.1	Effect of pH.....	57
5.3.2	Effect of adsorbent dose.....	58
5.3.3	Effect of contact time	59
5.3.4	Effect of initial dye concentration.....	60
5.3.5	Adsorption modelling	61
5.3.6	Factorial design analysis	69
5.4	Adsorption of methylene blue using rice husk from model wastewater	74
5.4.1	Effect of pH.....	74
5.4.2	Effect of initial concentration	75
5.4.3	Effect of adsorbent dose.....	75
5.4.4	Effect of particle size	76
5.4.5	Effect of contact time and comparison with hydrochar	77
5.4.6	Adsorption isotherm modelling in model wastewater	78
5.4.7	Adsorption kinetic modelling in model wastewater	83
5.5	Desorption and regeneration of rice husk	87
5.6	Reusing dye for cotton fabrics	89
6	Conclusion.....	91
7	Summary	93
8	Összefoglalás.....	97
9	New scientific results	101
10	Publications	103
11	Presentation in conferences	103
12	References	105
13	Appendices	125

Acknowledgment

I am deeply grateful for the invaluable support and guidance I have received throughout my Ph.D. journey. First and foremost, I extend my heartfelt thanks to my supervisor, Prof. Dr. Cecilia Hodùr, whose unwavering support, guidance, and encouragement have been instrumental in my academic success. I am forever thankful to her for the opportunity to pursue and complete my studies under her supervision.

To my family, dear wife, Indri Puspitasari, and lovely daughter, Iona Wafalia Hadid, your endless love, patience, and understanding have been my pillars of strength. Thank you for standing by me, cheering me on through every challenge, and being my source of inspiration. Also, I would like to thank Prof. Dr. Etelka Tombácz for her assistance and advice during my research studies. Additionally, I extend my appreciation to all my colleagues in the Department of Biosystems Engineering and the Department of Applied and Environmental Chemistry for their support and collaboration.

Special thanks to the Department of Agricultural Engineering at the University of Novi Sad, Serbia, for their cooperation and contribution to my research.

Further, I acknowledge the University of Szeged and the Tempus Foundation for their financial assistance during my studies.

I sincerely thank everyone who has played a part in my academic journey. Your support has been invaluable, and I am truly fortunate to have had such wonderful people by my side.

List of figures

Figure 1. Adsorption process using the sustainable dyeing concept	10
Figure 2. Industries responsible for the presence of dye effluent in the environment.....	13
Figure 3. Categorization of dyes according to ionic charges.....	13
Figure 4. Adsorption mechanism.....	20
Figure 5. Pathways of adsorption process.....	21
Figure 6. Methods for producing silica from rice husk	27
Figure 7. The three-dimensional depiction of the CIE L*a*b color space	30
Figure 8. Chemical content of RHs.....	40
Figure 9. Zeta potential value for (a) Hungarian rice husk (raw and hydrochar) and (b) Indonesian rice husk (raw and hydrochar).....	41
Figure 10. FT-IR absorption spectra for (a) Raw RH (b) after adsorption single solutions, (c) RH Hydrochar after adsorption binary solutions, and (d) after adsorption binary solutions..	44
Figure 11. SEM images of (a) Hungarian rice husk, (b) Indonesian rice husk, (c) Hungarian rice husk hydrochar, and (d) Indonesian rice husk hydrochar	45
Figure 12. Effect of pH on MB (a) and BR9 (b) removal by rice husks of different origins (concentration value: 2 g/L; initial concentration of dyes: 30 mg/L; temperature (T°): 25 °C; time (t): 120 min)	46
Figure 13. Effect of initial concentration on MB (a) and BR9 (b) removal by rice husks of different origins (pH: 10 for MB, 7 for BR; concentration value: 2 g/L; temperature (T°): 25 °C; time (t): 120 min).....	47
Figure 14. Effect of adsorbent dose on MB (a) and BR9 (b) removal by rice husks of different origins (pH: 10 for MB, 7 for BR9; initial concentration of dyes: 30 mg/L; temperature (T°): 25 °C; time (t): 120 min).....	48
Figure 15. Effect of contact time on MB (a) and BR9 (b) removal by rice husks of different origins (pH: 10 for MB, 7 for BR9; concentration value: 2 g/L; initial concentration of dyes: 30 mg/L; temperature (T°): 25 °C).....	49
Figure 16. Effect of temperature on MB (a) and BR9 (b) removal by rice husks of different origins (pH: 10 for MB, 7 for BR9; concentration value: 2 g/L; initial concentration of dyes: 30 mg/L; time (t): 120 min)	50
Figure 17. Experimental data and BET model fitting for (a) MB adsorbed using Indonesian rice husk, (b) MB adsorbed using Hungarian rice husk, (c) BR9 adsorbed using Indonesian rice husk, and (d) BR9 adsorbed using Hungarian rice husk.....	52
Figure 18. Experimental data and PSO model fitting for (a) MB adsorbed using Indonesian rice husk, (b) MB adsorbed using Hungarian rice husk, (c) BR9 adsorbed using Indonesian rice husk, and (d) BR9 adsorbed using Hungarian rice husk.....	57
Figure 19. Effect of pH on MB and BR9 removals by HRH (a) and IRH (b) using the following parameters: 500 mg of RH, 30 mg/L initial concentration, 60 min adsorption time, and 25 °C temperature	58
Figure 20. Effect of adsorbent dose on MB and BR9 removals by HRH (a) and IRH (b) using the following parameters: 30 mg/L initial concentration, pH 7, 60 min adsorption time, and 25 °C temperature	59
Figure 21. Effect of contact time on MB and BR9 removal by HRH (a) and IRH (b) using the following parameters: 500 mg of RH, pH 7, 30 mg/L initial concentration, 25°C temperature	60
Figure 22. Effect of initial dye concentration on MB and BR9 removals by HRH (a) and IRH (b) using the following parameters: 500 mg of RH, pH 7, 60 min adsorption time, and 25 °C temperature	61

Figure 23. Comparison of experimental data and BET multilayer isotherm models for (a) MB using HRH, (b) MB using IRH, (c) BR9 using HRH, and (d) BR9 using IRH.....	63
Figure 24. Comparison of experimental data and Elovich Equation model for (a) MB using HRH, (b) MB using IRH, (c) BR9 using HRH, and (d) BR9 using IRH	66
Figure 25. Intra-particle diffusion model for (a) HRH, and (b) IRH.....	67
Figure 26. The possible interactions between the rice husk adsorbent (cellulose unit) and dyes in binary adsorption	68
Figure 27. Cube plots of dye removals for (a) MB (%) and (b) BR9 (%) in binary adsorption	69
Figure 28. Main effect plots of dye removal for (a) MB (%) and (b) BR9 (%) during binary adsorption.....	72
Figure 29. Pareto charts of dye removal for (a) MB (%) and (b) BR9 (%) during binary adsorption.....	73
Figure 30. Normal plots of dye removal for (a) MB (%) and (b) BR9 (%) during binary adsorption.....	73
Figure 31. Interaction plots of dye removal for (a) MB (%) and (b) BR9 (%) during binary adsorption.....	73
Figure 32. Effect of pH on MB removal by rice husks of different origin (adsorbent dose: 600 mg, initial concentration of dyes: 60 mg/L, temperature: 25 °C, time: 60 min).....	74
Figure 33. Effect of initial concentration on MB removal by rice husks of different origins (pH: 12, adsorbent dose: 600 mg, temperature: 25 °C, time: 60 min).....	75
Figure 34. Effect of adsorbent dose on MB removal by rice husks of different origins (pH: 12, initial concentration of dyes: 60 mg/L, temperature: 25 °C, time: 60 min).....	76
Figure 35. Effect of particle size on MB removal by rice husks of different origins (pH: 12, adsorbent dose: 600 mg, initial concentration of dyes: 60 mg/L, temperature: 25 °C, time: 60 min)	77
Figure 36. Effect of contact time on MB removal by (a) HRH and HRH hydrochar, (b) IRH and IRH hydrochar (pH: 12, adsorbent dose: 600 mg, initial concentration of dyes: 60 mg/L, temperature: 25 °C).....	78
Figure 37. Comparison of experimental data and nonlinear isotherm models for (a) Hungarian rice husk and (b) Indonesian rice husk	79
Figure 38. Simulation of the Langmuir and Freundlich isotherm models for monolayer adsorption using (a) Hungarian rice husk and (b) Indonesian rice husk.....	82
Figure 39. Comparison of the experimental data and the Elovich model for (a) Hungarian rice husk and (b) Indonesian rice husk	84
Figure 40. Intraparticle diffusion model	86
Figure 41. Desorption of RH with HCl and NaOH solutions	87
Figure 42. Regeneration of RH adsorbent	88
Figure 43. Adsorption capacity of RH adsorbent	88
Figure 44. Cotton fabrics dyed with MB after its desorption from (a) HRH, and (b) IRH adsorbents	89

List of tables

Table 1. Specific properties and applications of various dyes.....	14
Table 2. Hazardous dyes with their adverse effect on biological systems and the environment	15
Table 3. The chemical structure and class of dye	18
Table 4. Technologies of wastewater treatment	19
Table 5. The nonlinear forms of adsorption isotherm and kinetic models	22
Table 6. Properties of RH	26
Table 7. Metal contents of RH.....	26
Table 8. Factorial designs for binary dye solutions	36
Table 9. FT-IR absorption bands of RH	43
Table 10. FT-IR absorption bands of RH (continued).....	43
Table 11. Isotherm parameters for MB and BR9 adsorption.....	53
Table 12. Comparison of the adsorption capacity of raw RH for MB removal.....	54
Table 13. Comparison of adsorption capacities of various adsorbents for BR9 removal.....	55
Table 14. Kinetic parameters for MB and BR9 adsorption	56
Table 15. Nonlinear isotherm parameters for MB and BR9 during binary adsorption	63
Table 16. Comparison of the adsorption capacity for cationic dyes in binary dye solutions using various adsorbents	64
Table 17. Nonlinear kinetic parameters for MB and BR9 during binary adsorption	65
Table 18. Intraparticle diffusion parameters for Methylene Blue and Basic Red 9 during binary adsorption	67
Table 19. Matrix and results of the 2 ³ full factorial design	69
Table 20. Estimated effects and coefficients for MB and BR9 during binary adsorption.....	70
Table 21. Analysis of variance for MB and BR9 during binary adsorption.....	71
Table 22. The multilayer isotherm model parameters for the adsorption of MB	80
Table 23. Monolayer isotherm model parameters for the adsorption of MB	82
Table 24. The kinetic parameters for the adsorption of MB.....	85
Table 25. Intraparticle diffusion parameters for MB adsorption on RHs	86
Table 26. Adsorption and desorption of MB for different adsorbents.....	89
Table 27. CIE L*a*b* value between cotton fabric from HRH and IRH recycling.....	90

1 Introduction

The dye industry is continuously developing and contributing to the world economy. The widespread use of dyes, with more than 100,000 kinds accessible for commercial purposes and an annual production of 1.6 million tons [1]. However, this industry is a major global polluter and uses large amounts of water, chemicals, and fuels, which are transformed into highly loaded wastewater [2], [3]. Industrial dyes present substantial environmental hazards due to their toxicity to species and their capacity to disrupt aquatic ecosystems [4]. The dyeing process, essential in textiles, paints, and pigments, produces significant amounts of wastewater containing dangerous compounds. Heavy metals, organic compounds, and salts in this wastewater can contaminate freshwater sources, posing a threat to human health and the survival of aquatic organisms [5]. These chemicals include cationic dyes such as methylene blue (MB) and basic red 9 (BR9).

Wastewater treatment technologies are needed to remove pollutants from dye wastewater, and dye recycling is required to achieve sustainability. Current wastewater treatment technologies include membrane technology, ultrasonication, biological techniques, coagulation/flocculation, photocatalysis, and adsorption [6]. Nevertheless, most of these techniques have inherent limitations such as substantial energy demands, chemical usage, and operational expenses [7]. Multiple studies have verified that adsorption is a highly effective method for removing dyes, demonstrating its superior ability to remove pollutants compared with other conventional techniques [8].

Adsorption is the most commonly used technology because it is cost-effective, environmentally friendly, simple, and easy to operate [9], [10]. Several studies have been conducted on the adsorption of cationic dyes using bioadsorbents such as date seeds, orange peels, dragon fruit peels, spent *Ganoderma lucidum* substrates, black tea leaves, and wood apple shells [11], [12], [13], [14], [15], [16]. These studies show that adsorption is an efficient and the most effective method for removing cationic dyes.

Various adsorbents have been studied in the scientific literature for their effectiveness in eliminating dyes from wastewater. These include ion-exchange materials, natural clays, activated carbon, and zeolites. Nevertheless, these adsorbents are frequently considered expensive [17]. Researchers developed several novel adsorbents from different natural sources to remove dyes as part of efforts to reduce costs. Over the past few decades, there has been significant interest in using biomass waste, particularly agricultural waste, to remove

pollutants. This waste is produced in large quantities due to the expanding food industry linked to the growing global population [18].

Adsorbent materials from natural resources are being developed, and agricultural waste is a prospective resource. Agricultural waste can be a new, inexpensive, efficient, and environmentally friendly material for wastewater treatment. Rice husk (RH), an agricultural waste material, can be used for wastewater treatment because it is water-insoluble and has a granular morphology, good mechanical qualities, and chemical stability. RH has excellent adsorption ability because it is rich in active functional groups such as carboxyl and phenolic groups [19], [20]. Therefore, RH can be an alternative to chemical materials in wastewater treatment and pollution mitigation solutions.

Indonesia is the fourth largest rice producer in the world. In 2023/2024, its rice production reached 31 million tons [21]. Its dry grain production in 2023 was 53.98 million tons, which was $\pm 64\%$ rice and $\pm 36\%$ by-product. The by-products of rice milling processes include RH (15–20%), bran (8–12%), and rice groats ($\pm 5\%$) [21]. Approximately ± 10.79 million tons of RH was produced in 2023. The utilization of RH from the rice milling process remains limited; it sometimes becomes waste and, thus, a source of environmental pollution [22]. Besides, Hungarian rice husks are used for composting, brick, and animal feed. Reusing rice husks as bioadsorbents can reduce waste generation in the agricultural sector.

Further, most studies on dye adsorption by bioadsorbents have concentrated on single component adsorption. Studying binary adsorption is more complex, and more parameters are needed to describe the process [23]. Textile industrial effluent contains several dyes that complicate adsorption due to various interactions and competition between adsorbates and adsorbents. Studies on the binary adsorption of dyes using multiple bioadsorbents, such as cellulose-based cotton fiber and activated carbon from kiwi, cucumber, and potato peels, have been reported [24], [25], [26].

The role of RH as a good bioadsorbent for removing cationic dyes from aqueous solutions has been studied intensively. MB and BR9 are widely studied because they are cationic dyes commonly used as coloring agents and in dye adsorption experiments; furthermore, they are nonbiodegradable and are toxic and carcinogenic upon short-time exposure [27], [28], [29], [30]. However, to the best of our knowledge, no study has been published on dye adsorption using RHs of different origins. Whether differences in chemical composition affect adsorption capacity is also unclear.

To achieve environmental sustainability and solutions to global challenges, adsorption was performed in this study according to the reduce–reuse–recycle principle. In particular, the goals were reducing pollutants from dyes, reusing water and rice husk, and recycling dyes for sustainable dyeing (Figure 1). Moreover, desorption and regeneration studies were carried out to investigate the recovery efficiencies and adsorption–desorption cycles, thus evaluating the sustainability and cost-effectiveness of RH as a bioadsorbents. The adsorption experiments were carried out taking into account the principles of circular economy to assess the environmental sustainability of RH.

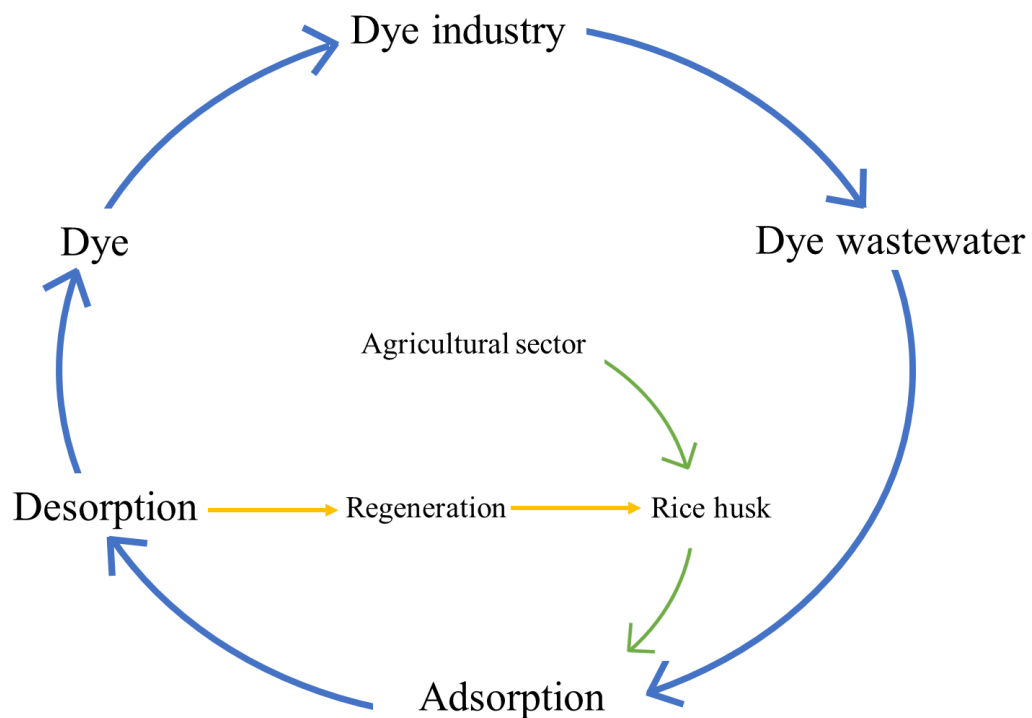


Figure 1. Adsorption process using the sustainable dyeing concept

2 Literature review

Historical records indicate that the application of dyes derived from natural sources predates 3500 BC when they were utilized to enhance the aesthetic appeal of objects. Initially, the only coloring agents available were natural dyes and pigments. These were derived from mineral sources and plants, such as *Rubia tinctorum* and *Paubrasilia echinata*, which contain chemical groups like naphthoquinones, anthraquinones, and flavonoids. Some coloring agents were also obtained from animals, precisely certain insect species such as cochineal (*Dactylopiidae coccus*). The dyes were used to color various items like utensils, weapons, and houses, among others, which held significant aesthetic and cultural value [31].

Dyes are categorized according to the origin of materials, the characteristics of chromophores, and the nuclear structures and industrial classification. Dyes are classified into natural and synthetic dyes based on their source of origin [32]. Natural dyes are derived from botanical and zoological sources, including hematoxylin, carmine, and orcein. Nevertheless, synthetic dyes are produced from organic and inorganic substances, and their classification is determined by their structure, color, particle charge, and techniques of application [33]. Natural dyes are both costly and environmentally benign. Synthetic dyes have gained significant interest in various industries due to their affordability, simplicity of production, and extensive color options. Nevertheless, synthetic dyes possess a substantial level of toxicity [34].

2.1 Dyes

Dyes are organic compounds composed of chromophores ($-\text{NO}_2$, $-\text{NO}$, $-\text{N}=\text{N}$) and auxochromes ($-\text{OH}$, $-\text{NH}_2$, $-\text{NHR}$, $-\text{NR}_2$, $-\text{Cl}$, $-\text{COOH}$, etc.). Chromophores are the components that give dyes their color, while auxochromes increase the intensity of the color of the dyes when applied to a substrate [35]. Dyes consist of a minimum of one chromophore and can absorb light within the visible spectrum, which ranges from 400 to 700 nanometers [36]. In general, dyes are capable of dissolving in water, resulting in the production of light hues. However, certain dyes can create intense shades even in very small amounts [35].

The effluents containing colored compounds discharged from various industrial sectors, such as textiles, cosmetics, laundry, paper, leather, printing, food and beverage, pharmaceuticals, and carpet manufacturing, are highly toxic and pose significant risks to aquatic ecosystems, human health, and the environment [37], [38], [39]. The textile industry is widely recognized as an important global industry, as seen in Figure 2. However, it is also responsible for the

significant pollutants of dyes, harmful metals/elements, and chemicals in the discharged wastewater [18].

Approximately 10,000 varieties of synthetic and natural dyes are manufactured annually worldwide, with a total weight ranging from 7×10^5 to 1×10^6 tons [40], [41]. A substantial quantity of dyes is lost during production and application procedures, with approximately 10-15% of dyes being directly discharged into wastewater [42], [43]. The dyeing sector is accountable for around 20% of the overall industrial water pollution, which amounts to an enormous 11 million tons of polluted water annually [43].

Wastewater that contains dye is frequently characterized by elevated pH levels, chemical oxygen demand, suspended particles, and salinity. In addition, the compounds present in dye wastewater are typically poisonous and can even be mutagenic and carcinogenic. These substances can cause significant harm to both humans and aquatic life [44]. Therefore, water pollution caused by dyes is a clear and escalating issue that requires immediate response.

The concentrations of dyes in industrial wastewater exhibit a broad range of values. In textile effluents, dye concentrations typically range from 10 to 50 mg/L. Reactive dyes in cotton factories are discharged at concentrations of 60 mg/L, with some reports indicating levels between 100 and 200 mg/L [45]. Abid et al. [46] documented dye concentrations in the effluents of 14 Ramadhan textile industries in Iraq, ranging from 20 to 50 mg/L. Sivakumar [47] reported an outflow concentration of 45 mg/L for the dye Acid Orange 10 from the final clarifier of a textile factory in India. According to Ghaly et al. [48] dye concentrations discharged from dye houses vary from 10 to 250 mg/L.

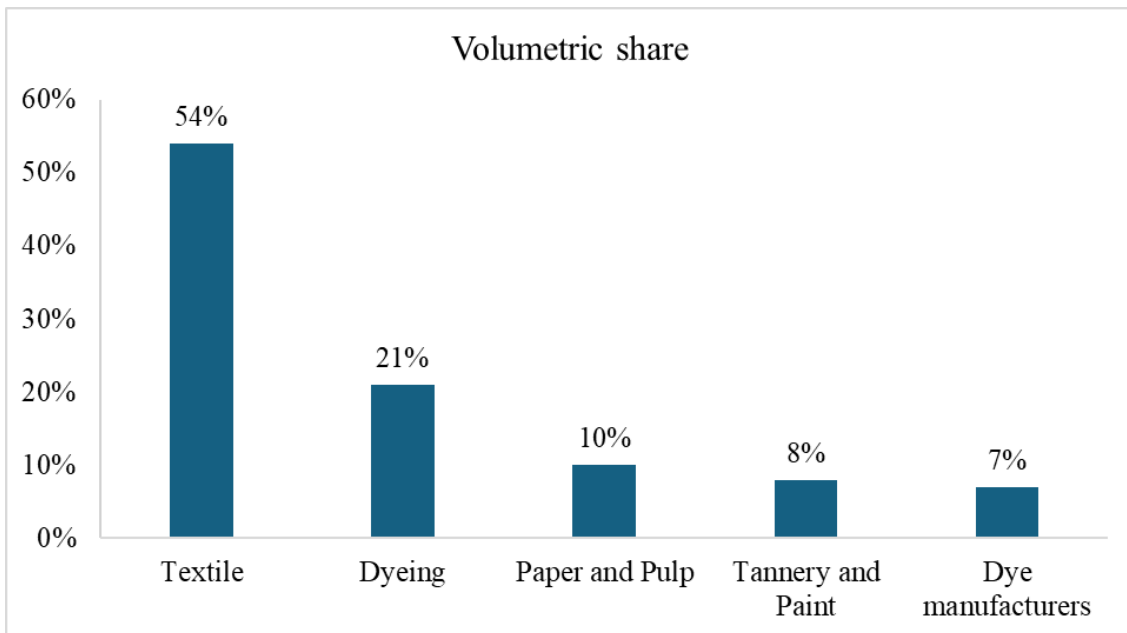


Figure 2. Industries responsible for the presence of dye effluent in the environment [37]

2.1.1 Categorization of dyes

Dyes are commonly categorized based on their structural or functional groups and color and their ionic charge when dissolved in water [1]. The categorization of dyes based on their ionic properties significantly impacts the effectiveness of dye adsorption. Meanwhile, dyes can be categorized according to their chemical structure into various types, including acridine, anthraquinone, azo, azine, diphenylmethane, indigoid, methine, nitro, nitroso, oxazine, phthalocyanine, thiazine, triphenylmethane, and xanthene [49], [50]. Figure 3 illustrates the categorization of dyes into ionic and non-ionic dyes.

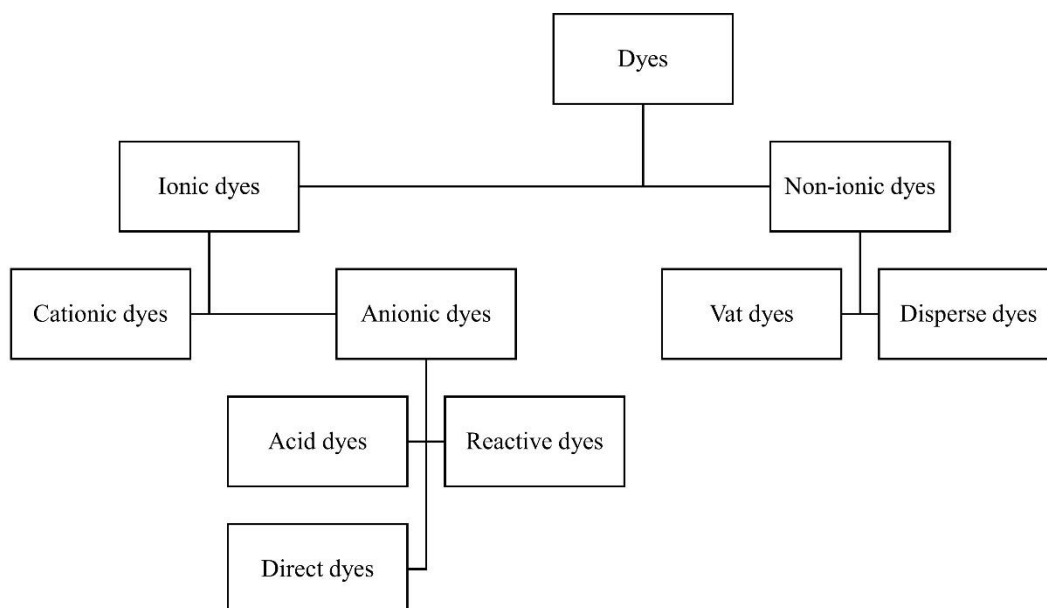


Figure 3. Categorization of dyes according to ionic charges [1], [51]

Even though structural classification offers detailed insights into dye characteristics like dye group and specific properties, categorization based on application proves more pragmatic as it allows for a general assessment of a dye's suitability for a given procedure without delving into complex nomenclature [52]. The specific properties and application of various dyes are shown in Table 1. Non-ionic dyes can be classified into vat dyes and disperse dyes. On the other hand, ionic dyes can be further divided into cationic (basic) dyes and anionic dyes (reactive, direct, and acidic). Except for dispersion dyes and vat dyes, most are soluble in water. It's common for many dyes to contain trace amounts of metals like copper, zinc, lead, chromium, and cobalt in their aqueous solutions, excluding vat and disperse dyes [53].

Table 1. Specific properties and applications of various dyes [54]

Dyes	Examples	Properties	Application
Acidic Acid	red 183, acid orange 10, acid orange 12, acid orange 8, acid red 73, acid red 18, sunset yellow, acid green 27, methyl orange, amido black 10B, indigo carmine	Water soluble, anionic	Nylon, wool, silk, paper, leather, ink-jet printing
Cationic	Methylene blue, Janus green, basic green 5, basic violet 10, rhodamine 6G	Water-soluble, releasing colored cations in solution. Some dyes show biological activity	Paper, polyacrylonitrile, Modified nylons, modified polyesters used in medicine as antiseptics
Disperse	Disperse orange 3, disperse red, disperse red 1, disperse yellow 1	Water-insoluble, non-ionic; for hydrophobic aqueous dispersion	Polyester, nylon, cellulose, cellulose acetate, acrylic fibers
Direct	Congo red, direct red 23, direct orange 39, direct blue 86	Water soluble, anionic, improves wash fastness by chelating with metal salts	Cotton, regenerated cellulose, paper, leather
Reactive	Reactive black 5, reactive green 19, reactive blue 4, reactive red 195, reactive red 198, reactive blue 19, reactive red 120	Extremely high wash fastness due to covalent bond formation with fiber, brighter dyeing than direct dyes	Cotton, wool, nylon, ink-jet printing of textiles

Vat	Vat blue 4, vat green 11, vat orange 15, vat orange 28, vat yellow 20	Use soluble leuco salts after reduction in an alkaline bath (NaOH)	Cellulosic fibers
-----	---	--	-------------------

2.1.2 Hazardous dyes

The contamination of wastewater with dyes affects the ability of the ecological system to perform essential activities for society. It poses a threat to the long-term sustainability of the environment [55]. Dyes cause severe environmental pollution because they are not easily degradable in natural environments [56]. Dyes are categorized as establishing pollutants due to their ability to move into the soil and groundwater through water bodies due to human and industrial activity [27], [57].

During migration, dyes have the potential to undergo decomposition or react with other molecules in the environment, resulting in the formation of a range of toxic and hazardous compounds. Waterways can be negatively affected by dye levels over one mg/L, which result from the direct release of dye wastewater. These high dye levels might have harmful environmental consequences due to their carcinogenic properties [49].

Dyes reduce the amount of sunlight that enters the water, alter the water's color, and disrupt the photosynthetic process, negatively affecting aquatic life [49]. These harmful compounds will not only harm organisms in the environment but also damage neurological systems and cause congenital disabilities in individuals who consume contaminated agricultural, forestry, and fishery goods [27]. The hazardous dyes which impact humans and the environment are shown in Table 2.

Table 2. Hazardous dyes with their adverse effect on biological systems and the environment [8]

No	Hazardous dyes	Environmental risks
1	Disperse Yellow 3	Carcinogenic effects like speeding up the development of hepatocellular tumors and malignant lymphomas
		Liver damage because of heavy metal intake from dyes
2	Malachite Green	Mutagenic impact
		Intercalates with the helical structure of DNA and RNA. - Strong carcinogenic effect
3	Disperse Blue 3	Tests for toxicity in bacteria, algae, and protozoa, as well as the Ames test's ability to detect mutagenesis effects in vitro
4	Rhodamine B	TA1538 and TA98 Salmonella strains have reversion mutations.
5	Acid orange 52	Mutagenic effects and an increase in DNA strand scission assay-based in vitro DNA synthesis
6	Methylene Blue	Inhibition in the growth of microalgae

7	Procion Red MX-5B	Production of hazardous metabolites during the adsorption process
8	Remazol Black B	Hazardous metabolites in water bodies
9	Reactive Red 120	Hazardous for aquatic species
10	Reactive Black 5	In soils, they show adverse effects on the overall growth of plant material and germination of seeds
11	Sunset Yellow	Genetic damage induced on meristematic cells
12	Direct Red 23	For the ecosystem, this dye is poisonous, teratogenic, carcinogenic, and mutagenic
13	Reactive red 198	Gene mutation, cancer, cutaneous stimulation, allergy, and dermatitis in humans
14	Congo Red	Adverse effects on wildlife and plants
15	Crystal violet	When inhaled or consumed, this dye is poisonous and may cause skin irritation

2.1.3 Methylene blue (MB) and Basic red 9 (BR9)

Basic dyes are colorless in their original state, and their color becomes visible only when they are in the form of salts, typically chlorides. However, they can also exist as oxalates or double salts that contain zinc chloride [58], [59]. Basic dyes have superior color brilliance and intensity than acid dyes and other dye classes. However, it is essential to note that they are dangerous and toxic to both humans and the environment [52], [58], [59]. Basic dyes are a type of dye that possess a positive charge and are commonly used in the coloring of various materials. The main constituents of these structures are cyanine, triarylmethane, anthraquinone, diarylmethane, diazahemicyanine, oxazine, hemicyanine, thiazine, and hemicyanine [60].

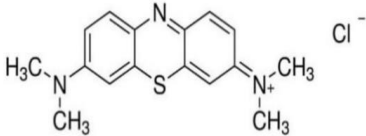
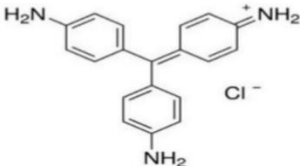
MB dye, known as methyl thioninium chloride, is a heterocyclic aromatic chemical compound with the molecular formula $[C_{16}H_{18}N_3SCl]$ [61]. MB, a cationic dye extensively employed in diverse industrial domains such as paper, pharmaceutical, textile, rubber, plastic, food, leather, and cosmetic industries, presents substantial environmental hazards due to its elevated toxicity in comparison to negatively charged dyes [62], [63], [64]. The intrinsic properties of MB, such as its excellent chemical stability, substantial molecular weights, and restricted ability to biodegrade, are responsible for its harmful impact on the environment, even when present in low quantities [65].

MB is a commonly found cationic dye recognized for being persistent and negatively impacting health, such as toxicity, carcinogenicity, and mutagenicity. Prolonged exposure to MB can lead to significant health consequences, such as anemia, cancer, vomiting, eye irritation, nausea, methemoglobinemia, cognitive impairment, and water pollution [66], [67] [7]. Hence, the

necessity to reduce the environmental consequences of wastewater contaminated with MB emphasizes the requirement for extensive treatment approaches to prevent degradation of the environment and protect human health. Further, MB was selected as an initial dye for the model wastewater experiment. MB is a frequently employed model dye due to its representation of typical cationic dyes, which are commonly present in industrial wastewater. The data obtained from studies using MB serve as a valuable baseline for understanding the adsorption capacity and mechanisms that may apply to other similar dyes. MB has a high molar absorptivity, which allows for straightforward and precise quantification via UV-Vis spectroscopy. This property enables convenient monitoring of MB concentrations in solution before and after interaction with an adsorbent. Additionally, MB has been extensively used in previous studies and provides a rich source of comparative data. This facilitates the process of contextualizing and validating new findings within the existing body of literature.

BR9 is a triamino derivative of triphenylmethane and has the largest dye group within the triarylmethane dye class. It is commonly used in the textile, paper, leather, and ink industries because of its bright color, low energy consumption, and high solubility [68], [69], [70]. Under anaerobic conditions, BR9 decomposes into carcinogenic aromatic amines and its release into the environment in the form of wastewater can cause hazardous effects such as cancer, skin irritation, mutations, and allergic dermatitis [70]. According to the European Textile Ecology standard and the International Agency for Research on Cancer (IARC), BR9 is a carcinogenic dye because it endangers the health of humans and other organisms and biodegrades poorly [68], [71]. The chemical structure and class of dye of MB and BR9 are shown in Table 3.

Table 3. The chemical structure and class of dye

Dye	Common name	C.I. No.	Class	Molar absorptivity ($M^{-1} cm^{-1}$)	Chemical structure
C.I. Basic Blue 9	Methylene Blue	C.I. 52015	Thiazine	4×10^4 to 9.5×10^4 [72]	
C.I. Basic Red 9	Basic Red 9/Pararosaniline	C.I. 42500	Triarylmethane	3.7×10^4 [73]	

2.2 Wastewater treatment

Water is an essential factor for all life and human survival and has a vital role in the drinking water supply and economic sectors [74]. The need for water in household and industrial activities is still increasing every year. Nowadays, the world faces a water crisis due to industrial globalization, increasing residential and commercial areas, and agricultural lands that lead to enormous wastewater production [75].

According to global trends, in high-income countries, municipal and industrial wastewater treatment is about 70 %, the percentages drop to 38 % and 28 % in upper-middle-income and lower-middle-income countries, respectively. Besides, in low-income countries, only 8 % undergo treatment of any kind, and over 80 % of all wastewater is discharged without treatment [76]. Wastewater treatment is an essential factor in industrial processes because wastewater containing hazardous pollutants has negatively affected all environmental elements, such as air, soil, and water [77].

In general, the wastewater treatment methods are biological, chemical, physical, and the combination of each method [78]. The essential process of wastewater treatment is divided into five steps such as 1) pre-treatment using physicochemical and mechanical methods; 2) primary treatment using physicochemical and chemical methods; 3) secondary treatment using physicochemical and biological methods; 4) tertiary treatment or final treatment using physical

and chemical methods; and finally, 5) sludge treatment [79]. For instance, wastewater treatment technologies include biological techniques, photocatalysis, membrane technology, ultrasonication, adsorption, and coagulation/flocculation. Efficient wastewater treatment is the basic need of the present society. The application of wastewater treatment could be a solution for protecting the environment. The advantages and disadvantages of technologies of wastewater treatment are shown in Table 4.

Table 4. Technologies of wastewater treatment

Type of treatment	Advantages	Disadvantages	References
Biological	potential for removing metals	technology is still under development	[80]
Photocatalysis	high degradation rate	potential to harmful due to exposure to carcinogenic UV light	[81]
Membrane technology	membrane properties could be adjusted	membrane fouling	[82], [83]
	small occupation area		
	high processing efficiency		
Ultrasonication	compact	require high energy	[84], [85]
	environmentally friendly		
Adsorption	simple design	require regeneration of the adsorbent	[10], [86], [87], [88]
	cost-effectiveness		
	excellent approach for removing organic pollutants		
Coagulation/flocculation	simple process	require high dosage	[86], [89],
	good for reclamation or removed pollutants	produce massive sludge and large particles	[90]

2.2.1 Adsorption

Adsorption is a change in concentration of a given substance at the interface compared with the neighboring phases [91]. Adsorption can occur in the following systems: solid-liquid, solid-gas, liquid-gas, and liquid-liquid.

Nowadays, adsorption is one of the most common methods used in industrial wastewater treatment. For instance, adsorption could be used to remove and recover heavy metals in wastewater, even at a low concentration. Therefore, adsorption is a practice and simple process to apply in wastewater treatment compared with other methods. Adsorption methods have several parameters to determine an effective technique, such as pH, adsorbent dose, temperature, and contact time.

The solution pH plays an essential role in the adsorption process; determining the initial pH condition is vital for increasing pollutants' removal effectivity. pH condition in the solution affects the ability between hydrogen ions in the functional group such as hydroxyl (OH), carboxyl (COOH), amine (NH), and metal ions on the adsorbent surface [92].

The adsorbent dose is one of the critical parameters in the adsorption method due to the adsorbent capacity's effect on the adsorbate initial concentration and plays an important role in determining the optimum process [93]. The increasing adsorbent dose could increase removal capacity due to greater surface area and more active adsorption sites [94].

The temperature is one of the parameters that impact the adsorption process due to affecting physicochemical reactions. In endothermic reactions, the increasing temperature would increase the reaction rate, whereas, in exothermic reactions, the increasing temperature would decrease the reaction rate [95].

Adsorption capacity could be described by contact time. Therefore, the adsorption process requires a specific time to reach equilibrium which is the time when the adsorption is completed [86]. In the application of contact time, there is time variation to achieve maximum process depending on adsorbent material and adsorbate.

2.2.2 Adsorption mechanism

The adsorption method is widely used in wastewater treatment due to effective and efficient factors. During adsorption, several steps occur until the process finishes. The adsorption mechanism is shown in Figure 4.

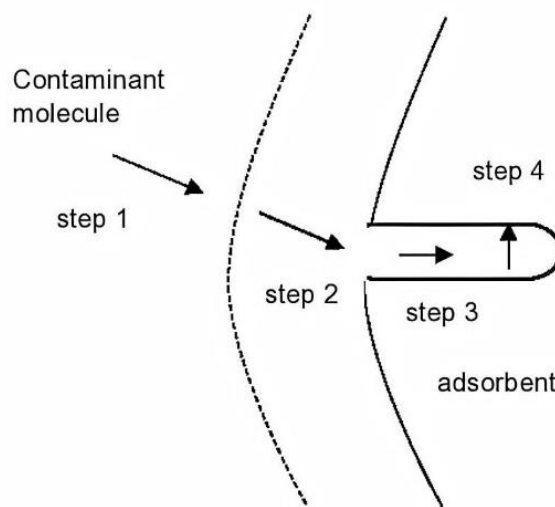


Figure 4. Adsorption mechanism [96]

The adsorption mechanism followed four steps, i.e. [97]:

- 1) The solution transfers the contaminant molecules/solute to the boundary layer of the adsorbent.
- 2) Diffusion occurs from the boundary layer to external surface of the adsorbent.
- 3) Transport from the external surface to active sites of pores.
- 4) The adsorption of the sorbate to the solid phase.

Adsorption processes are divided into two types, shows in Figure 5. Physical adsorption (physisorption) and chemical adsorption (chemisorption) have different processes. The physisorption responsible for attractive forces in molecules and generally occurred with a relatively low degree of specificity, whereas chemisorption responsible for the structure of chemical compounds due to involves electrons exchanges [98], [99].

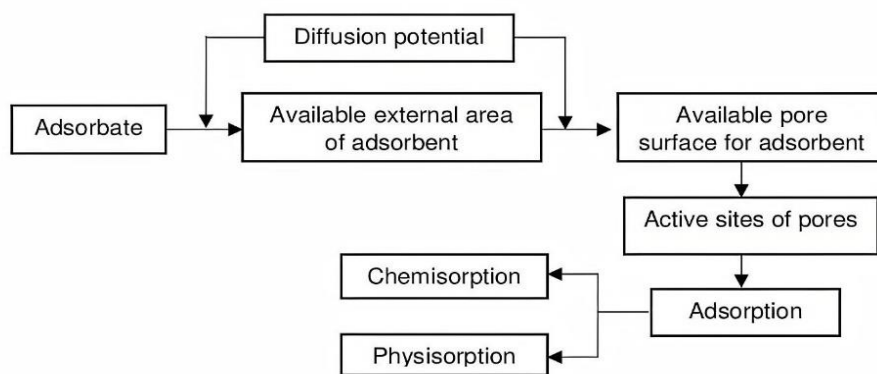


Figure 5. Pathways of adsorption process [100]

2.2.3 Adsorption modelling

The common method for evaluating the adsorption mechanism is adsorption isotherm and kinetics. The adsorption isotherm is described of equilibrium concentration between the solute concentration in the liquid and that on the surface of the adsorbent [101]. In contrast, adsorption kinetics is described diffusion behavior the adsorption rate of solute [102]. The nonlinear forms of adsorption isotherm and kinetic models shows in Table 5.

Table 5. The nonlinear forms of adsorption isotherm and kinetic models

Isotherm models	Equation nonlinear form	Parameters
Langmuir	$q_e = \frac{Q_m K_L C_e}{1 + K_L C_e}$	C _e : equilibrium concentration of adsorbate q _e : amount of sorbed per gram of adsorbent Q _m : maximum monolayer coverage capacity of sorbent K _L : Langmuir isotherm constant related to the energy of adsorption
Freundlich	$q_e = K_f C_e^n$	K _f : Freundlich isotherm constant, an approximate indicator of adsorption capacity n: adsorption intensity/heterogeneity parameter
Harkins–Jura	$q_e = \left(\frac{A}{B - \log C_e} \right)^{1/2}$	A: Harkins–Jura isotherm parameter B: equilibrium constant of Harkins–Jura
Aranovich–Donohue	$q_e = \left(\frac{Q_m K_1 C_e}{1 + K_1 C_e} \right) \left(\frac{1}{(1 - K_2 C_e)^{n_2}} \right)$	K ₁ and K ₂ : equilibrium constant of Aranovich–Donohue n ₂ : modified form of the second term on the right side of the BET Equation
Brunauer–Emmett–Teller	$q_e = Q_m \frac{K_S C_{eq}}{(1 - K_L C_{eq})(1 - K_L C_{eq} + K_S C_{eq})}$	K _S : the equilibrium constant of adsorption of the first layer K _L : the equilibrium constant of adsorption for upper layers of adsorbate on the adsorbent
Kinetic models	Equation nonlinear form	Parameters
Pseudo-first-order	$q_t = q_e (1 - e^{-k_1 t})$	q _t : amount of metal sorbed at time t k ₁ : the first-order rate constant
Pseudo-second-order	$q_t = \frac{q_e^2 k_2 t}{1 + k_2 q_e t}$	k ₂ : the second-order rate constant.

Elovich	$q_t = \frac{1}{\beta} \ln(1 + \alpha\beta t)$	α : the Elovich Equation constant β : the constant of desorption.
Intra-particle diffusion	$q_t = k_{id}\sqrt{t} + C$	k_{id} : the constant of intra-particle diffusion C: is a constant describing the boundary layer thickness

According to Table 5, there are several models in isotherm adsorption. However, Langmuir and Freundlich are standard models used for monolayer adsorption. Langmuir isotherm model has two key points in the adsorption process. First, homogeneous adsorption occurs in the adsorbent. Second, adsorbed molecules form a saturated layer on the adsorbent surface so that maximum and monolayer adsorption occurs. The Freundlich isotherm model assumes adsorption capacity has relation to the ion concentration at equilibrium, and adsorption occurs in the heterogeneous surface, also not suitable for low sorbate concentration [103], [104].

Furthermore, the standard model in the kinetic models is pseudo-first-order and pseudo-second-order. The kinetic model could explain the adsorption process and possible rate-controlling steps, such as chemical reaction processes or mass transport [105]. Generally, when adsorption occurs through diffusion through the interface, the kinetic model follows pseudo-first-order. However, pseudo-second-order has a benefit where equilibrium adsorption capacity could be calculated from the model and no need to calculate adsorption equilibrium capacity from the experiment [106].

2.2.4 Adsorbent

The adsorbent is an essential factor in the adsorption process. Adsorbents can capture pollutants substances onto itself and has porosity also insoluble in water [107]. The utilization of adsorbent usually considers several aspects, such as cost and adsorbent characterization. However, the cost and characteristics of these compounds can influence maximum removal in wastewater.

Firstly, the adsorbent key factor is adsorption capacity, where the adsorbent could adsorb the adsorbate onto its surface. Secondly, excellent adsorbent criteria are short adsorption periods in the adsorption process [108]. Thirdly, adsorbent with high porosity has a higher surface area with high adsorption capacity [109].

Adsorbents could be classified into two types that are conventional and non-conventional adsorbents. Conventional adsorbents consist of activated carbons, ion-exchange resins (polymeric organic resins), and inorganic materials such as activated alumina, silica gel, zeolites, and molecular sieves. Non-conventional adsorbents consist of industrial/agriculture by-products such as sawdust, bark, solid waste, red mud, etc., and biological by-product such as biomasses, peat, chitosan, other polysaccharides [110].

Non-Conventional/Natural adsorbent origin is from natural materials or industrial waste/by-products such as agriculture, food, etc. It has a low cost and could be directly used or after minor treatment [111]. For instance, agriculture waste is one of the foremost abundant renewable resources globally and available in a considerable amount [112], becoming a source of porous materials rich in active functional groups [113]. Therefore, agriculture waste is a potential material that could be utilized in wastewater treatment.

Currently, the researcher is focused on developing a natural adsorbent as an alternative for substituting a chemical adsorbent [114]. The main advantages of natural adsorbents are increase efficiency economically due to a low cost and provide a high removal rate for the highly toxic wastewater [115]. However, natural adsorbents also have disadvantages such as the adsorption process running slow and pH parameter as the main factor to influence the adsorption effect [116].

Several natural adsorbents have been studied for pollutants removal from wastewater. For instance, Bellahsen et al. [117] applied natural adsorbents from the banana peel, compost, bark, wheat husk, wheat bran, sugar beet pulp, and pomegranate peel for the adsorption of ammonium. The result shows pomegranate peel powder (PPP) could achieve 97% removal however, other materials showed a negative and low adsorption ability.

Furthermore, Baby et al. [118] reported that the use of agricultural waste palm kernel shell as an adsorbent to remove heavy metals-contaminated water. In this study, heavy metals such as Pb^{2+} , Cr^{6+} , Cd^{2+} , and Zn^{2+} could be removed effectively from the water. The optimum condition of contact time was 60 minutes for Pb^{2+} and Cr^{6+} and 90 and 120 minutes for Cd^{2+} and Zn^{2+} , respectively. The percentage of removal obtained 99% for Pb^{2+} and Cr^{6+} , and Zn^{2+} and Cd^{2+} obtained 83%. The adsorption capacity of Pb^{2+} and Cr^{6+} was achieved 49.64 mg/g and 49.55 mg/g, respectively, whereas Cd^{2+} and Zn^{2+} were achieved 43.12 mg/g and 41.72 mg/g, respectively.

Other than that, Zulkania et al. [119] found that the application of activated carbon and bio-sorbent produced from palm fibre wastes (PFW) and activated by phosphoric acid. The adsorbent was investigated to remove MB with the effect of adsorbent type and phosphoric acid concentration. The contact time was found in 90 minutes. The result shows optimum adsorption was obtained using activated carbon with 10% (v/v) bio-sorbent activating agent concentration and using bio-sorbent with 30% (v/v) activating agent concentration. The adsorption capacity and percentage of removal from activated carbon were 9.85 mg/g and 98.5 %, respectively, while bio-sorbent was achieved 9.98 mg/g and 99.8%, respectively.

The modification of rice husk (RH) or rice husk ash (RHA) was investigated by Phan et al. [120] used Triamine-activated rice husk ash (TRI-ARHA) is a potential natural adsorbent for nitrate and other anions removal. The TRI-ARHA shows a nitrate adsorption capacity (>160 mgNO₃⁻/g) compared to the anion exchange resin akulite A420 (~ 80 mgNO₃⁻/g), with 10 cycles of adsorption-desorption. Similar result were obtained by Mor et al. [121] using the activated rice husk ash (ARHA) to remove phosphate in wastewater and water. The ARHA would enhance the adsorption capacity for phosphate with maximum removal of 89% with pH 7, 2 g/L doses, and a time of 120 minutes.

Furthermore, the study by Thuy et al. [122] applied magnesium chloride modified carbonized rice hull (MCRH) to remove ammonium from synthetic and domestic wastewaters. During the 27 hours long treatment, MCRH with 1.8 g/L concentration could remove of ammonium reached 90.7 % (capacity of 41.0 mg/g) for 81.3 mg/L synthetic wastewater and 86.8 % for real domestic wastewater. The Langmuir model was the best model for this study, and based on the Dubinin-Radushkevich model, ammonium was physically adsorbed on MCRH.

Mitra et al. [123] showed that the addition of RH as an adsorbent in continuous column mode for the removal of Pb (II) and Cr (VI) ions with pH 2-6. The result shows increasing influent concentration (10-30 mg/L) indicates the increased capacity of adsorbent for Pb (II) and Cr (VI) from 5.72 to 22.99 mg/L and 2.8-10.18 mg/L, respectively. According to the result, statistical analysis obtained the Thomas model and the Yoon–Nelson model.

2.3 Application of rice husk

The material used in wastewater treatment has an excellent property for increasing wastewater quality. Nowadays, researchers use natural materials as an alternative for substituting chemical materials. In previous research, measurements of the properties of those materials have been taken. For instance, RH has properties in the presence of carboxyl and silanol groups. Besides

the use of RH for wastewater treatment, the application of RH could be used in varied sectors as in below [124]:

- a) Bio-fertilizer
- b) Control of pest
- c) Insulation of thermal

RH is formed from a combination of cellulose, hemicellulose, lignin, and carbon with appreciable amounts of silica and other minor substances, as shown in Table 6.

Table 6. Properties of RH

No	Properties	Values [125]	Amount (%) [126]	Amount (%) [127]	Amount (%) [128]
1	Bulk density	86–114 kg/m ³	0.72	-	-
2	Moisture contents	8.68–10.44%	9.38	-	-
3	Particle size	0.212–0.850 mm	-	-	-
4	Calorific values	3000 KCal/kg	-	-	-
5	Ash	-	11.34	-	17–20
6	Volatile Matter	-	6.74	-	-
7	Carbon	-	20.63	-	-
8	Silica	-	-	15–17	-
9	Cellulose	-	-	25–30	28.6–43.3
10	Hemicellulose	-	-	18–21	22–29.7
11	Lignin	-	-	26–31	19.2–24.4

In RH properties, there are polysaccharides such as cellulose and hemicellulose, where cellulose contains β -glucose monomers, whereas hemicellulose contains other sugars such as mannose, arabinose, galactose, rhamnose, and xylose. Furthermore, RH has a lignin component and polymeric aromatic structures that involve the oxidative coupling of 4-hydroxyphenylpropanoids, coniferyl, synapyl alcohols, and primarily p-coumaric [129].

The metal contents in the original RH are shown in Table 7. The ion K high element was 2.676 mg/g, followed by Ca. The eutectic reaction occurs in Na, K, and SiO₂ during the burning process of RH.

Table 7. Metal contents of RH [130]

Sample	Metal contents (mg/g)						
	Al	Fe	Na	Mg	Mn	Ca	K
Rice husk	0.04	0.12	0.	0.36	0.36	1.47	2.68

The rice husk goes through several steps until it is ready for use in various applications. Rice husk processing could produce silica through thermal and chemical methods. Figure 6 shows the method used for producing silica from rice husk.

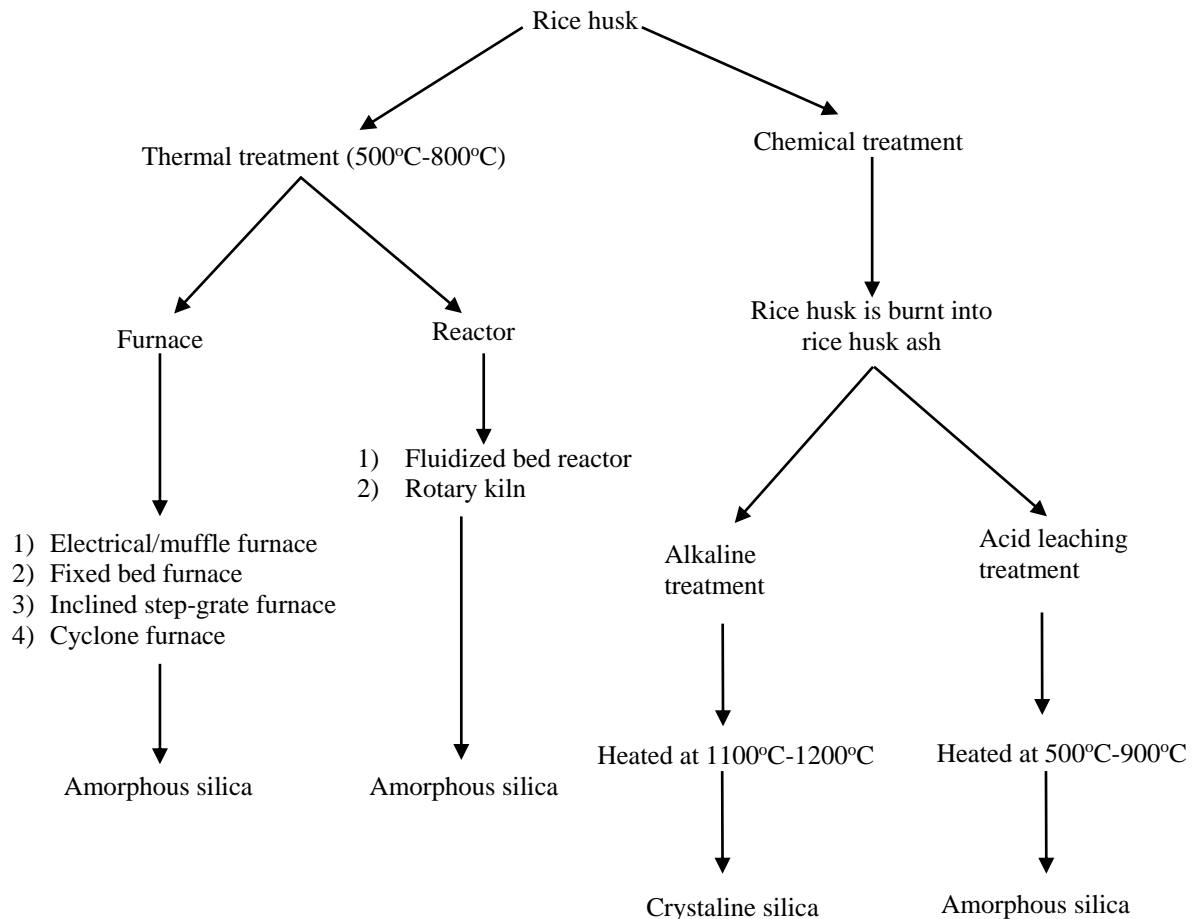


Figure 6. Methods for producing silica from rice husk [131]

The thermal treatment uses a physical process to produce silica. In thermal treatment, RH would be burning at a temperature of 500-800°C with two pieces of equipment, such as a furnace and a reactor; both thermal treatments produce amorphous silica. This treatment was relatively easy due to there is no chemical added to the process. Otherwise, in chemical treatment, there is two preparation before heated such as alkaline and acid leaching. The temperature for burning at 1100-1200°C and 500-900°C for produce crystalline and amorphous silica, respectively.

2.3.1 Rice husk and its modification as a bioadsorbent for dyes removal

The research conducted by Alver et al. [63] used the magnetic alginate/rice husk bio-composite beads for MB adsorption. The result shows that the maximum adsorption capacity of magnetic

alginate/rice husk beads was obtained at 274.9 mg/g with the optimum pH solution (range 6-10). Besides, in a study by Sharma et al. [132], RH and RHA were used for the adsorption of MB in aqueous waste. The higher capacities for removing MB by adjusting pH around 7, time of 30 minutes, and temperature setting of 323°K.

In the study by Quansah et al. [133], RH utilization for removing MB and crystal violet (CV). The RH used varying dosages in the 0.05-1.0 g range, with the concentration of dye MB and CV 400 mg/L and 300 mg/L, respectively. The result shows the optimum temperature at 75°C with removal percentage of MB and CV was from 53.7% to 97.7% and 57.4% to 98.2%, respectively. Therefore, the total removal percentages of MB and CV were 95% at pH 4-10. Besides, the study by Yusmaniar et al. [134] used mesoporous silica adsorbents from rice husk ash to remove methyl orange dyes. The result shows the percentage of removal and adsorption capacity was 74.6% and 0.2 mg/g, respectively, with the optimum condition at pH 2 and contact time is 30 minutes.

The research by Moeinian and Mehdinia [135] used the silica derived from RH prepared in a furnace at 800°C for 4 hours after acid leaching with sulfuric acid and chloride acid. The result shows that the maximum removal efficiency of MB by the rice husk silica was 96.7%. The optimum condition of MB concentration is 10 mg/L, the adsorbent dosage is 1 g/L, the contact time is 60 minutes, and the pH is 8. Moreover, the study by da Rosa et al. [136] used the delignification process from RH waste as an adsorbent for removing MB. The study showed that the adsorbent capacity and equilibrium were obtained at 1350 mg/g and around 30 seconds, respectively.

The study by Malik et al. [137] used the RH, rice husk char (RHC), and chemically modified rice husk char (CMRHC) for the removal of congo red (CR) dye. The result shows that the percentage removal of CR in RH and RHC was 88.7% and 92.3%, respectively, whereas CMRHC with pH 6 could remove 98.9%. Furthermore, the research by Dahlan et al. [138] used magnetic adsorbent rice husk ash (MRHA) to remove brilliant green (BG) dye from an aqueous medium. The result shows the percentage of removal BG obtained 96.7% with the optimum condition at pH 7, the dosage of adsorbent is 2 g, the concentration of dye is 200 mg/L; contact time is 60 minutes, temperature 50°C, and speed of agitation is 150 rpm.

The adsorption of malachite green (MG) was studied by Zou et al. [139] using the natural rice husk (NRH) and oxalic acid-modified rice husk (MRH). The result shows that the maximum adsorption capacities of NRH and MRH were achieved at 28 mg/g and 54 mg/g, respectively.

The study by Bayrak Tezcan et al. [140] reported the removal of basic yellow 51 (BY51) using rice husk (RH) and burned rice husk (BRH). The results show that maximum adsorption capacities were obtained at 38.8 for RH and 49 mg/g for BRH.

2.4 Implementing color evaluation from reusing of dyes for cotton fabrics

In the realm of color quality evaluation, traditional methodologies have centered around colorimetric approaches, notably employing systems such as the CIE L*a*b framework established by the Commission Internationale de L'éclairage. This framework, incorporating metrics such as lightness (L*), chromaticity coordinates for redness or greenness (a*), and yellowness or blueness (b*), serves as a cornerstone for commercial standardization and gradation across diverse applications, including photography and image processing [141], [142].

Its designation as a chromatic value color space stems from its capacity to encapsulate the vast spectrum of visually perceptible color shades encountered in surface colors, underscoring its utility and versatility in color characterization [142]. The adoption of the CIE L*a*b color space rests upon two pivotal considerations: its fidelity to human visual perception and its formulation on a device-independent mathematical model. This device independence ensures the consistent and faithful representation of color values across varied devices, irrespective of calibration settings, thereby guaranteeing accurate color reproduction across monitors, screens, and printers [143].

While colorimetric systems boast multifaceted functionalities, their primary emphasis typically lies in quantifying CIE L*a*b parameters, such as $\Delta(L^*, a^*, b^*)$, to gauge color quality, alongside ΔE for evaluating color tolerance within the continuous dyeing spectrum. However, their efficacy in monitoring color uniformity remains somewhat limited [141]. The three-dimensional depiction of the CIE L*a*b color space, as depicted in Figure 7, facilitates precise color characterization by utilizing L*, a*, and b* coordinates, organized along three opponent axes.

Rooted in color-opponent theory, this model posits that colors cannot concurrently manifest as red and green or yellow and blue. Accordingly, disparities in L*, a*, and b* values, denoted as ΔL^* , Δa^* , and Δb^* respectively, may assume positive or negative magnitudes, with the aggregate color difference, ΔE^* , consistently yielding positive values [144].

- ΔL^* (L* sample minus L* standard) = difference in lightness and darkness (+ = lighter, - = darker)

- Δa^* (a^* sample minus a^* standard) = difference in red and green (+ = redder, - = greener)
- Δb^* (b^* sample minus b^* standard) = difference in yellow and blue (+ = yellower, - = bluer)
- ΔE^* = total color difference

The inevitable divergence in coloration between batches of textile materials underscores the imperative for consensus between clients and manufacturers regarding acceptable quality standards. Objective color assessment, facilitated by instruments such as colorimeters or spectrophotometers, supplants subjective evaluations, furnishing quantitative metrics for precise identification, specification, and alignment of colors, thereby mitigating human errors and ensuring product integrity [145].

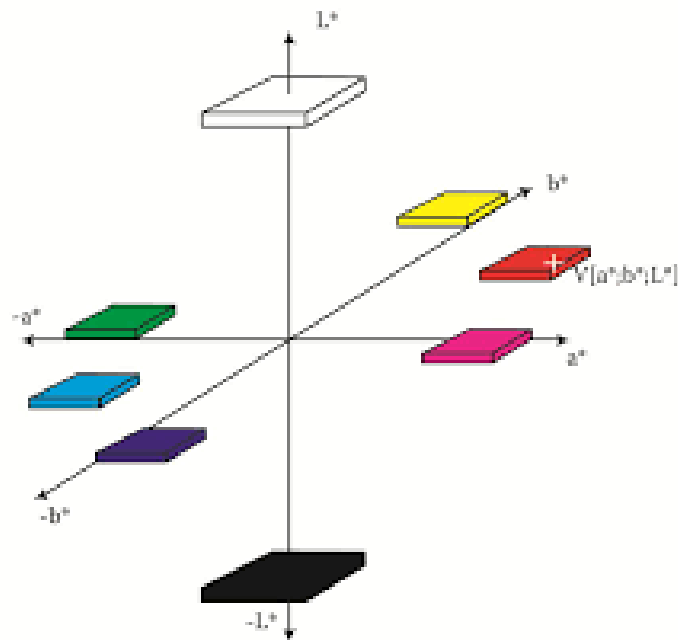


Figure 7. The three-dimensional depiction of the CIE L*a*b color space [146]

3 Aims

The primary objective of this Ph.D. thesis is to develop a highly efficient bioadsorbent from RHs of different origins for dye removal and recovery from aqueous solutions. This study promises to improve sustainable and environmentally friendly wastewater treatment technologies, including reducing wastewater pollutants, recycling and recovering dye, and reusing agricultural waste.

To achieve this overarching goal, the following specific objectives have been delineated:

1. Characterization of the physicochemical properties of the Hungarian rice husk (HRH) and Indonesian rice husk (IRH) utilizing appropriate analytical techniques and methodologies.
2. Examination of the influential parameters governing the adsorption of MB and BR9 adsorption from single dye solution by the HRH and IRH using batch adsorption experiments.
3. Determination of kinetic and isotherm models that properly describe the mechanisms and properties of MB and BR9 adsorption from single dye solution by the HRH and IRH.
4. Examination of the influential factors affecting the adsorption of MB and BR9 adsorption from binary dyes solution by the HRH and IRH using batch adsorption experiments.
5. Determination of kinetic and isotherm models that properly describe the mechanisms and properties involved in the adsorption of MB and BR9 from binary dyes solution by the HRH and IRH.
6. Verify the efficiency of the HRH and IRH in removing MB from real wastewater using batch adsorption experiments.
7. Identification of the influential parameters affecting the adsorption of MB from real wastewater by the HRH and IRH.
8. Determination of kinetic and isotherm models that properly describe the mechanisms and properties of MB adsorption from real wastewater by the HRH and IRH.
9. Implementation of the hydrogen carbonization method to enhance the adsorptive properties of the RH for MB removal.
10. Exploration of the novel physicochemical properties of the RH Hydrochar.

11. Comparison of the contact time parameters for MB adsorption from real wastewater between the RH Hydrochar and raw RH.
12. Investigation of the desorption and regeneration studies of HRH and IRH.
13. Investigation on the recovered of MB dye for cotton fabrics.

4 Materials and Methods

4.1 Dyes preparation

4.1.1 Single and binary dye solutions

MB and BR9 solutions were prepared by dissolving 1 g of the dye (MB from Molar Chemical, Halásztelek, Hungary and BR9 from Sigma–Aldrich, St. Louis, MI, USA) in 1 L of distilled water. Further, MB (Molar Chemical) and BR9 (Sigma-Aldrich) were diluted using stock solutions (1000 mg/L) and mixed for binary solutions. The mixture was diluted with distilled water to obtain the target concentration. Sodium hydroxide (NaOH) and hydrochloric acid (HCl) solutions were used to modulate the pH levels of the dye solutions. All the substances utilized in the experiments, including MB, BR9, NaOH, and HCl, were of analytical reagent quality.

4.1.2 Methylene blue model wastewater stock solution

A wastewater stock solution containing MB (1000 mg/L) was prepared to imitate the composition of dye-containing wastewater originating from textile industries. The solution was prepared by dissolving 1 g of MB (Molar Chemical, Hungary), 22.5 g of Na₂SO₄, and 5 g of Na₂CO₃ in 1 L of distilled water, which was maintained at a temperature of 80 °C for 1 h [147]. The pH of the dye solutions was modified using sodium hydroxide (NaOH) and hydrochloric acid (HCl) solutions. All chemicals utilized in this study were of analytical reagent quality.

4.2 Bioadsorbent preparation

The raw materials (RHs) for the experiments were obtained from Indonesia and Hungary. Indonesian rice or *Oryza sativa subsp. Japonica* (tropical japonica) rice was harvested in the 2020 cropping season in Cianjur City, Indonesia, by smallholder farmers in a rainfed rice field where the irrigation source was rainwater and a small amount of fertilizer was used. Hungarian rice or *Oryza sativa subsp. Japonica* var.M488 (Hungarian Plant Breeding) was harvested in the 2020 cropping season in Kisújszállás City, Hungary. It was produced by Nagykun 2000 Mezőgazdasági Zrt using Kubani technology, namely, seedbed preparation, sowing in warm weather (20 April and 10 May), and germination in flooded troughs. At the beginning of sowing, the area was watered constantly, with one-third of each plant in water. Each RH sample was washed using distilled water until the pH was constant and then vacuum-dried in an oven at 105 °C for 120 min without inert gases. Finally, the dried material was crushed and ground to the desired size (<250 μm) for the adsorption experiments.

4.3 Hydrochar preparation

Hydrothermal carbonization was carried out in a 2 dm³ batch reactor (Parr 4520, Moline, Illinois, USA). The reactor, equipped with an electric heater and stirrer controlled by a Parr 4842 microprocessor control unit, was loaded with 100 g of material and 400 g of distilled water, then sealed hermetically. Nitrogen was used to purge any remaining oxygen. The mixture was heated to the desired temperature (with a tolerance of $\pm 2^\circ\text{C}$), and the pressure was increased to the set value by introducing 99% pure nitrogen (Messer Tehnogas AD, Novi Sad, Serbia). The experiment was performed at a temperature of 250 °C, with a pressure of 8.0 MPa, a reaction time of 120 minutes, a stirrer speed of 670 min⁻¹, and a dry matter concentration in the reactor of $18.17 \pm 0.264\%$. After the reaction time, the reactor was cooled with water. Once the temperature of the solid-liquid mixture inside the reactor dropped to 30°C, the pressure control valve was opened, and the mixture was removed. The mixture was then filtered to separate the process water from the wet hydrochar using gravity filtration with circular filter paper (20 µm, Ø110 mm, 5892 white ribbon ashless, Schleicher and Schuell, Dassel, Germany) and a vacuum pump. The wet hydrochar was dried to a constant weight for 24 hours at 105 ± 2°C in an oven (Sterimatic, ST-11, Instrumentaria, Zagreb, Croatia). The resulting dry hydrochar was then analyzed further.

4.4 Characterization of RH

4.4.1 Chemical content analysis

Lignin and cellulose analyses were conducted according to the method of Chesson [148]. A mixture containing 1 g of dried sample (a) and 150 mL of distilled water was heated in a water bath at 90–100 °C for 1 h. The mixture was filtered, and the residue washed using 300 mL of hot water. The residue was dried in an oven until the weight was constant (b). The residue was mixed with 150 mL of 0.5 M sulfuric acid (H₂SO₄) and heated in the water bath at 90–100 °C for 1 h. The mixture was filtered, washed using 300 mL of distilled water, and the residue dried (c). The dried residue was soaked in 10 mL of 72 (m/m%) H₂SO₄ at room temperature for 4 h. Afterwards, 150 mL of 0.5 M H₂SO₄ was added to the mixture, which was refluxed in the water bath for 1 h. The solid was washed using 400 mL of distilled water, heated in the oven at 105 °C, and weighed until a constant weight (d) was reached. Finally, the solid was heated until it became ash, which was then weighed (e). The percentages of cellulose, lignin, and ash were calculated using Equations (1)–(3):

$$\% \text{ Cellulose} = \frac{c - d}{a} 100 \quad (1)$$

$$\% \text{ Lignin} = \frac{d - e}{a} 100 \quad (2)$$

$$\% \text{ Ash} = \frac{e}{a} 100 \quad (3)$$

4.4.2 Zeta potential

A Nano ZS (Malvern, UK) dynamic light scattering apparatus with a 4 mW He–Ne laser source ($\lambda = 633 \text{ nm}$) was used for zeta potential measurements. RH suspensions were placed in disposable zeta cells (DTS1070) and analyzed at 25°C . Suspensions were prepared as follows: 10 mg of RH was added into 10 mL of sodium chloride (0.01 M) at various pH. The pHs were adjusted before measurement with 0.1 M HCl or 0.1 M NaOH and checked after the analysis.

4.4.3 Fourier Transform Infrared Spectroscopy (FT-IR) analysis

FT-IR analysis was performed using a Bruker Vertex 70 spectrophotometer (Ettlingen, Germany) with a spectral resolution of 4 cm^{-1} . Each spectrum was recorded from 500 to 4500 cm^{-1} and composed from the average of 16 scans. After grinding the sample, 100 mg potassium bromide (KBr) pellets were prepared with 1 w/w% of sample content and measured in transmission mode.

4.4.4 Scanning Electron Microscopic (SEM) analysis

The morphology of the adsorbent surface was investigated with a Hitachi S-4700 Type II scanning electron microscopic (SEM) (Hitachi, Japan) using an accelerating voltage of 10 kV.

4.4.5 Batch adsorption studies

4.4.5.1 *Single dye solution*

IRH and HRH were used to remove MB and BR9 in batch adsorption experiments. Batch adsorption was performed to determine the effects of certain parameters—pH, contact time, initial dye concentration, adsorbent dose, and temperature—on their adsorption performance. The influence of various pH values on MB and BR9 adsorption was investigated (pH 5–10 for MB and pH 3–7 for BR9) by adjusting the initial pH of the solutions using 0.1 M HCl or 0.1 M NaOH. The influence of the initial dye concentration (30, 60, 90, and 120 mg/L), adsorbent dose (125, 250, and 500 mg), contact time (5–120 min), and temperature (25°C , 35°C , and 45°C) were investigated to obtain the optimal MB and BR9 adsorption conditions. In batch

adsorption experiments, 250 mL of each aqueous dye solution was used, with a stirring speed of 100 rpm. (do you have a photo??)

4.4.5.2 Binary dye solutions

Batch adsorption experiments were conducted to assess the effect of pH (within the 3–7 pH range), adsorbent dose (250, 375, and 500 mg), contact time (5– 60 min), and initial concentration (between 30 and 120 mg/L) for MB and BR9 removal in binary adsorption. Further, 250 mL of binary dye solutions with a constant 25°C temperature and stirring speed of 100 rpm were applied for the experiment. Important factors that influenced MB and BR9 adsorption were identified using 23 factorial designs in Minitab® 20 statistical software (Table 8). Initial concentrations of binary dye solutions (30 mg/L for each dye), stirring speed (100 rpm), and optimum time (60 min) were kept constant.

Table 8. Factorial designs for binary dye solutions

Factor	Coded symbol	Low level (-1)	High level (+1)
Adsorbent type	A	IRH	HRH
pH	B	3	7
Dose	C	250	500

4.4.5.3 Methylene blue model wastewater experiment

The HRH and IRH were used in a batch adsorption experiment to remove MB from the model wastewater. The impact of pH on the adsorption of MB was examined in the pH range of 4–12 by modifying the initial pH of the solutions with either 0.1 M or 1 M HCl and 0.1 M or 1 M NaOH. In addition, the study examined the impact of various factors influencing the optimal conditions of MB removal, including the initial concentration (ranging from 60 to 300 mg/L), adsorbent dose (ranging from 0.2 to 1 g), particle size (ranging from 0.25 to 2 mm), and contact time (ranging from 0 to 60 min). The adsorption of MB using RH hydrochar The hydrochar experiment was conducted under optimal conditions to compare with the results obtained for raw RHs. The batch adsorption experiments were carried out using 250 mL of MB model wastewater that was stirred at 100 rpm.

4.4.5.4 Dyes measurement

After the adsorption process, the solution was centrifuged at 4000 rpm for 15 min using a Heraeus Megafuge 16R centrifuge (Thermo Scientific, Waltham, MA, USA). The dye concentration in the solution was measured spectrophotometrically using a Biochrom WPA Lightwave II UV/visible Spectrophotometer (Cambridge, UK) and Agilent Cary 60 UV–vis

spectrophotometer (Penang, Malaysia) at 664 and 545 nm (λ_{max}) for MB and BR9, respectively. The dye removal percentage was calculated using Equation (4):

$$\% \text{ Removal} = \frac{c_i - c_f}{c_i} 100 \quad (4)$$

where c_i (mg/L) and c_f (mg/L) are the initial and final dye concentrations, respectively, in the aqueous solution. The amount of adsorbed dye in the aqueous solution was estimated using Equation (5):

$$q_e = (c_i - c_e) \frac{V}{m} \quad (5)$$

where q_e is the amount of adsorbate adsorbed by the adsorbent; c_i (mg/L) and c_e (mg/L) are the initial and equilibrium dye concentrations, respectively, in the aqueous solution; V (L) is the solution volume; and m (g) is the mass of the adsorbent in volume (V). Each reported experimental result is the average of three replicate measurements, and error bars represent the standard error of the average.

4.4.6 Isotherm and kinetic studies

4.4.6.1 Single and binary dye solutions

Isotherm studies were conducted using 500 mg of the adsorbent and 250 mL of the dye solution (30–120 mg/L concentrations) at pH 10 for MB and pH 7 for BR9 and binary solutions. Adsorption was conducted for a contact time of 2 h for single solution and 1 h for binary solutions at room temperature. Two nonlinear isotherm models were used to evaluate the adsorption isotherms of MB and BR9 namely, Harkins–Jura and Brunauer–Emmett–Teller (BET) multilayer for single solutions and extended Langmuir and Brunauer–Emmett–Teller (BET) multilayer for binary solutions.

Kinetic studies were performed by adding 500 mg of the adsorbent to the 250 mL dye solution at a fixed concentration (30 mg/L) at room temperature and the optimum pH (10 for MB and 7 for BR9 and binary solutions). The amount of adsorbed dye was recorded from 5 min to 120 min for single solution and from 5 min to 60 min for binary solutions. The adsorption kinetics for MB and BR9 were examined using nonlinear kinetic models: pseudo-first-order (PFO) and pseudo-second order (PSO) for single solution and pseudo-first-order (PFO), pseudo-second-order (PSO), Elovich, and Intra-particle diffusion for binary solutions.

4.4.6.2 Methylene blue model wastewater

The isotherms were obtained by employing a dose of 600 mg of adsorbent and 250 mL of MB model wastewater at concentrations ranging from 60 to 300 mg/L under a pH of 12. The adsorption experiments were carried out at room temperature for 60 min. The adsorption isotherms of MB were evaluated using three nonlinear isotherm models: the Harkins–Jura (HJ), Aranovich–Donohue (AD), and Brunauer–Emmett–Teller (BET) multilayer models.

The kinetics of adsorption was investigated by adding 600 mg of adsorbent to 250 mL of 60 mg/L MB model wastewater. The experiments were carried out at room temperature and pH 12. The amount of adsorbed MB was measured for a 60-min period. The adsorption kinetics of MB were analyzed using four nonlinear kinetic models, namely, the pseudo-first-order (PFO), pseudo-second-order (PSO), Elovich, and intraparticle diffusion models.

4.5 Desorption and regeneration of adsorbent

To assess the feasibility of adsorbent regeneration, we selected two potential solvents for desorption: 1 M HCl and 1 M NaOH solutions. To choose the most appropriate solvent, we conducted an initial desorption experiment. For this purpose, the MB-containing RH was added to 250 mL of HCl or NaOH solution at a stirring speed of 100 rpm for 60 min. Following the desorption process, the solutions were centrifuged at a speed of 4000 rpm for 5 min using a Heraeus Megafuge 16R centrifuge (Thermo Scientific, Waltham, MA, USA). The dye concentration was measured spectrophotometrically using an Agilent, Cary 60 UV–vis spectrophotometer (Penang, Malaysia) at 664 nm. The amount of MB desorbed and the MB desorption efficiency (%) [149] were calculated based on Equations 6 and 7, respectively:

$$q_{e,d} = \frac{c_d \times V}{m} \quad (6)$$

$$\% \text{ Desorption} = \frac{q_{e,d}}{q_{e,a}} 100 \quad (7)$$

where $q_{e,d}$ and $q_{e,a}$ are the amount of MB desorbed and adsorbed, respectively; c_d (mg/L) is the concentration of desorbed MB; V (L) represents the solution volume, and m (g) represents the mass of the adsorbent in volume (V).

Following each cycle, the adsorbent was cleaned with distilled water. Then, it was dried in an oven at 80 °C for 15 min in preparation for adsorption in the subsequent cycle. To evaluate the regeneration of the adsorbent, we performed a minimum of four successive adsorption/desorption cycles. Then, the MB-containing RH was brought into contact with the

most effective regenerating solvent, following the same approach as in the batch adsorption process. Every reported experimental outcome is the mean value of three repeated measurements, and the error bars indicate the standard deviation of the mean values.

4.6 Application dyes for textile cotton fabric

After desorption and separation with a centrifuge, the method of Moon and Chae [150] was modified slightly and then applied to carry out the dyeing process. Accordingly, 150 mL filtrate was used for dyeing cotton fabrics at 80 °C for 60 min. The cotton fabric was dried at room temperature followed by color measurements.

5 Results and Discussion

5.1 Characterization of RH

5.1.1 Chemical content

RH is a lignocellulosic material that can be utilized as an adsorbent for dye removal. The chemical content of RH can be analyzed through various treatment methods, including acid pretreatment. Sulfuric and hydrochloric acid solvents are commonly used for this treatment. Acid pretreatment is suitable for lignocellulosic materials due to its ability to break down the rigid structure of lignocellulosic materials into cellulose and lignin [151], [152].

The chemical content of RH was investigated and is shown in Figure 8. IRH has higher cellulose and ash contents than HRH, but HRH has higher lignin content. The higher ash content in IRH may influence its adsorption capacity [28], [29]. In general, RH contains 28.6–43.3 cellulose, 19.2–24.4 lignin, and 11.3–20 ash [30], [31]. Cellulose contains β -glucose monomers, whereas lignin contains polymeric aromatic structures that involve the oxidative coupling of 4-hydroxyphenylpropanoids and the three primary monolignols (coniferyl, sinapyl, and p-coumaryl alcohols) [32].

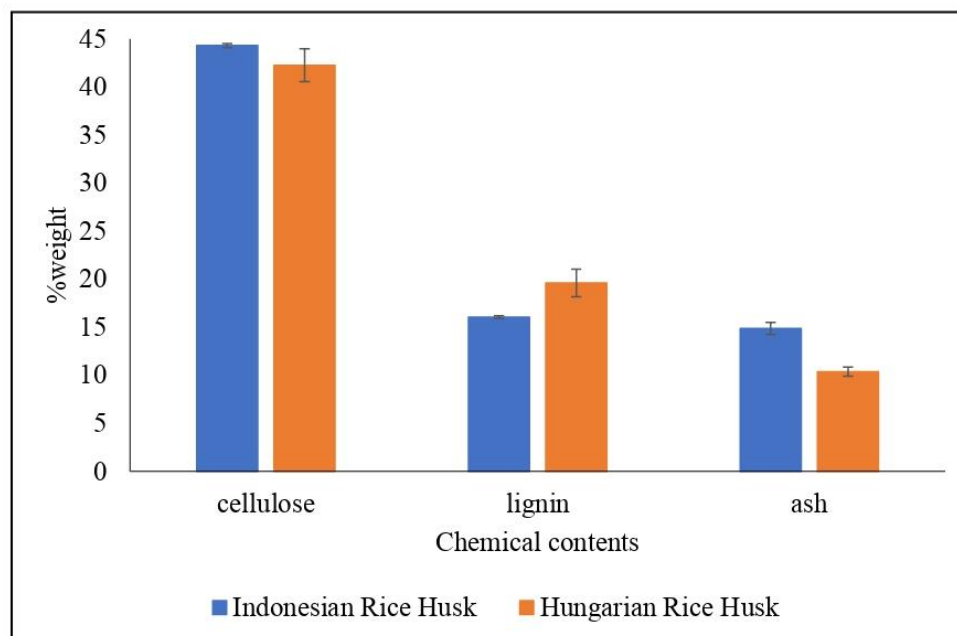


Figure 8. Chemical content of RHs

5.1.2 Zeta potential values

The zeta potential is an essential tool for understanding the charge characteristics of particles. Zeta potential measurement is also known as electrokinetic potential measurement, which is conducted to analyze particle charges and predict the stability of nanoparticles in a colloidal dispersion [153]. The zeta potential values of the RHs are shown in Figure 9a,b. There is a lack of zeta potential measurement where environmental changes, such as changes in pH and ion strength, occur [154]. The zeta potential sign is negative at all studied pH values. An increase in pH can decrease the zeta potential value, thus increasing the negative charges on the RH surface. RH functional groups, such as carboxyl and phenolic groups, contribute significantly to the RH surface charge.

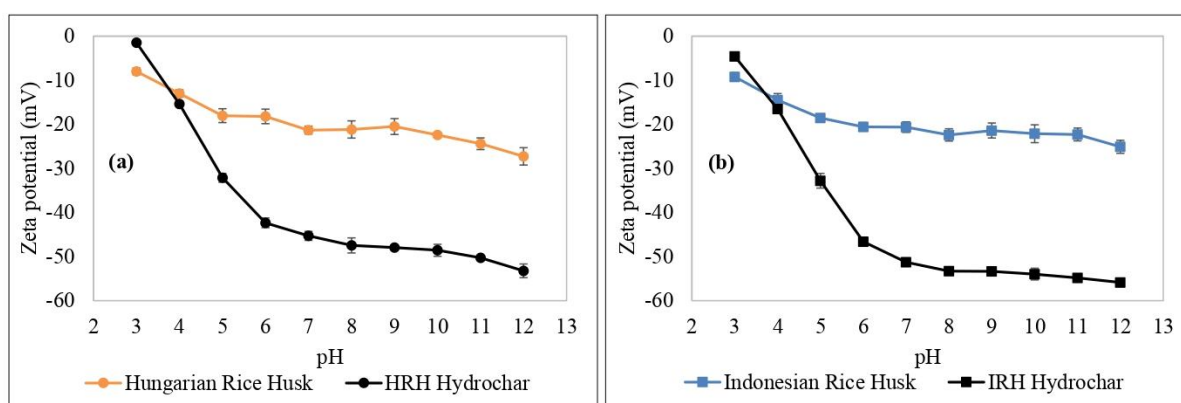


Figure 9. Zeta potential value for (a) Hungarian rice husk (raw and hydrochar) and (b) Indonesian rice husk (raw and hydrochar)

The increasing pH can enhance the deprotonation of the surface groups because of the weakening interaction between the surface functional groups and H^+ . Meanwhile, at more acidic pH values, the RH surface shows high protonation of the surface due to the association between the surface functional groups and H^+ [155], [156]. The negative surface contributes to the RH functional group's ability to adsorb positive ions [157]. At pH 12, the zeta potential of HRH and HRH hydrochar achieved maximum values of -27.2 mV and -53.2 mV, respectively. Meanwhile, IRH and IRH hydrochar achieved maximum values of -25.1 mV and -55.8 mV, respectively. Therefore, RH and RH hydrochar can be considered proper adsorbents for cationic dye removal.

5.1.3 Fourier Transform Infrared Spectroscopy (FT-IR) analysis

FT-IR analysis were conducted to characterize the RH samples before and after the adsorption of dyes (Table 9 and Figure. 10). The bands observed were similar to the ones investigated by Antil et al. [158]. Before adsorption, the band at 3427 cm^{-1} (IRH) and 3411 cm^{-1} (HRH) is due

to O–H bonds stretching in lignocellulose materials. The bands at 2929 cm^{-1} (IRH) and 2925 cm^{-1} (HRH) can be attributed to C–H bonds stretching. Further, the bands at 1736 cm^{-1} (IRH) and 1735 cm^{-1} (HRH) due to C=O bonds stretching of aldehyde groups in the hemicellulose component [159]. The bands at 1646 cm^{-1} (IRH) and 1654 cm^{-1} (HRH) can be attributed to O–H bonds. The bands at 1102 cm^{-1} (IRH) and 1099 cm^{-1} (HRH) can be ascribed to stretching Si–O–Si bonds. Finally, the bands at 804 cm^{-1} (IRH) and 800 cm^{-1} (HRH) refer to the presence of Si–O bonds in the rice husk structure.

The bands shift after MB adsorption. The bands at 3407 cm^{-1} and 3444 cm^{-1} are due to the O–H bonding interaction between MB and RH. The bands at 2925 cm^{-1} and 2933 cm^{-1} indicate the stretching vibration of the $-\text{CH}_3$ in the dimethylamino groups. The band at 1605 cm^{-1} is attributed to the heterocyclic stretching vibration of C=N. The bands at 1335 cm^{-1} and 1331 cm^{-1} are ascribed to the stretching vibrations of the C–N bonds in the dimethylamino groups [59].

After BR9 adsorption, the bands shift to 3399 cm^{-1} and 3382 cm^{-1} due to the stretching vibrations of O–H and N–H bonds. The bands at 2921 cm^{-1} and 2933 cm^{-1} are due to the symmetric and asymmetric stretching vibrations of the C–H bonds in the $-\text{CH}_3$ and CH_2 groups. The bands at 1593 cm^{-1} and 1519 cm^{-1} are ascribed to the stretching vibrations of C=N and C=O bonds, respectively. The bands at 1164 cm^{-1} and 1168 cm^{-1} indicate the stretching vibrations of C–N bonds.

After the adsorption of MB and BR9 in binary solutions, the original band positions shifted, and new bands appeared. The band at 1602 cm^{-1} due to C=N and C=O bonds stretches. The bands at 1334 cm^{-1} and 1166 cm^{-1} can be attributed to C–N bonds stretching: the former band is specific for dimethylamino groups [160].

The IR spectra of RHs change after hydrogen carbonization. The bands seen at 3408 cm^{-1} and 3423 cm^{-1} correspond to the stretching vibrations of O–H bonds, which are distinctive features of alcohol groups in cellulose, hydroxyl groups in water, and phenol in lignin [161]. The band at 2929 cm^{-1} can be attributed to the vibrational motion of C–H bonds in $-\text{CH}_3$ and $-\text{CH}_2$ groups. The band at 1701 cm^{-1} corresponds to the stretching vibrations of C=O bonds in cellulose and lignin [162]. The presence of C=C bonds in the aromatic rings of lignin is indicated by the bands observed at 1608 cm^{-1} and 1598 cm^{-1} . Additionally, the bands observed at 1112 cm^{-1} and 1110 cm^{-1} indicate the existence of C–O stretching vibrations in the raw

materials of lignocellulose, whereas the bands at 798 cm^{-1} and 800 cm^{-1} can be attributed to C–H bonds in the aromatic rings.

Table 9. FT-IR absorption bands of RH

Absorption band (cm^{-1})						
IRH	HRH	IRH + MB	HRH + MB	IRH + BR9	HRH + BR9	Assignment
3427	3411	3407	3444	3399	3382	O–H and N–H
2929	2925	2925	2933	2921	2933	C–H, $-\text{CH}_3$ or $-\text{CH}_2$
1736	1735	-	-	-	-	C=O
1646	1654	-	-	-	-	O–H
-	-	1605	1605	1593	1519	C=N and C=O
-	-	1335	1331	-	-	C–N
-	-	-	-	1164	1168	C–N
1102	1099	-	-	-	-	Si–O–Si
804	800	-	-	-	-	Si–O

Table 10. FT-IR absorption bands of RH (continued)

Absorption band (cm^{-1})				
IRH (MB+BR9)	HRH (MB+BR9)	IRH Hydrochar	HRH Hydrochar	Assignment
3413	3422	3423	3408	O–H and N–H
2927	2927	2929	2929	C–H, $-\text{CH}_3$ or $-\text{CH}_2$
1733	1738	1701	1701	C=O
1647	1652	-	-	O–H
1602	1602	-	-	C=N and C=O
		1598	1608	C=C
1334	1334	-	-	C–N
1166	1166	-	-	C–N
1098	1098	1110	1112	Si–O–Si
803	808	800	798	Si–O

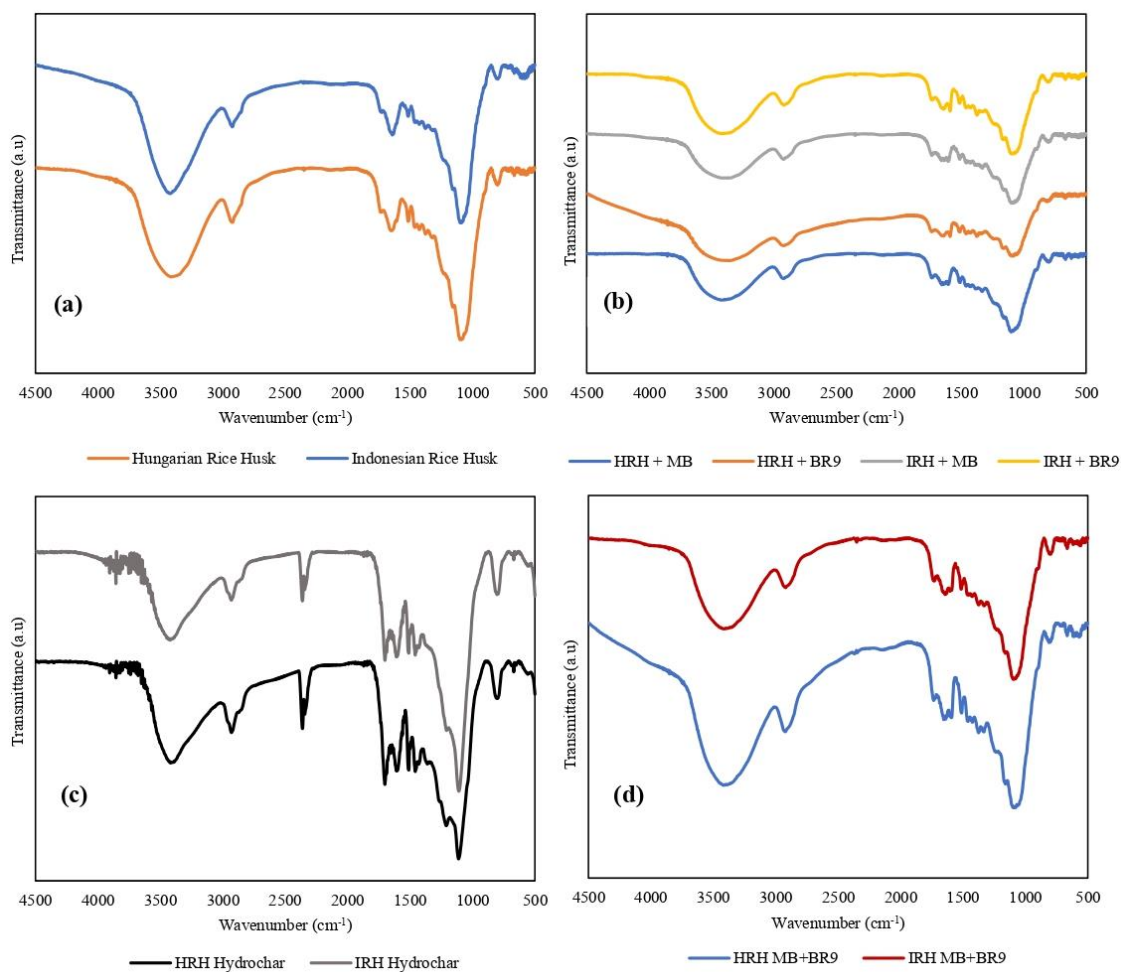


Figure 10. FT-IR absorption spectra for (a) Raw RH (b) after adsorption single solutions, (c) RH Hydrochar after adsorption binary solutions, and (d) after adsorption binary solutions

5.1.4 Scanning Electro Microscopic (SEM) analysis

The surface morphology of RH and its hydrochar can be analyzed by SEM, as shown in Figure 11. The micrographs show that the surfaces were highly irregular and could not be characterized by any well-defined morphology, containing only a few fine particles (Figure 11a,b). This characteristic is ascribed to the fiber structure of the raw biomass material. After hydrothermal carbonization, the previous surface of the raw RH changes, revealing degradation during the carbonization process. The RH is transformed into smaller particles with rough surfaces and porous structures. The observed change is probably caused by structural reorganization during hydrothermal carbonization [163], [164].

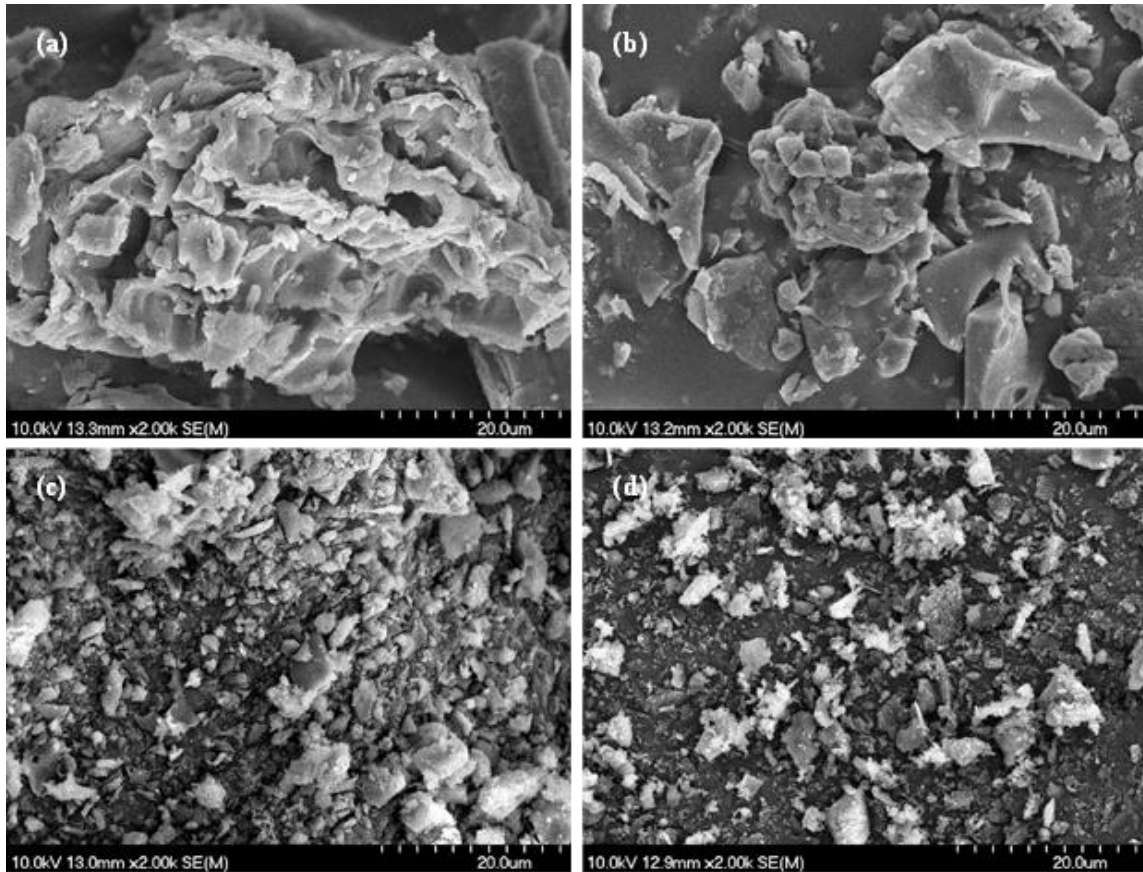


Figure 11. SEM images of (a) Hungarian rice husk, (b) Indonesian rice husk, (c) Hungarian rice husk hydrochar, and (d) Indonesian rice husk hydrochar

5.2 Adsorption of cationic dyes using RH from aqueous solution

5.2.1 Effect of pH

The solution pH affects the ability of hydrogen ions (H^+ or protons) to bind to functional groups on an adsorbent surface, for example, carboxyl (COOH), amine (NH), phenolic hydroxyl (OH), and metal ions [92]. The MB removal percentages at pH 5–10 are shown in Figure 12a. IRH and HRH achieve a maximum MB removal percentage of 96% at pH 10. This result is supported by the zeta potentials of IRH and HRH, which are equal at pH 10. These findings agree with those of Labaran et al. [165], where MB removal occurred under alkali conditions.

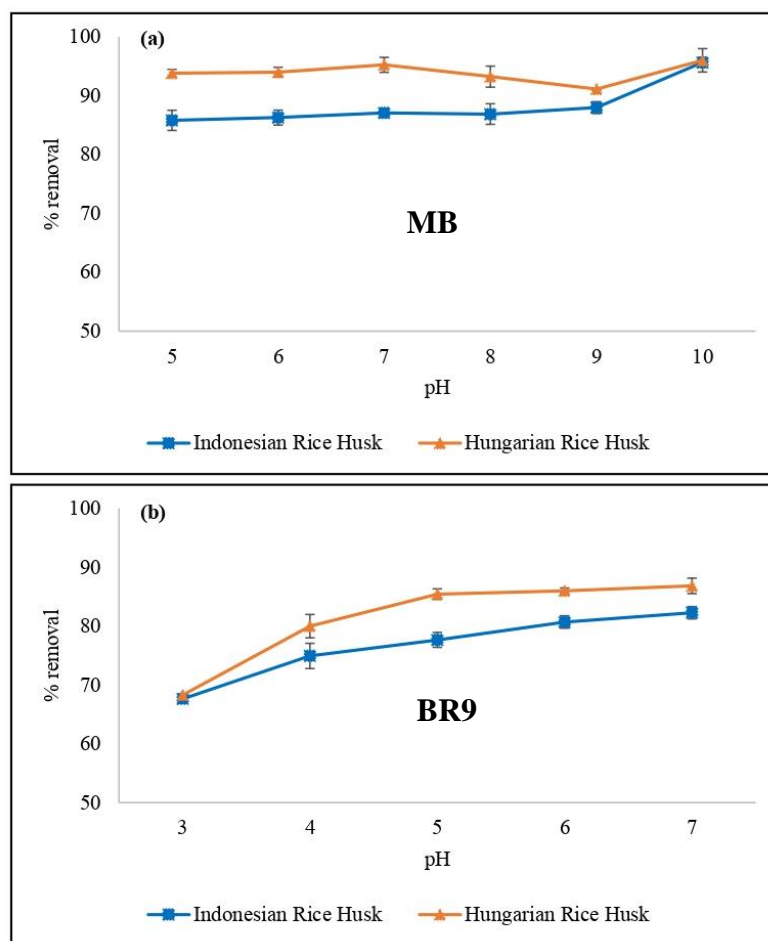


Figure 12. Effect of pH on MB (a) and BR9 (b) removal by rice husks of different origins (concentration value: 2 g/L; initial concentration of dyes: 30 mg/L; temperature (T°): 25 $^\circ\text{C}$; time (t): 120 min)

The BR9 removal percentages at pH 3–7 are shown in Figure 12b. IRH and HRH achieve maximum BR9 removal percentages of 82% and 87%, respectively, at pH 7. This result is confirmed by the zeta potential of HRH, which is higher than that of IRH at pH 7. These findings agree with those reported in a previous study on the use of activated *Gossypium hirsutum* seeds for BR9 removal [70].

The dye removal percentage increases under alkali conditions for MB and neutral conditions for BR9 but decreases under acidic conditions. This is because of the protonation and deprotonation of the functional groups on the adsorbent surface and the dye molecules. At low (acidic) pH values, the number of hydrogen ions (H^+ or protons) in the solution increases and more functional groups on the RH surface are protonated. This competition with H^+ ions for surface sites reduces the probability of cationic MB adsorption on the RH surface. However, increasing the pH toward alkali conditions reduces the number of hydrogen ions (H^+ or protons) near the surface. Thus, the functional groups on the RH surface become more deprotonated,

thereby affecting the charge density and strengthening the Coulomb interaction between the negative charge of the adsorbent and the positive charge of the dye molecules [166], [167].

5.2.2 Effect of initial dye concentration

The effects of various initial dye concentrations (30, 60, 90, and 120 mg/L) on MB and BR9 removal by IRH and HRH at room temperature were studied, as shown in Figure 13a,b. The amounts of MB (120 mg/L) adsorbed using IRH and HRH in the aqueous solutions are 55.6 mg/g and 55.7 mg/g, respectively. The amounts of BR9 (120 mg/L) adsorbed using IRH and HRH are 53.9 mg/g and 54.3 mg/g, respectively.

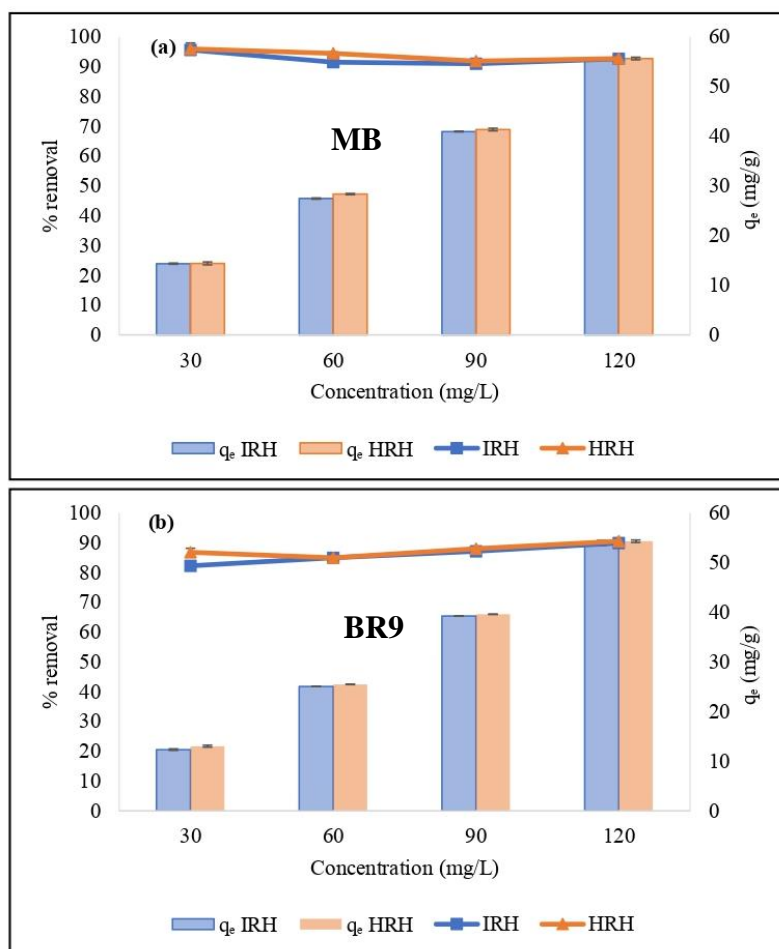


Figure 13. Effect of initial concentration on MB (a) and BR9 (b) removal by rice husks of different origins (pH: 10 for MB, 7 for BR; concentration value: 2 g/L; temperature (T°): 25 $^\circ$ C; time (t): 120 min)

As the initial dye concentration increases, the amount adsorbed (mg/g) at equilibrium (q_e) increases. At higher initial concentrations, the driving forces increase and the RH surface is saturated because the number of unoccupied active sites on the adsorbent decreases. The mass transfer of dyes from the solutions to the RH surface reduces, reducing the adsorption rate

[117], [168], [169]. Therefore, adsorption depends on the initial dye concentration. In general, no significant differences are observed between the use of IRH or HRH at various initial dye concentrations.

5.2.3 Effect of adsorbent dose

The effects of different adsorbent doses (125, 250, and 500 mg) on adsorption were studied using 250 mL of each dye solution. The adsorbent dose is an important parameter for determining optimal adsorption conditions because the adsorbent capacity is affected by the initial dye concentration [93]. The maximum MB removal percentage of IRH and HRH at 500 mg is 96%. An increase in the adsorbent dose from 0.5 g/L to 2 g/L can improve the removal percentage. The effects of the doses of the two adsorbents are shown in Figure 14a,b.

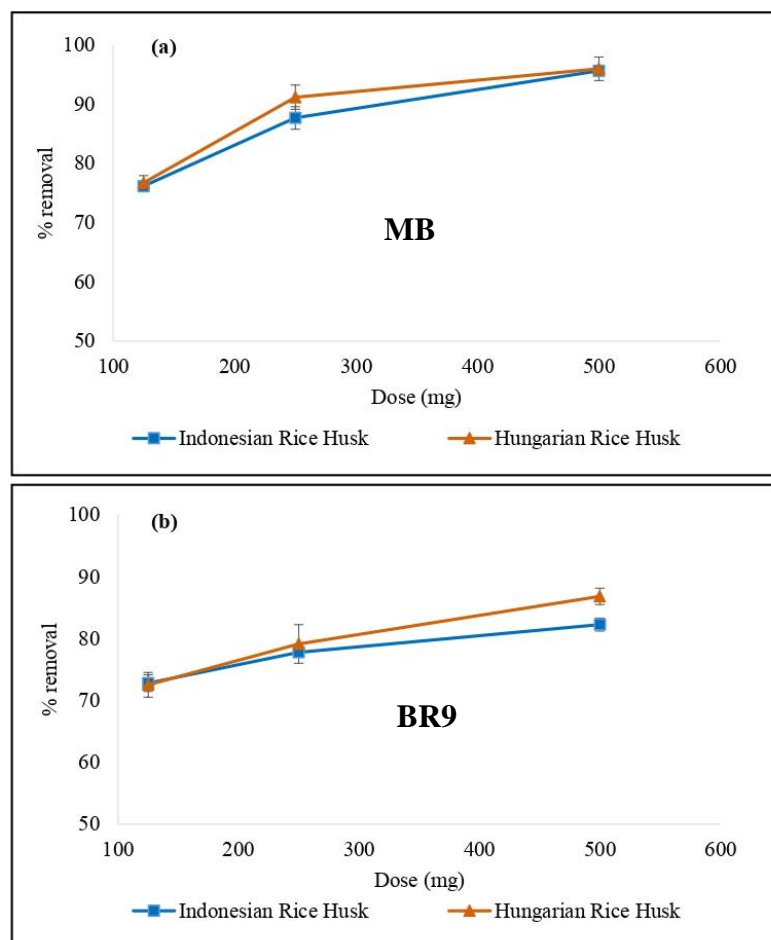


Figure 14. Effect of adsorbent dose on MB (a) and BR9 (b) removal by rice husks of different origins (pH: 10 for MB, 7 for BR9; initial concentration of dyes: 30 mg/L; temperature (T°): 25 $^\circ$ C; time (t): 120 min)

The maximum BR9 removal percentages of IRH and HRH are 82% and 87%, respectively. The removal patterns for both dyes are similar—the removal percentage improves with the adsorbent dose. Increasing the adsorbent dose can enhance the removal capacity by increasing

the active adsorption sites and surface areas [170], [171], thus increasing the available active sites for the adsorption of dyes.

5.2.4 Effect of contact time

The contact time parameter is used to determine the equilibrium time. Depending on the adsorbent material and the adsorbate, the adsorption process requires a certain period to achieve equilibrium [86]. Here, the adsorption was conducted from 5 min to 120 min to understand the effect of contact time. Every 5 min during the adsorption process, samples are taken to obtain removal percentages. The effects of contact on the adsorption performance of the two adsorbents are shown in Figure 15a,b.

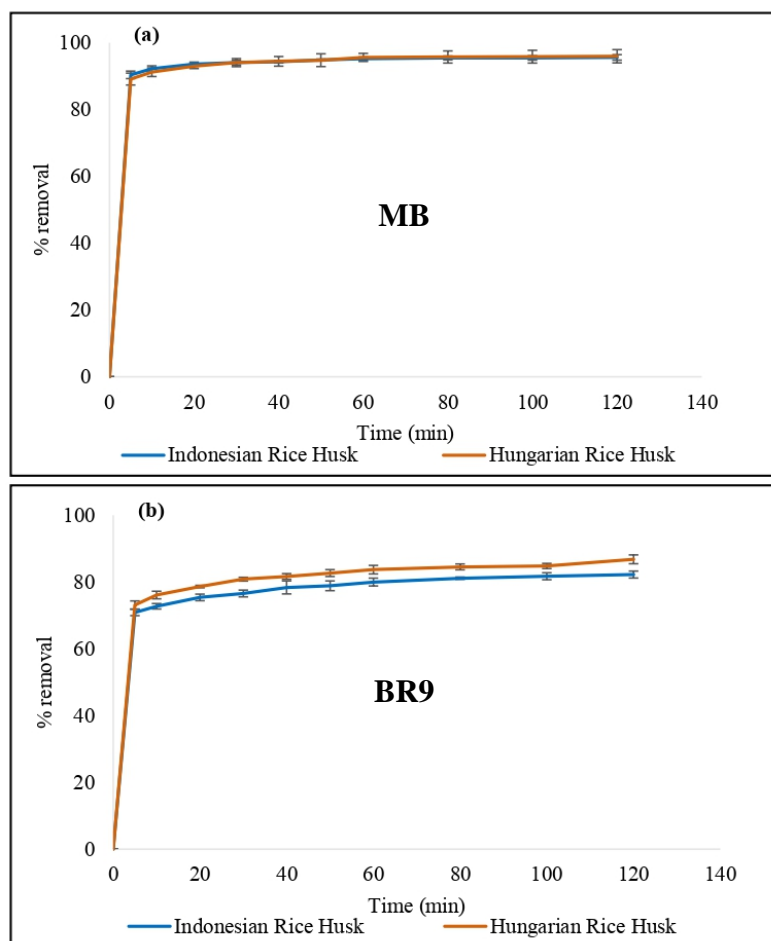


Figure 15. Effect of contact time on MB (a) and BR9 (b) removal by rice husks of different origins (pH: 10 for MB, 7 for BR9; concentration value: 2 g/L; initial concentration of dyes: 30 mg/l; temperature (T°): 25 °C)

The adsorption process consists of three phases: initial, intermediate, and equilibrium [172], [173]. The adsorption process starts in the initial phase, which is fast and has high removal rates. The MB and BR9 removal percentages of HRH within 5 min are 89% and 73%, respectively, whereas those of IRH are 90% and 71%, respectively. In the intermediate phase,

the removal rate gradually slows down. The removal rate becomes constant (equilibrium phase) within 120 min, at which the MB and BR9 removal rates of HRH (IRH) are 96% (96%) and 87% (82%), respectively. HRH generally exhibits a higher removal percentage than IRH.

5.2.5 Effect of temperature

The physicochemical reactions in the adsorption process are influenced by temperature. An increase in temperature typically increases the dye molecule's mobility from a solution to an adsorbent surface [174]. The effect of temperature (25 °C, 35 °C, and 45 °C) was examined, as shown in Figure 16a,b. The MB removal percentages of IRH at 25 °C, 35 °C, and 45 °C are 96%, 96%, and 96%, respectively, whereas those of HRH at 25 °C, 35 °C, and 45 °C are 96%, 96%, and 97%, respectively. MB adsorption is independent of temperature. In particular, this parameter is not always beneficial to the process and thus can be neglected in some cases [175].

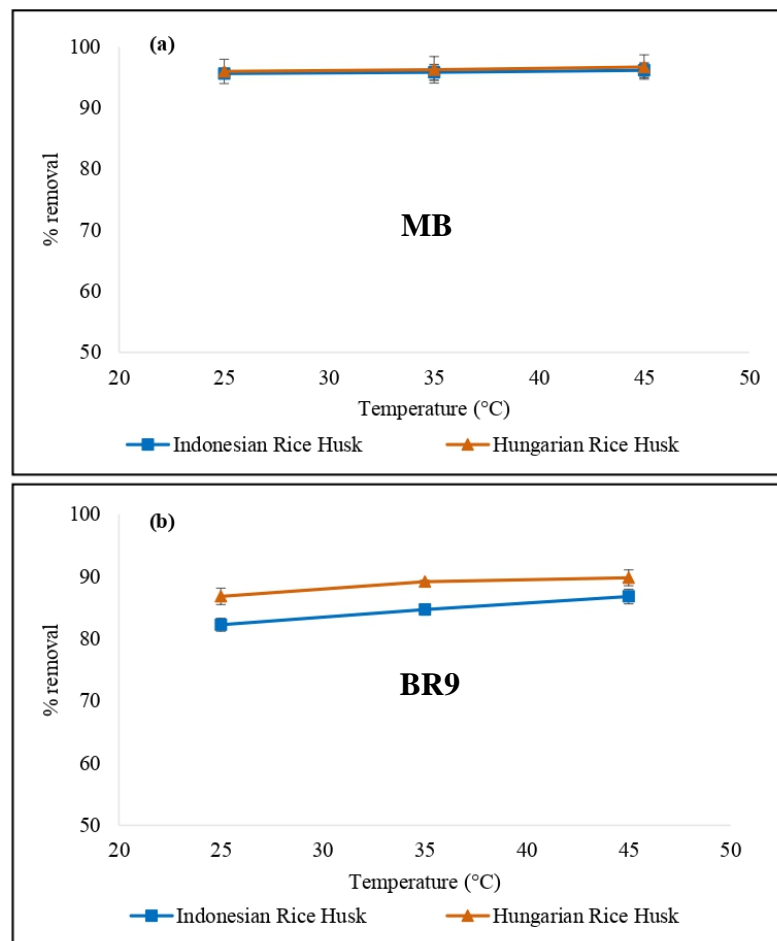


Figure 16. Effect of temperature on MB (a) and BR9 (b) removal by rice husks of different origins (pH: 10 for MB, 7 for BR9; concentration value: 2 g/L; initial concentration of dyes: 30 mg/L; time (t): 120 min)

BR9 removal using IRH and HRH gave similar results. The removal percentages of IRH at 25 °C, 35 °C, and 45 °C are 82%, 85%, and 87%, respectively, and those of HRH at 25 °C, 35 °C, and 45 °C are 87%, 89%, and 90%, respectively. The same results were obtained by Zhao et al. [176]. However, the effect of temperature is not highly significant in this study; the associated differences in removal percentage are relatively small. The effect of temperature is strongly dependent on the adsorbent surface nature (energetically homogeneous or heterogeneous) for adsorption from aqueous solutions [177].

5.2.6 Adsorption isotherm modelling in single solution

The adsorption isotherm describes the relationship between the amount of adsorbate adsorbed by the adsorbent (q_e) and the equilibrium concentration of adsorbate (c_e) at a constant temperature. The parameters obtained from adsorption equilibrium models provide helpful information about surface properties, adsorption mechanisms, and the adsorbent–adsorbate relationship [172].

The capacities of IRH and HRH to adsorb MB and BR9 were investigated via batch adsorption experiments at different initial dye concentrations and constant adsorbent doses at a given temperature. The adsorption equilibrium data for MB and BR9 were studied using the Harkins–Jura and Brunauer–Emmett–Teller (BET) multilayer isotherm models. The experimental data and isotherm models are compared in Figure 17a–d.

In this experiment, the isotherm shape can be described as a C-type isotherm. A C-type (constant partition) isotherm is a partition of solutes that takes place between the aqueous phase and the interfacial layer of a solid [178]. Therefore, the BET multilayer model is more appropriate for the adsorption isotherm in this study. MB and BR9 aggregated in the adsorption experiment; the self-association of these dyes in aqueous solutions has been reported in the literature [179]. Organic dyes in aqueous solutions frequently self-aggregate into dimers, trimers, and higher-order aggregates based on concentration [180].

Fujita et al. [181] found that MB exists as dimers in an aqueous solution or as aggregates on the surface. A monomer–dimer can exist in the concentration range of 10^{-3} – 10^{-6} M [182]. According to Fernández-Pérez et al. [183] and Fernández-Pérez and Marban [184], the aggregation of MB molecules in a solution forms dimers at concentrations below 3.4×10^{-5} M, monomers at a concentration of 1.1×10^{-6} M, and tetramers at a concentration of 3.5×10^{-3} M. The monomer–dimer equilibrium for MB has been investigated at concentrations of 2×10^{-6} – 5×10^{-5} M [185]. Pathrose et al. [186] found that BR9 can form dimers and aggregates

at concentrations of 10^{-2} – 10^{-5} M. According to Figure 17a–d, MB concentrations of 2.8×10^{-5} M (~9 mg/L) and BR9 concentrations of 4.1×10^{-5} (~12 mg/L) tend to increase to infinity, since the aggregation is perceptible in the aqueous solution and on the surface.

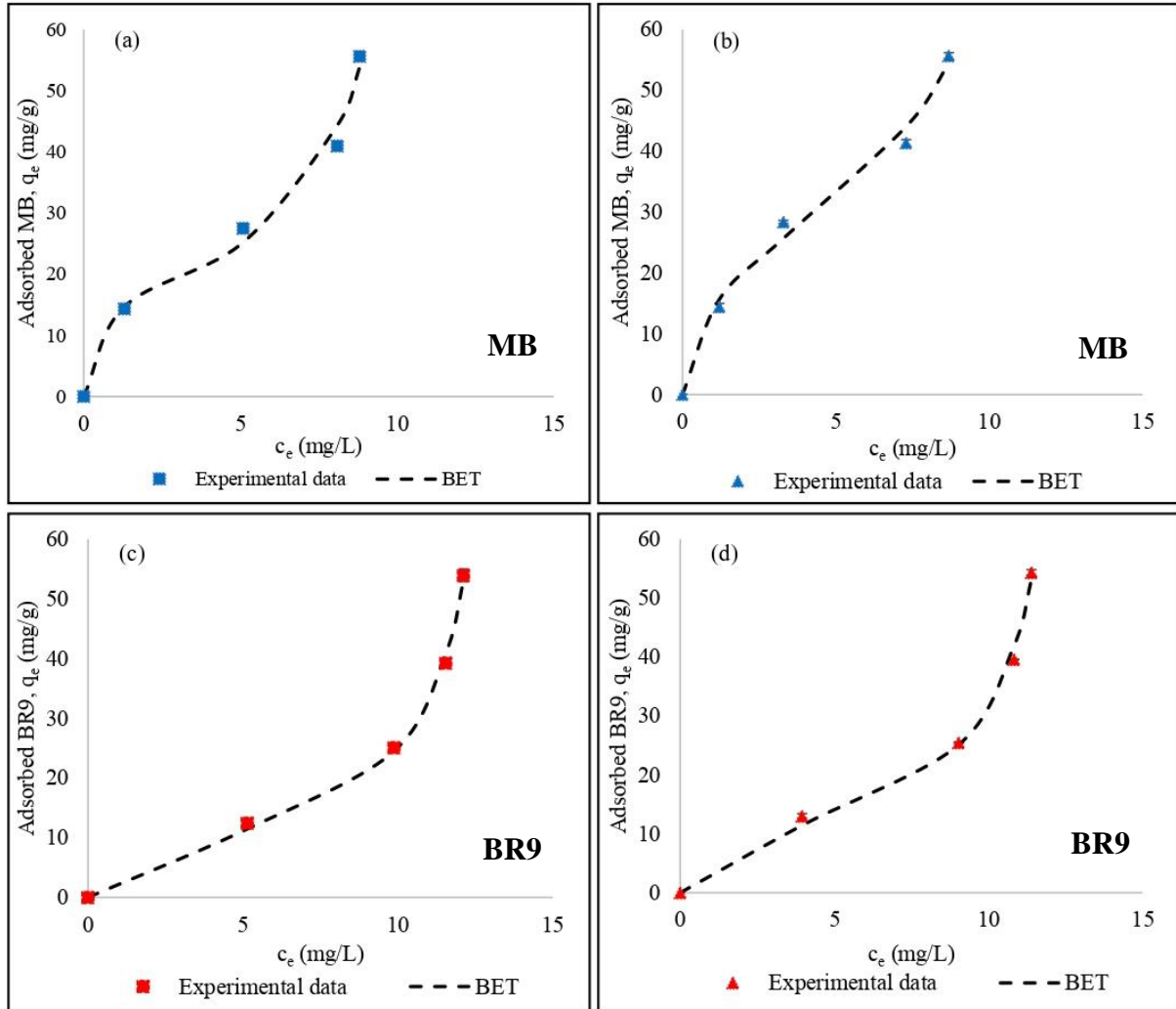


Figure 17. Experimental data and BET model fitting for (a) MB adsorbed using Indonesian rice husk, (b) MB adsorbed using Hungarian rice husk, (c) BR9 adsorbed using Indonesian rice husk, and (d) BR9 adsorbed using Hungarian rice husk

Table 10 shows the isotherm parameters of the Harkins–Jura and the BET multilayer models obtained via nonlinear fitting. Based on the correlation coefficient (R^2) and the nonlinear chi-square (χ^2) (Table 10), the BET multilayer adsorption isotherm fits the experimental adsorption data better. Equation (8) presents the Harkins–Jura Equation form for determining the isotherm parameter [187]:

$$q_e = \left(\frac{A}{B - \log C_e} \right)^{1/2} \quad (8)$$

C_e is the equilibrium concentration of adsorbate, A is the Harkins–Jura isotherm parameter, and B is the Harkins–Jura isotherm constant. The Harkins–Jura adsorption isotherm describes heterogeneous pore distribution and multilayer adsorption [188].

Table 11. Isotherm parameters for MB and BR9 adsorption

Isotherm Model	Parameter	IRH		HRH	
		MB	BR9	MB	BR9
Harkins–Jura	A	26.38	10.32	39.37	12.85
	B	1.20	1.18	1.30	1.18
	R^2	0.960	0.974	0.970	0.963
	χ^2	0.28	0.18	0.20	0.25
BET	Q_m (mg/g)	15.02	7.27	24.50	8.32
	K_L	0.08	0.07	0.07	0.07
	K_S	4.78	983.02	1.10	114.40
	R^2	0.979	0.995	0.981	0.989
	χ^2	0.14	0.04	0.13	0.08

The BET multilayer isotherm is a theoretical model commonly used in gas–solid equilibrium systems [101], [189]. However, the classical BET Equation can be modified for liquid phase adsorption and has three degrees of freedom (Q_m , K_s , and K_L) [190]. The BET Equation for liquid phase adsorption [190] is expressed using Equation (9):

$$q_e = Q_m \frac{K_S C_e}{(1 - K_L C_e)(1 - K_L C_e + K_S C_e)} \quad (9)$$

Q_m is the amount adsorbed during complete monolayer adsorption, K_s is the equilibrium constant of adsorption of the first layer, and K_L is the equilibrium constant of adsorption of the upper layers of the adsorbate on the adsorbent.

In the BET multilayer isotherm model, the maximum adsorption capacity can reach infinity [190] The isotherm modeling in this study is similar to that of Vargas et al. [191], who used sisal fibers (*Agave sisalana*) for MB removal, and that of Côrtes et al. [192], who used fish scales for BR9 removal.

A comparison of the adsorption capacities of IRH and HRH for MB removal is given in Table 11. In the literature, the highest adsorption capacity for MB removal is 1346.7 mg/g [132], while the lowest is 1.6 mg/g [193]. Particle size has a vital role in adsorption capacity, and a varying adsorbent particle size correlates directly with particle diffusion into pores [194].

Table 12. Comparison of the adsorption capacity of raw RH for MB removal

No	Origins	Adsorption Capacity (mg/g)	Particle Size	pH	References
1	India	1347.7	400–841 μm	7	[132]
2	China	19.7	0.425–0.850 mm	7	[139]
3	Malaysia	1.6	NA	5.8	[193]
4	Iran	24.7	<250 μm	10	[195]
5	Brazil	52.2	5 mm	11	[196]
6	Thailand	21.9	<400 μm	5.7–6.2	[67]
7	Nigeria	13.5	NA	10	[165]
8	Korea	25.4	0.075–1.16 mm	7	[133]
9	Indonesia	15.0	<250 μm	10	This study
10	Hungary	24.5	<250 μm	10	This study

The chemical composition of RH, which includes lignin and silica, can affect the adsorption capacity of RH. The chemical composition of an adsorbent can affect the bonding strength between the adsorbate and the functional groups on the adsorbent surface [133]. The use of chemical fertilizers and the composition of soil chemistry in a paddy field can vary the chemical composition of RH [197]. Therefore, the wide range of RH chemical compositions reveals their dependence on, among others, RH origin, farm climate, and crop technology. Based on studies of MB adsorption using RHs of different origins, RH origin is a factor that influences MB adsorption capacities.

In our study, the adsorption capacities of IRH and HRH for MB removal are 15.0 mg/g and 24.5 mg/g, respectively. According to the results, HRH has a higher adsorption capacity because it contains less ash. However, IRH and HRH have better adsorption capacities compared with other RHs. As a bioadsorbent, RH can also be used for wastewater treatment because it is abundant and environmentally friendly. Other advantages, such as simplicity and low costs, can be achieved using raw RH.

The adsorption capacities of various adsorbents for BR9 removal have been investigated and compared (Table 12). The highest adsorption capacity for BR9 removal was reported by Kong et al. [198], while the lowest was obtained by Zhao et al. [56]. In the current study, the IRH and HRH adsorption capacities for BR9 removal are 7.2 mg/g and 8.3 mg/g, respectively. HRH has a higher adsorption capacity for BR9 removal than IRH.

Table 13. Comparison of adsorption capacities of various adsorbents for BR9 removal

No	Adsorbent	Adsorption Capacity (mg/g)	Particle Size	pH	References
1	Fish Bones	14.8	50–200 μm	7	[199]
2	Activated <i>Gossypium Hirsutum</i> Seeds	67.1	NA	8	[70]
3	Leather Activated Carbon	139.3	105–149 μm	8	[198]
4	Malted Sorghum Mash	58.5	2 mm	4–9	[200]
5	Triptycene-Based Porous Polymer	586.2	NA	2–9	[201]
6	Multi-Walled Carbon Nanotubes	55.5	NA	8	[202]
7	Pistachio Nut Shells	118.2	1 mm	12	[203]
8	Alkali-Activated Diatomite	9.8	NA	9	[176]
9	Eggshell Membrane	48.0	250–350 μm	6	[204]
10	<i>Astragalus</i> Root	20.2	125 μm	10	[205]
11	Indonesian Rice Husk	7.2	<250 μm	7	This study
12	Hungarian Rice Husk	8.3	<250 μm	7	This study

Many agricultural and waste materials have been utilized as adsorbents to remove BR; however, to the best of our knowledge, raw RH has not been used. From environmental and economic points of view, RH can be utilized as an alternative adsorbent to elucidate BR9 adsorption.

5.2.7 Adsorption kinetic modelling in single solution

A kinetic model can describe adsorption processes and possible rate-controlling steps such as mass transport and chemical reaction processes [105]. Two kinetic Equations, namely, pseudo-first-order (PFO) [206] and pseudo-second order (PSO) [207], were used to investigate the MB and BR9 adsorption kinetics. Their nonlinear forms are expressed as Equations (10) and (11):

$$q_t = q_e (1 - e^{-k_1 t}) \quad (10)$$

$$q_t = \frac{q_e^2 k_2 t}{1 + k_2 q_e t} \quad (11)$$

where q_e and q_t represent the adsorption capacities (mg/g) of the adsorbent at equilibrium and at time t (min), respectively. k_1 is the first-order rate constant and k_2 is the second-order rate constant.

The PFO kinetic model describes the adsorption process as controlled by the diffusion step; it follows a physical adsorption mechanism (physisorption kinetics). By contrast, the PSO kinetic model describes the adsorption rate as affected by the chemical interaction between the adsorbate and the adsorbent; it follows a chemical adsorption mechanism (chemisorption

kinetics) [208], [209]. The kinetic parameters for MB and BR9 adsorption are shown in Table 13.

Table 14. Kinetic parameters for MB and BR9 adsorption

Kinetic Model	Parameter	IRH		HRH	
		MB	BR9	MB	BR9
Pseudo-first order	q_e (mg/g)	14.19	11.83	14.20	12.38
	k_1	0.61	0.43	0.54	0.41
	R^2	0.637	0.474	0.666	0.736
	χ^2	0.001	0.01	0.003	0.01
Pseudo-second order	q_e (mg/g)	14.32	12.13	14.38	12.71
	k_2	0.23	0.1	0.16	0.08
	R^2	0.945	0.825	0.956	0.921
	χ^2	0.0002	0.005	0.0004	0.004

Based on the correlation coefficient (R^2) and the nonlinear chi-square (χ^2) result in Table 13, all the experimental data fit the PSO kinetic model better than the PFO kinetic model. Thus, chemisorption controls the MB and BR9 adsorption processes, where functional groups play a central role [210], [211]. Chemisorption occurs through the sharing or exchange of electrons between the negatively charged RH functional groups, as evidenced by the zeta potential measurement, and the positively charged cationic dyes [212]. The initial concentration selected during the adsorption kinetic process affects the kinetic model. A relatively high initial concentration tends to be relatively stable during the adsorption process and better fits a PFO kinetic model. Conversely, a PSO kinetic model fits better when the initial concentration is relatively low and changes significantly during the adsorption process [213].

In addition, the PSO kinetic rate k_2 for MB adsorption (0.16–0.23 g/mg/h) is higher than the PSO kinetic rate k_2 for BR9 adsorption (0.08–0.1 g/mg/h). This result suggests the formation of covalent bonds between the MB molecules and the RH surface [214]. The experimental data and calculated (PSO kinetic model) adsorption kinetics are represented by plotting time (min) against q_e (mg/g) in Figure 18a–d. The experimental q_e data closely match the calculated q_e data from the PSO kinetic model.

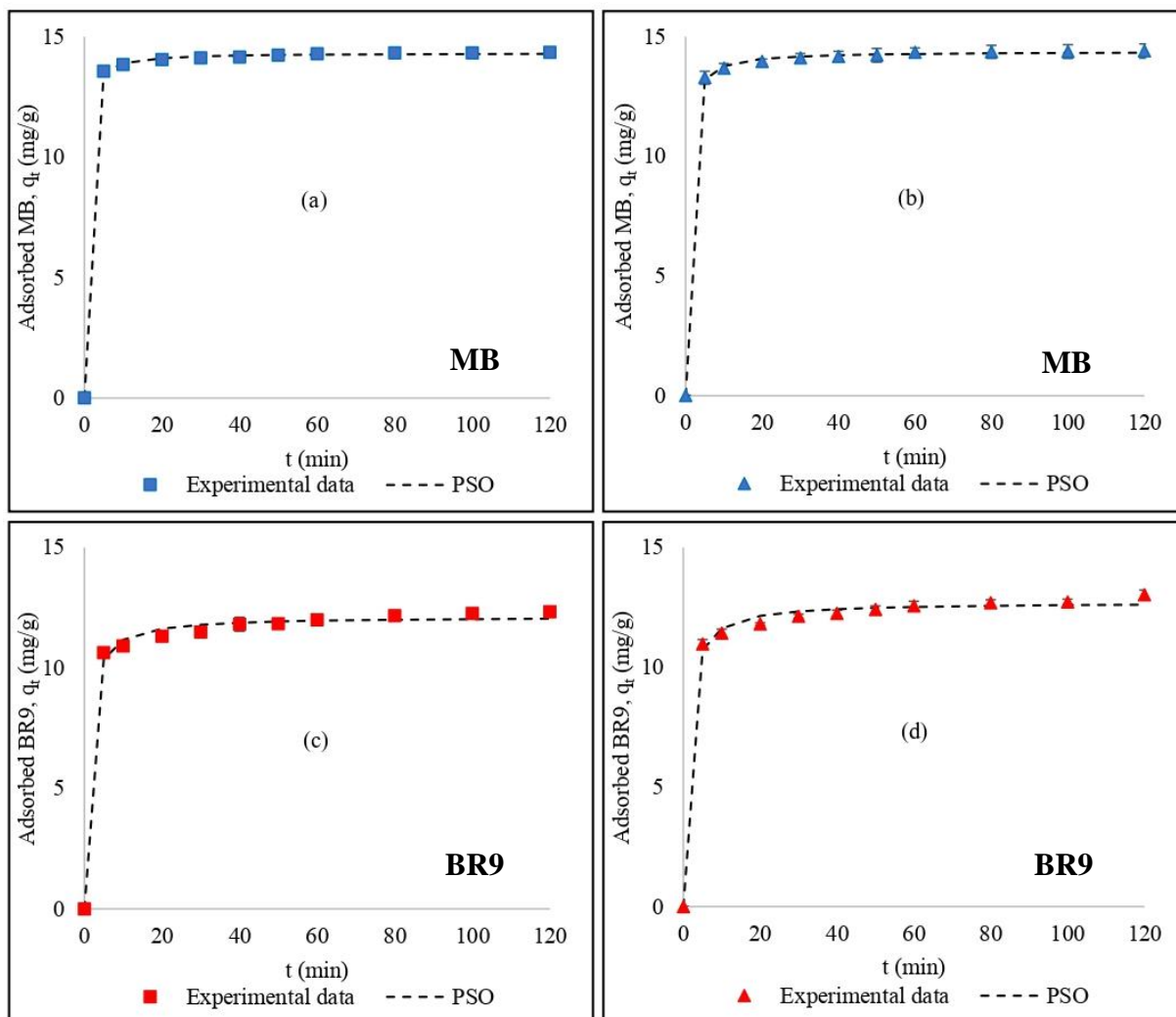


Figure 18. Experimental data and PSO model fitting for (a) MB adsorbed using Indonesian rice husk, (b) MB adsorbed using Hungarian rice husk, (c) BR9 adsorbed using Indonesian rice husk, and (d) BR9 adsorbed using Hungarian rice husk

5.3 Binary adsorption of cationic dyes using RH from aqueous solution

5.3.1 Effect of pH

The effect of pH was studied to determine the optimal pH for removing MB and BR9. The removal percentages of these dyes by HRH and IRH increase with the increase of pH from 3 to 7 (Figure 19a,b). Generally, removal percentages for adsorption of cationic dyes will increase at high pH values (basic condition) and decrease at low pH values (acidic condition) [215]. At lower pH values the removal percentages are lower due to more H^+ ions in the solution. The H^+ ions compete for the adsorbent sites with cationic dyes during the adsorption process [216]. Meanwhile, under basic conditions, the adsorbent is more negatively charged. Hence, the electrostatic interaction between the positively charged of cationic dye molecules and the negatively charged of RH adsorbent increases the removal percentage [217].

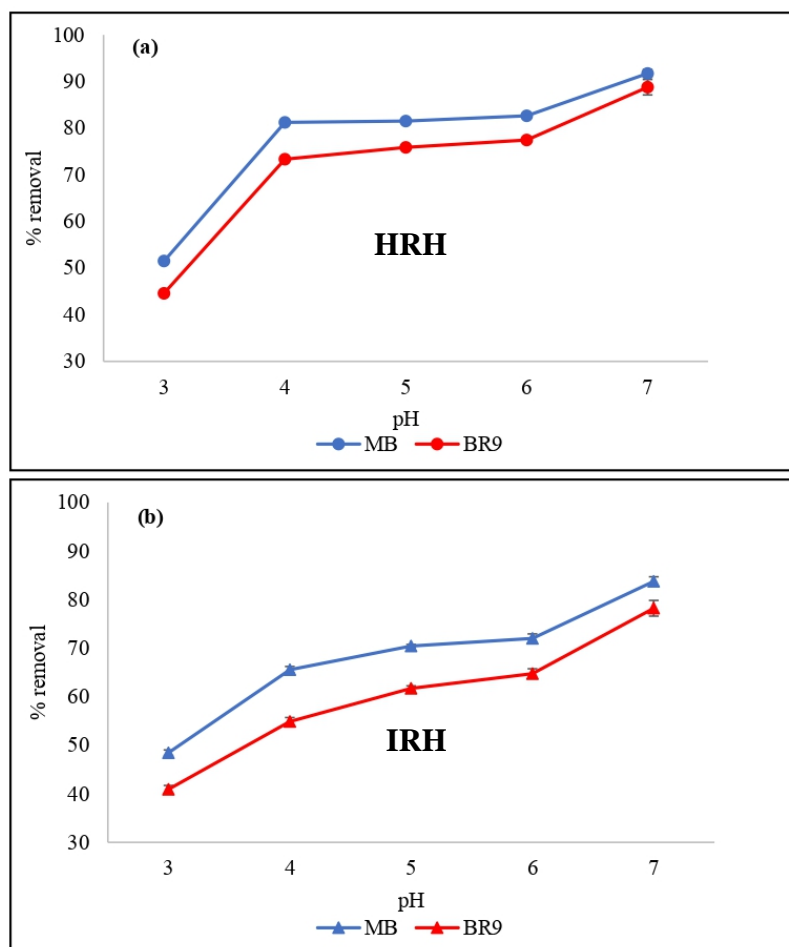


Figure 19. Effect of pH on MB and BR9 removals by HRH (a) and IRH (b) using the following parameters: 500 mg of RH, 30 mg/L initial concentration, 60 min adsorption time, and 25 °C temperature

5.3.2 Effect of adsorbent dose

The effect of the adsorbent dose was also examined (Figure 20a,b). At the highest adsorbent dose (500 mg), MB and BR9 removal percentages by HRH were as high as 91.7% and 88.8%, respectively. For IRH, these values were 83.8% and 78.2%, respectively. However, the adsorption capacities for MB and BR9 by HRH decreased from 22.4 to 13.8 mg/g and from 20.3 to 13.3 mg/g, respectively. Meanwhile, using IRH, the adsorption capacities were decreased from 20.2 to 12.6 mg/g for MB and from 16.8 to 11.7 mg/g for BR9. The increasing RH dose increases the removal percentage and decreases the adsorption capacities due to more available unoccupied adsorbent sites on the RH surface [218]. Based on these results, 500 mg of RH was selected as the very good adsorbent dose and used in a subsequent experiments.

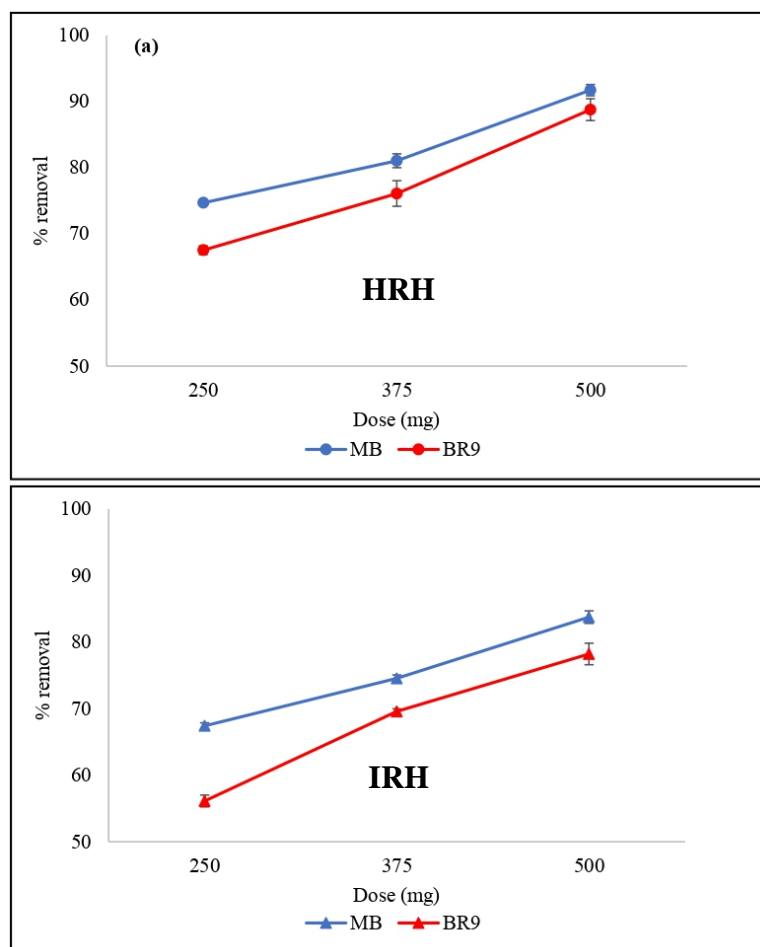


Figure 20. Effect of adsorbent dose on MB and BR9 removals by HRH (a) and IRH (b) using the following parameters: 30 mg/L initial concentration, pH 7, 60 min adsorption time, and 25 °C temperature

5.3.3 Effect of contact time

Adsorption varies with the contact time, and contact time is vital to dye removal efficiency (Figure 21a,b). Increasing the contact time from 0 to 60 min increases the MB and BR9 removal from binary dyes solution due to increased interaction probability of MB and BR9 dyes with the surface of RH bioadsorbent [219]. Removal of MB and BR9 on HRH or IRH was initially rapid because of the more available adsorption sites [28]. Removal within 5 min using HRH was 76.7% for MB and 69.7% for BR9. In the same timeframe, removal by IRH was 71.9% for MB and 63.5% for BR9. After the initial removal, as active sites were increasingly occupied adsorption gradually slowed and stabilized [220]. Adsorption equilibrium was reached within 60 min. Moreover, removal rates by HRH were found to be 91.7% for MB and 88.8% for BR9 and 83.8% for MB, and 78.2% for BR9 by IRH.

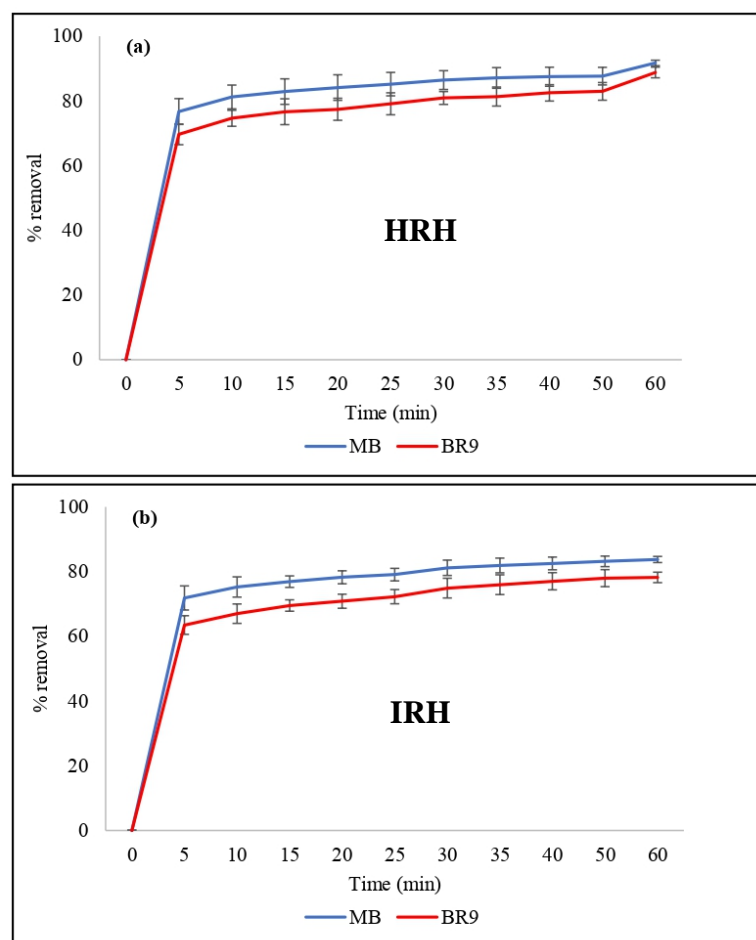


Figure 21. Effect of contact time on MB and BR9 removal by HRH (a) and IRH (b) using the following parameters: 500 mg of RH, pH 7, 30 mg/L initial concentration, 25°C temperature

5.3.4 Effect of initial dye concentration

The impact of various initial concentrations of dye (30, 60, 90, and 120 mg/L) was assessed to explore adsorption capacity (Figure 22a,b). Adsorption at equilibrium increased with increasing initial concentration of dye. The adsorption capacities of HRH for 120 mg/L MB and BR9 were 50.7 and 48.5 mg/g, respectively, and 50.1 and 47.4 mg/g for IRH, respectively. At lower initial dye concentrations, fewer dye molecules were adsorbed, as expected [221]. Increasing MB and BR9 concentration led to lower active sites of the bioadsorbent owing to the high adsorption rate of MB and BR9 at the beginning of the adsorption process [149]. Additionally, increasing the initial dye concentrations increased mass transfer during adsorption; therefore, higher equilibrium values were obtained, thereby reducing the removal percentage of dyes [149], [222].

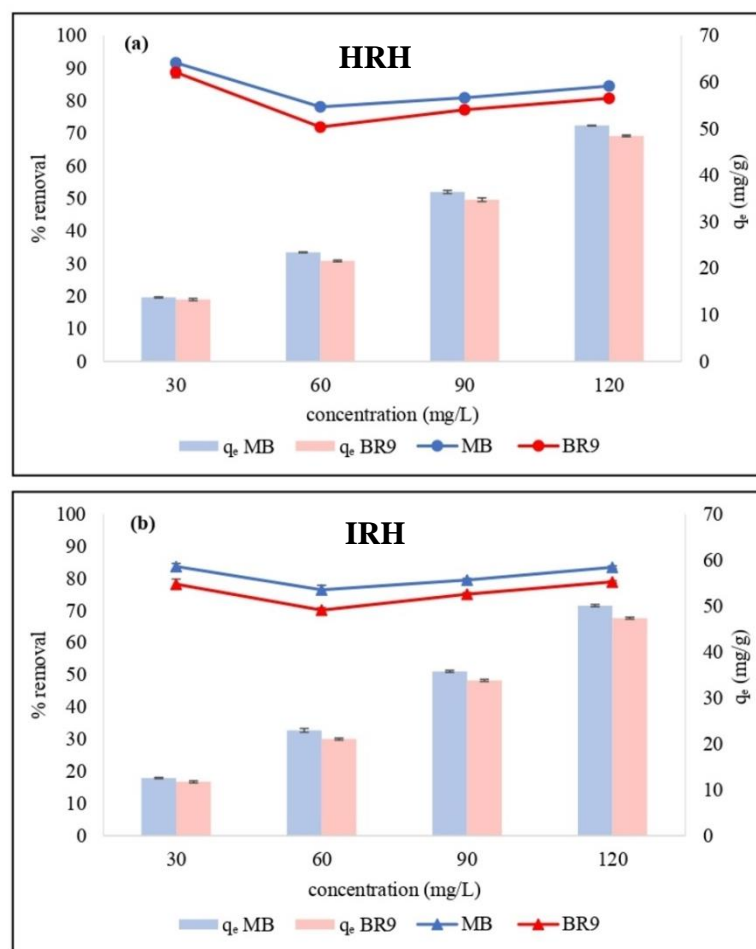


Figure 22. Effect of initial dye concentration on MB and BR9 removals by HRH (a) and IRH (b) using the following parameters: 500 mg of RH, pH 7, 60 min adsorption time, and 25 °C temperature

5.3.5 Adsorption modelling

Adsorption isotherm and kinetic of MB and BR9 were constructed to identify the binary adsorption mechanisms. Langmuir and Brunauer–Emmett–Teller (BET) multilayer isotherm models were evaluated using varying initial dye concentrations, amounts of RH, and temperature. The BET multilayer model could be fitted to the experimental data (Figure 23a–d).

Ionic dyes tend to undergo self-association (aggregation) in aqueous solutions. Ionic dyes can form dimers, trimers, and micelles during adsorption. Several factors can influence this condition, including pH, concentration, temperature, etc. [223]. In a previous research, MB formed aggregates below 3.4×10^{-5} M [184], while BR9 was liable to form aggregations and dimers between concentrations of 10^{-2} and 10^{-5} M [186]. The result show that MB and BR9 tend to form dimers and aggregates in aqueous solution at concentrations of 6.2×10^{-5} M (~ 20 mg/L) (Figure 23a,b) and 8.7×10^{-5} M (~ 25 mg/L) (Figure 23c,d), respectively.

The Langmuir isotherm describes the adsorption process at homogeneous adsorbent sites [224]. The Langmuir model Equation [139] is calculated as Equation (12):

$$q_e = \frac{Q_m K_L C_e}{1 + K_L C_e} \quad (12)$$

where C_e is the concentration at equilibrium, q_e is the adsorbate amount on the adsorbent, Q_m is the amount required for monolayer adsorption, and K_L is the Langmuir isotherm constant related to the energy of adsorption. The extended Langmuir model [225] was used to evaluate binary adsorption as follows:

$$q_{ei} = \frac{K_{Li} Q_{mi} C_{ei}}{1 + \sum K_{Li} C_{ei}} \quad (13)$$

Based on Equation 13, the individual equilibrium capacity for the binary adsorption of MB and BR9 is calculated as Equations (14) and (15):

$$q_{e1} = \frac{K_{L1} Q_{m1} C_{e1}}{1 + K_{L1} C_{e1} + K_{L2} C_{e2}} \quad (14)$$

$$q_{e2} = \frac{K_{L2} Q_{m2} C_{e2}}{1 + K_{L1} C_{e1} + K_{L2} C_{e2}} \quad (15)$$

where q_{e1} and q_{e2} are the amounts of solutes (MB and BR9) adsorbed by the adsorbent (mg/g); C_{e1} and C_{e2} are adsorbate concentrations at equilibrium (mg/L); Q_{m1} and Q_{m2} represent the maximum adsorption capacities (mg/g); and K_{L1} and K_{L2} are the Langmuir constants (L/mg). The BET isotherm model characterizes multilayer adsorption and is derived from the generalized Langmuir model [226]. The liquid phase adsorption of BET multilayer isotherm Equation [190] is given as Equation (9).

The BET multilayer isotherm model best fit experimental results based on correlation coefficients (R^2) and nonlinear chi-square (χ^2) (Table 14). This model shows that the adsorption of MB and BR9 formed more than one layer of adsorbate on RH surfaces [191]. The difference in the Q_m value in Table 14 is because the Langmuir isotherm model supposes the adsorption process occurred only on a monolayer. Therefore, the Q_m calculated in the BET model is less than the Q_m calculated in the Langmuir model [227].

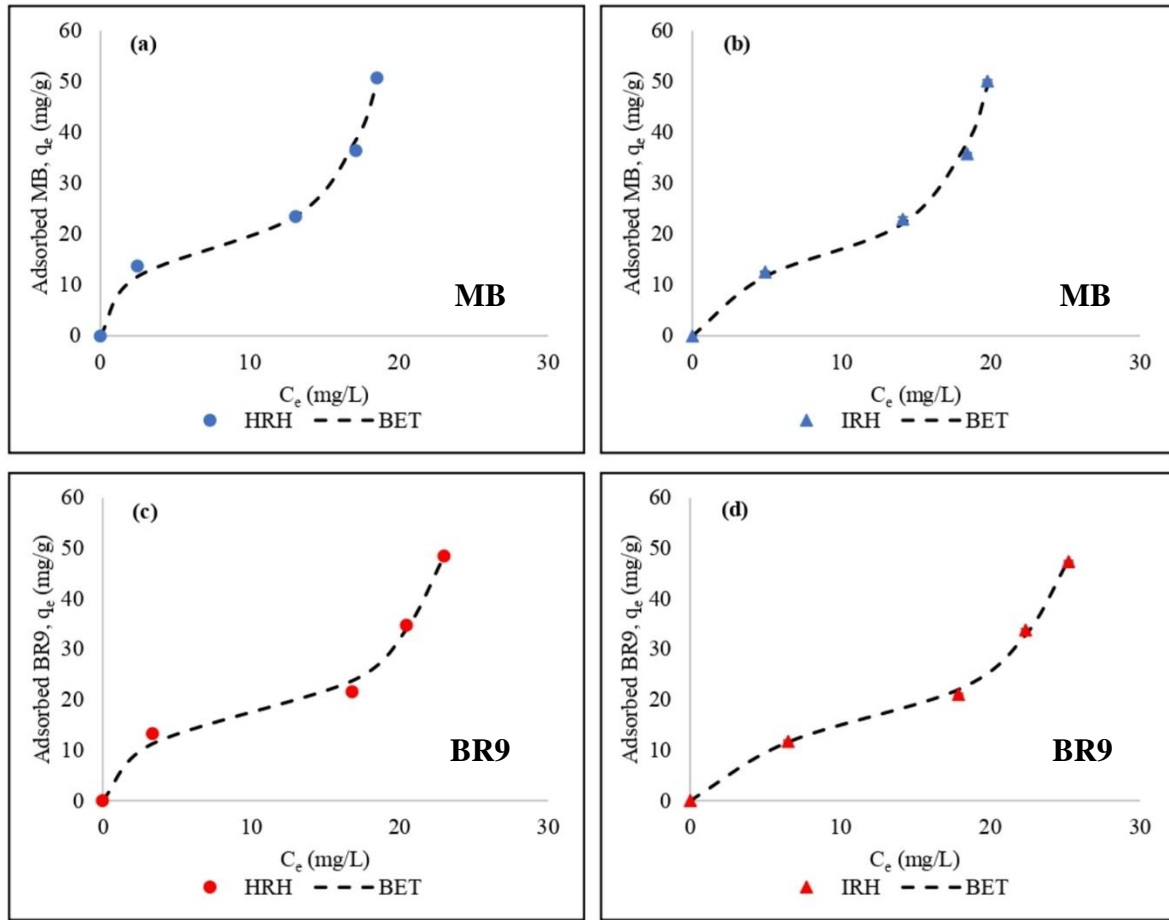


Figure 23. Comparison of experimental data and BET multilayer isotherm models for (a) MB using HRH, (b) MB using IRH, (c) BR9 using HRH, and (d) BR9 using IRH

Table 15. Nonlinear isotherm parameters for MB and BR9 during binary adsorption

Model	Parameter	Indonesian Rice Husk		Hungarian Rice Husk	
		MB	BR9	MB	BR9
Extended Langmuir	Q_m (mg/g) (10^5)	9.8	9.6	6.1	9.9
	K_L (10^{-6})	2.2	1.7	3.9	1.8
	R^2	0.834	0.844	0.764	0.744
	χ^2	1.07	0.97	1.52	1.59
BET	Q_m (mg/g)	9.3	9.6	10.4	10
	K_L	0.04	0.03	0.04	0.03
	K_S	1.3E+04	2.5	2E+06	1.5E+07
	R^2	0.991	0.997	0.987	0.987
	χ^2	0.06	0.02	0.08	0.08

The Langmuir model uses the same value for monolayer and maximum adsorption capacities. However, the monolayer and maximum adsorption capacities are different for the BET multilayer model. The maximum adsorption capacity for the BET multilayer model can be infinite [190]. This can be proven by comparing the Q_m values between the Langmuir and BET multilayer isotherm. Based on these results, the Q_m calculated by the BET multilayer model

agrees with the q_e experimental after reaching equilibrium, which were 12.6–13.8 mg/g for MB and 11.7–13.3 mg/g for BR9 (Table 16).

K_s was higher than K_L , which showed that the affinity of the first layer between the RH surface and dyes is greater than in the second layer [228]. Similar results were obtained by the BET model for the removal of dyes using different bioadsorbents, such as sugarcane bagasse [223], soybean hull [229], and banana pseudostem [230].

Table 15 compares the adsorption capacities of HRH and IRH for cationic dyes in binary dye solutions from various adsorbents. The result shows that the raw material of HRH and IRH provides good adsorption capacities. Utilization of HRH and IRH without chemical/physical modification can reduce energy and chemical consumption during bioadsorbent preparation. In addition, rice husk as a low-cost bioadsorbent is abundantly available in large quantities, has eco-friendly components, and is excellent in the regeneration–reusability for removing dyes [231]. Therefore, HRH and IRH become promising alternative bioadsorbent compared to other adsorbent materials and have the potential for cationic dyes removal from binary dye solutions.

Table 16. Comparison of the adsorption capacity for cationic dyes in binary dye solutions using various adsorbents

No	Adsorbent	Adsorbate	Adsorption capacity (mg/g)	Particle Size	pH	Reference
1	Medlar nut activated carbon	Basic yellow 28	37	NA	12	[232]
		Methylene blue	135.2			
2	Ziziphus mauritiana nut activated carbon	Basic blue 41	190.8	NA	12	[233]
		Basic yellow 28	133.1			
3	Cellulose-based modified citrus peels	Methylene blue	795.1	0.2 mm	NA	[28]
		Crystal violet	884.1			
4	Cotton–graphene oxide composite	Methylene blue	35.7	NA	7	[234]
		Crystal violet	19.2			
5	Functionalized microcrystalline cellulose	Methylene blue	100.2	NA	NA	[25]
		Neutral red	76.7			
6	Bombax buonopozense bark	Basic blue 41	75.1	NA	8.5	[235]
		Safranin	80.6			
7	Hungarian rice husk	Methylene blue	10.4	<250 μ m	7	This study
		Basic red 9	10			
8	Indonesian rice husk	Methylene blue	9.3	<250 μ m	7	This study
		Basic red 9	9.6			

To describe the binary adsorption mechanism, we used three kinetic models, such as the pseudo-first-order [206] (Equation 10), pseudo-second-order kinetics [207] (Equation 11), and the Elovich Equation [236] (Equation 16):

$$q_t = \frac{1}{\beta} \ln(1 + \alpha\beta t) \quad (16)$$

where q_e is the adsorbate amount on the adsorbent (mg/g) at equilibrium; q_t represents the adsorbate amount on the adsorbent (mg/g) at time t (min); k_1 is the constant of first-order (L/min); k_2 is the constant of second-order (g/mg/min); α represent the Elovich Equation constant (mg/g/min); and β (mg/g) is the constant of desorption.

The pseudo-first-order (PFO) and pseudo-second-order (PSO) models were applied to understand the adsorption kinetic behavior. PFO and PSO are commonly used to define adsorption mechanisms in physical adsorption (physisorption) and chemical adsorption (chemisorption) processes, respectively [237]. PFO and PSO models did not result in the best coefficient correlations and nonlinear chi-squares (χ^2) (Table 16). Besides, the calculated q_e value obtained from both models was lower than the experimental q_e value.

The Elovich model describes the adsorption process that occurs quickly at the initial stage, which then decreases over time due to the activation energy changes on the adsorbent surface [238]. This Equation describes an adsorption mechanism for a heterogeneous adsorbent [236], [239], [240]. The α value for MB was higher than for BR9, indicating faster initial adsorption [241]. According to correlation coefficients (R^2) and nonlinear chi-square (χ^2) for nonlinear kinetic models for binary adsorption indicated the Elovich Equation as the best fit (Table 16 and Figure 24a–d). Based on this result, chemisorption took place during adsorption. Other researchers also applied the Elovich Equation to analyze the adsorption kinetics of MB [238] and BR9 [68].

Table 17. Nonlinear kinetic parameters for MB and BR9 during binary adsorption

Model	Parameter	Indonesian Rice Husk		Hungarian Rice Husk	
		MB	BR9	MB	BR9
Experimental	q_e (mg/g)	12.6	11.7	13.8	13.3
Pseudo-first-order	q_e (mg/g)	12.1	11.1	12.9	12.1
	k_1	0.4	0.3	0.4	0.4
	R^2	0.545	0.844	0.574	0.788
	$\chi^2 (10^{-2})$	1.2	2.1	1.1	2.3
Pseudo-second-order	q_e (mg/g)	12.5	11.8	13.4	12.8
	$k_2 (10^{-2})$	8.4	6	8	6.1
	R^2	0.883	0.955	0.868	0.915
	$\chi^2 (10^{-3})$	3	6.2	3.6	9.1
Elovich Equation	α	2.6E+07	1.4E+05	2.7E+07	4.3E+05
	B	1.7	1.4	1.6	1.4
	R^2	0.931	0.967	0.913	0.943
	$\chi^2 (10^{-3})$	1.7	4.6	2.3	6.2

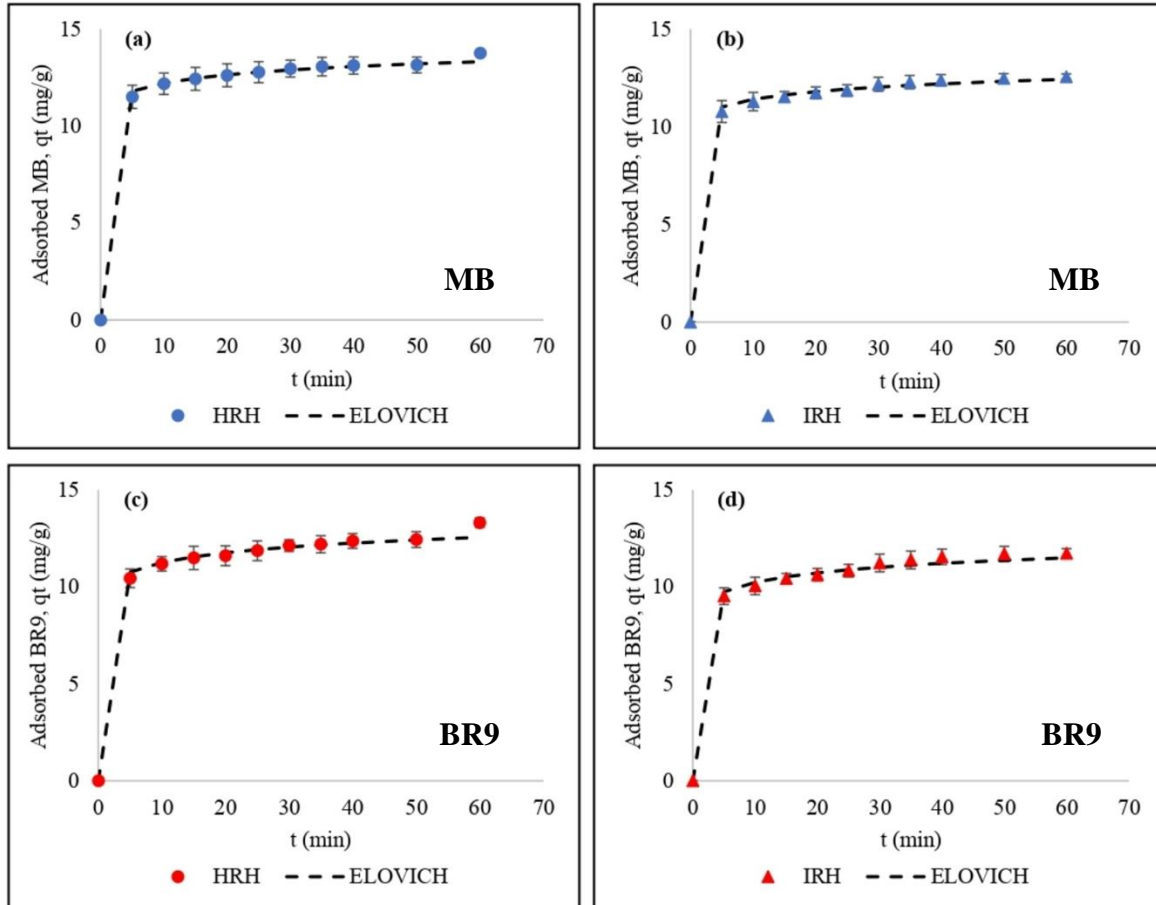


Figure 24. Comparison of experimental data and Elovich Equation model for (a) MB using HRH, (b) MB using IRH, (c) BR9 using HRH, and (d) BR9 using IRH

PFO and PSO models cannot describe the diffusion mechanism on the binary adsorption of MB and BR9. Therefore, the intra-particle model was applied to determine the rate-limiting of dye adsorption onto RH adsorbent. The intra-particle diffusion model [242] is calculated as Equation (17):

$$q_t = k_{id}\sqrt{t} + C \quad (17)$$

Here, k_{id} is the constant of intra-particle diffusion (mg/g/min), and C is a constant describing the boundary layer thickness. The linearized intra-particle diffusion kinetic model was applied to plot q_t vs $t^{1/2}$; the fitted (straight) line did not fit the experimental (Figure 25a,b). This result indicated a rate-limiting step of adsorption, which did not occur only by intra-particle diffusion [243]. Hence, the adsorption of MB and BR9 occurred in three different steps.

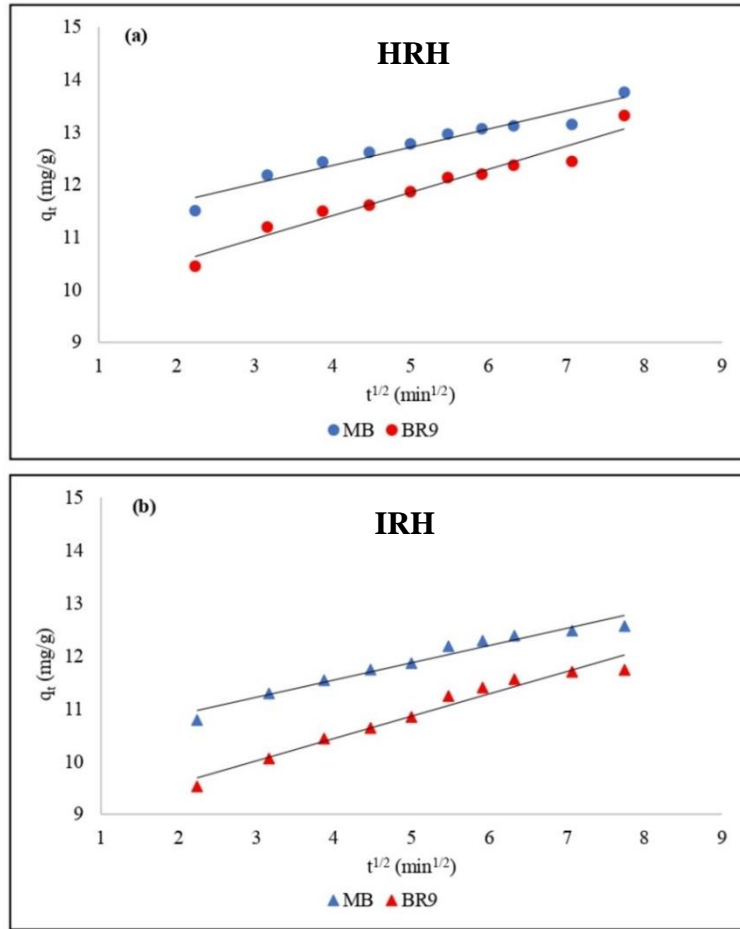


Figure 25. Intra-particle diffusion model for (a) HRH, and (b) IRH

Firstly, the solution transfers MB and BR9 to the surface of the rice husk adsorbent. Secondly, intra-particle diffusion takes place as the dyes reach the pores of the rice husk adsorbent. The strength of adsorption for monolayer and multilayer are different in this stage. Adsorption strength was higher for monolayer adsorption because the adsorbate easily adsorbs on the surface of the rice husk [244]. This condition can be confirmed based on the BET isotherm model, which yielded the higher value for the first layer constant (K_s) compared to those for the upper layers of adsorbates on the adsorbent (K_L). The last step is the equilibrium stage [245]. The C value was not equal to zero (C value range of 8.7–11 mg/g in Table 17), which implies that mass transfer and intra-particle diffusion contributed the most during the removal of MB and BR9 in binary adsorption [242], [246]

Table 18. Intraparticle diffusion parameters for Methylene Blue and Basic Red 9 during binary adsorption

Model	Parameter	Indonesian Rice Husk		Hungarian Rice Husk	
		MB	BR9	MB	BR9
Intra-particle diffusion	k_{id}	0.3	0.4	0.3	10.4
	C	10.2	8.7	11	9.6

The mechanism of adsorption can be explained by considering the structure of the adsorbates and the surface characteristics of the adsorbents. Both MB and BR9 are cationic dyes and dissociate into $\text{MB}^+ + \text{Cl}^-$ ions and $\text{BR9}^+ + \text{Cl}^-$ ions in aqueous solutions. Besides, rice husk is a lignocellulose comprising cellulose, hemicellulose, lignin, silica, and other minor components [247]. These components form many functional groups on the rice husk surface, and it becomes effective bioadsorbent due to their availability and low cost for application in wastewater treatment. Cellulose has many polar O and H atoms that play important roles in intramolecular and intermolecular hydrogen bonding [248]. Therefore, the possible interactions between rice husk adsorbents (cellulose unit) and dyes in binary adsorption are hydrogen bonding, electrostatic, and π - π stacking, as shown in Figure 26.

Hydrogen bonding interactions occur between the surface O-H groups of rice husk and $-\text{N}(\text{CH}_3)_2$ groups of dyes [249]. Functional groups such as phenolic and carboxyl groups have a strong negative charge evident from zeta potential analysis and can interact with MB and BR9 by electrostatic interactions [243], [246]. Further, the benzene ring in MB and BR9 possibly forms a π - π stacking interaction during binary adsorption. Besides, due to binary adsorption, the competitive adsorption of the dyes can take place. Thus, an adsorbent site on the surface of the rice husk could be partially overlapped with MB and BR9 [25].

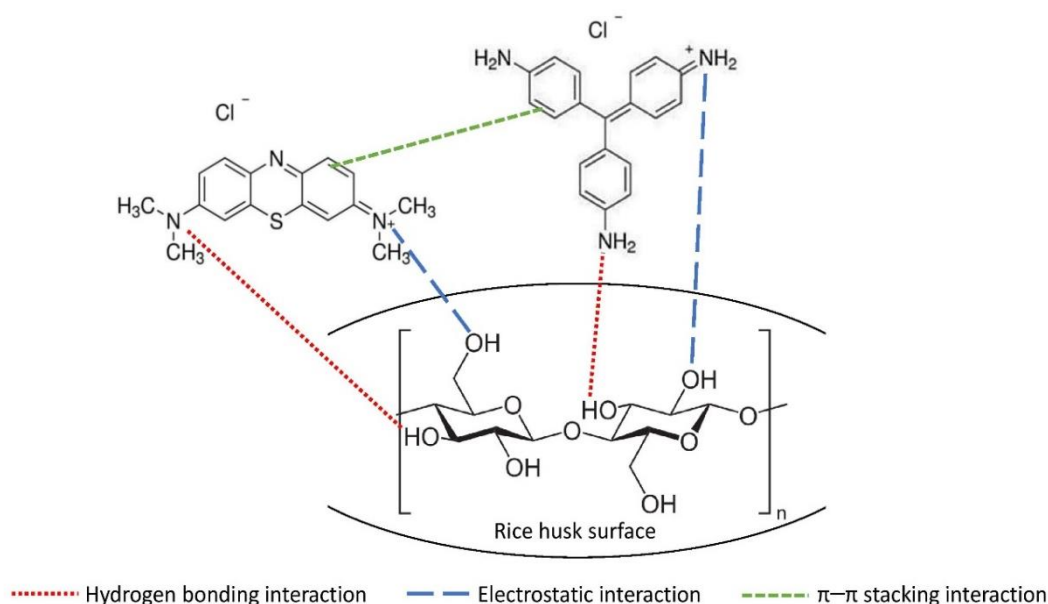


Figure 26. The possible interactions between the rice husk adsorbent (cellulose unit) and dyes in binary adsorption

5.3.6 Factorial design analysis

Factorial design analysis was used to evaluate factors for MB and BR9 removal in binary adsorption. The factorial design allows significant factors to be retained and insignificant factors to be neglected. This property reduces the number of experiments required. However, applying such an approach results in higher removal percentages [250]. Influences on the adsorption of MB and BR9 onto HRH and IRH were evaluated considering main effects, Pareto charts, normal probability plots, and interaction effects (Table 18).

Further, cube plots are provided to illustrate interactions of each factor (Figure 27a,b). These plots show that increasing pH from 3 to 7 and adsorbent from 250 to 500 mg enhances removal significantly for both dyes. In addition, HRH was the more efficient adsorbent. The highest removal was 91.7% for MB and 88.8% for BR9 at pH 7 using 500 mg of HRH.

Table 19. Matrix and results of the 2³ full factorial design

Run number	Codes value of variables			Removal (%)		Standard deviation	
	Adsorbent Type	pH	Dose	MB	BR9	MB	BR9
1	-1	-1	-1	47.1	39.4	0.3	0.6
2	1	-1	-1	48.0	40.6	0.3	0.6
3	-1	1	-1	67.4	56.1	0.5	0.9
4	1	1	-1	74.7	67.5	0.2	0.7
5	-1	-1	1	48.5	40.9	0.6	0.8
6	1	-1	1	51.5	44.6	0.3	0.2
7	-1	1	1	83.8	78.2	0.9	1.6
8	1	1	1	91.7	88.8	0.8	1.7

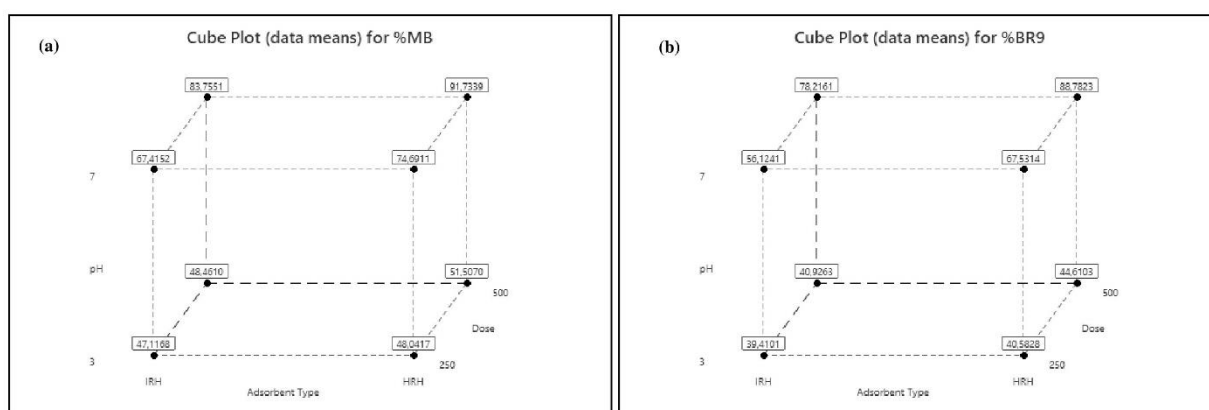


Figure 27. Cube plots of dye removals for (a) MB (%) and (b) BR9 (%) in binary adsorption

The main effect, interaction effect, coefficients, standard deviations, regression coefficients, T , and probability (P) values are provided in Table 19. The main factors (adsorbent type, pH, dose) for both dyes were significant ($p < 0.05$). At the same time, all two-way interactions for MB and BR9 in binary adsorption were significant, excluding two-way interactions (adsorbent type*dose) for BR9. However, three-way interactions for MB and BR9 were not significant.

When a factor effect is positive, removal efficiency increases at high levels; when negative, removal efficiency decreases from low to high levels [251]. Further, the model exhibited an adjusted R² of 99.89% for MB and 99.71% for BR9, which satisfied the statistical model.

Table 20. Estimated effects and coefficients for MB and BR9 during binary adsorption

Term	Effect	Coefficient	SE Coefficient	T-Value	P-Value	VIF
MB dye						
Constant		64.1	0.1	560.7	0	
Adsorbent Type	4.8	2.4	0.1	21.0	0	1
pH	30.6	15.3	0.1	133.9	0	1
Dose	9.5	4.8	0.1	41.8	0	1
Adsorbent Type*pH	2.8	1.4	0.1	12.3	0	1
Adsorbent Type*Dose	0.7	0.4	0.1	3.1	0	1
pH*Dose	7.1	3.6	0.1	31.3	0	1
Adsorbent Type*pH*Dose	-0.4	-0.2	0.1	-1.6	0.1	1
S	0.56					
R ²	99.92%					
Adjusted R ²	99.89%					
Predicted R ²	99.83%					
BR9 dye						
Constant		57.0	0.2	281.3	0	
Adsorbent Type	6.7	3.4	0.2	16.5	0	1
pH	31.3	15.6	0.2	77.1	0	1
Dose	12.2	6.1	0.2	30.1	0	1
Adsorbent Type*pH	4.3	2.1	0.2	10.6	0	1
Adsorbent Type*Dose	0.4	0.2	0.2	1.0	0.3	1
pH*Dose	9.5	4.7	0.2	23.3	0	1
Adsorbent Type*pH*Dose	-0.8	-0.4	0.2	-2.1	0.1	1
S	0.99					
R ²	99.80%					
Adjusted R ²	99.71%					
Predicted R ²	99.54%					

Dye removal efficiencies (%) are calculated after discarding adsorbent type*pH*dose (A*B*C) interactions for both dyes and neglecting adsorbent type*dose (A*C) interactions for BR9 as follows:

$$\begin{aligned}
 MB \text{ removal} = & 38.28 - 2.182 A + 2.297 B - 0.03324 C \\
 & + 0.7052 A * B + 0.002824 A * C + 0.014287 B * C
 \end{aligned} \tag{18}$$

$$\begin{aligned}
 BR9 \text{ removal} = & 35.03 - 1.995 A + 0.733 B - 0.04561 C \\
 & + 1.070 A * B + 0.018900 B * C
 \end{aligned} \tag{19}$$

Equations (18) and (19) describe how experimental variables and their interactions influence dye adsorption. Positive values indicate that dye removal increases when the effect increases and vice-versa [252]. Therefore, as adsorbent type (A) increased from low to high, percentage removal decreased to 2.182% for MB and to 1.995% for BR9. Also, as pH (B) increased from low to high, MB and BR9 removal increased to 2.297% and 0.733%, respectively. Finally, as adsorbent dose (C) was increased from low to high, percentages decreased by 0.03324% for MB and by 0.04561% for BR9.

Table 21. Analysis of variance for MB and BR9 during binary adsorption

Source	DF	Adjusted SS	Adjusted MS	F-Value	P-Value
MB dye					
Model	7	6667.7	952.5	3037.9	0
Linear	3	6310.1	2103.4	6708.3	0
Adsorbent Type	1	138.6	138.6	442.1	0
pH	1	5624.5	5624.5	17938.3	0
Dose	1	547.0	547.0	1744.5	0
2-Way Interactions	3	356.9	119.0	379.4	0
Adsorbent Type*pH	1	47.8	47.8	152.3	0
Adsorbent Type*Dose	1	3.0	3.0	9.5	0.01
pH*Dose	1	306.2	306.2	976.4	0
3-Way Interactions	1	0.8	0.8	2.4	0.1
Adsorbent Type*pH*Dose	1	0.8	0.8	2.4	0.1
Error	16	5.0	0.3		
Total	23	6672.8			
BR9 dye					
Model	7	7688.1	1098.3	1113.3	0
Linear	3	7037.2	2345.7	2377.7	0
Adsorbent Type	1	270.0	270.0	273.6	0
pH	1	5871.0	5871.0	5951.1	0
Dose	1	896.2	896.2	908.4	0
2-Way Interactions	3	646.7	215.6	218.5	0
Adsorbent Type*pH	1	109.9	109.9	111.4	0
Adsorbent Type*Dose	1	1.1	1.1	1.1	0.3
pH*Dose	1	535.8	535.8	543.1	0
3-Way Interactions	1	4.2	4.2	4.3	0.1
Adsorbent Type*pH*Dose	1	4.2	4.2	4.3	0.1
Error	16	15.8	1.0		
Total	23	7703.9			

Interaction effects can be evaluated by the analysis of variance (ANOVA). ANOVA separates variation into its components (Table 20). ANOVA provides the sum of squares to evaluate the contributions of different factors. F ratios compare respective mean–square–effects to mean–square–error, and p values provide the lowest significance level that leads to the null hypothesis refusal [253]. Main factors (adsorbent type, pH, dose) and two-way interactions were highly significant ($p < 0.05$) and corroborated with the model and experimental results at a 95% confidence level [254]. Conversely, three-way interactions were insignificant ($p > 0.05$).

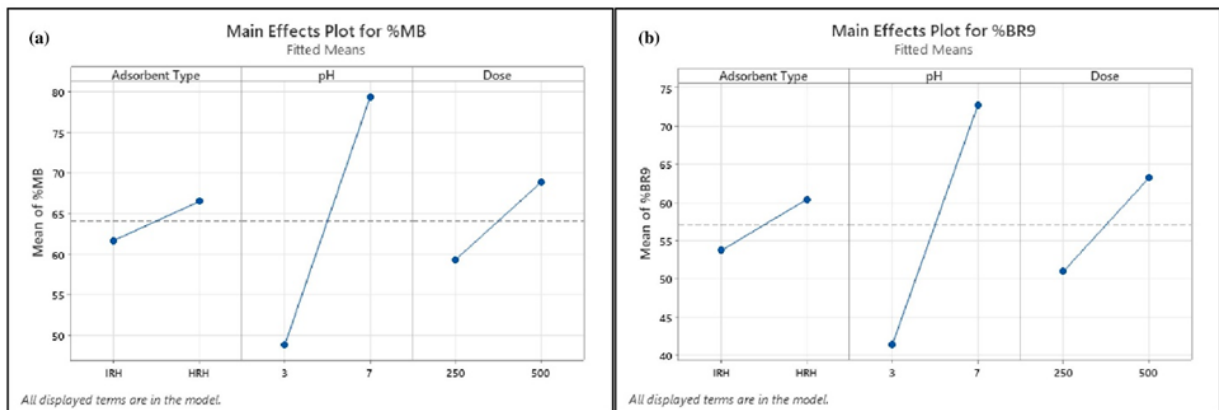


Figure 28. Main effect plots of dye removal for (a) MB (%) and (b) BR9 (%) during binary adsorption

Main effect plots reveal which factors exhibit the greatest impact on the response (i.e., removal efficiency) (Figure 28a,b). Each factor level affects response differently. The impact on the response is small when the slope is close to zero [255]. Thus, pH displayed the strongest positive influence on removal efficiency, followed by adsorbent dose.

Pareto charts (Figure 29a,b) were explored to illustrate information obtained from normal plots (Figure 30). Values to the right of the reference line (2.1 for %MB and 2.12 for %BR9) were significant. The vertical line indicates the minimum effect degree for a 95% confidence level [256]. Main factors (adsorbent type, pH, and dose) for both dyes and their interactions were significant. However, three-way interactions and adsorbent type*dose in BR9 (Figure 29b) were insignificant.

We considered normal plots to assess each factor and interaction (Figure 30a,b). Normal plots are employed to discriminate real effects from chance results. Each factor is defined as a point on the normal plots. A point located farthest from the line indicates the highest impact [253], [255]. Normal plots could be divided into two areas: factors in the area above a standardized impact of 50% demonstrate positive effects and vice versa [251].

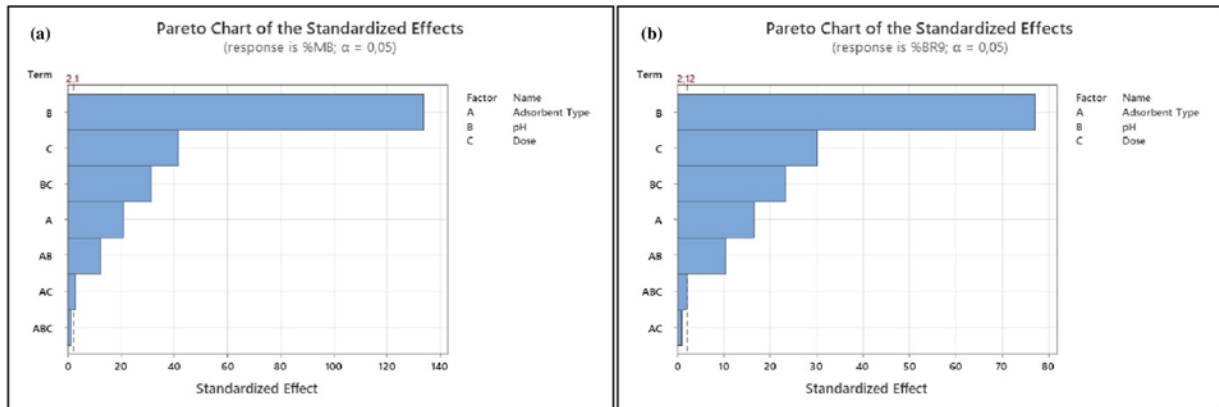


Figure 29. Pareto charts of dye removal for (a) MB (%) and (b) BR9 (%) during binary adsorption

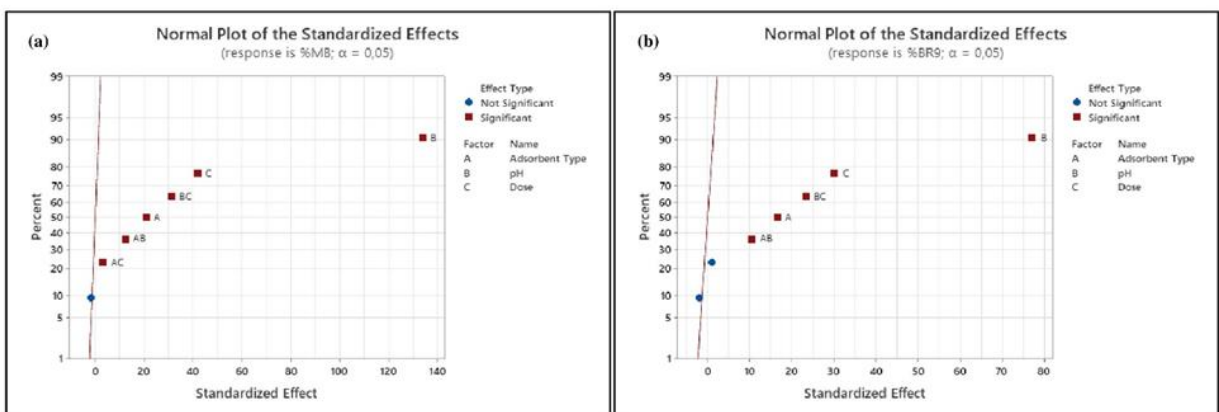


Figure 30. Normal plots of dye removal for (a) MB (%) and (b) BR9 (%) during binary adsorption

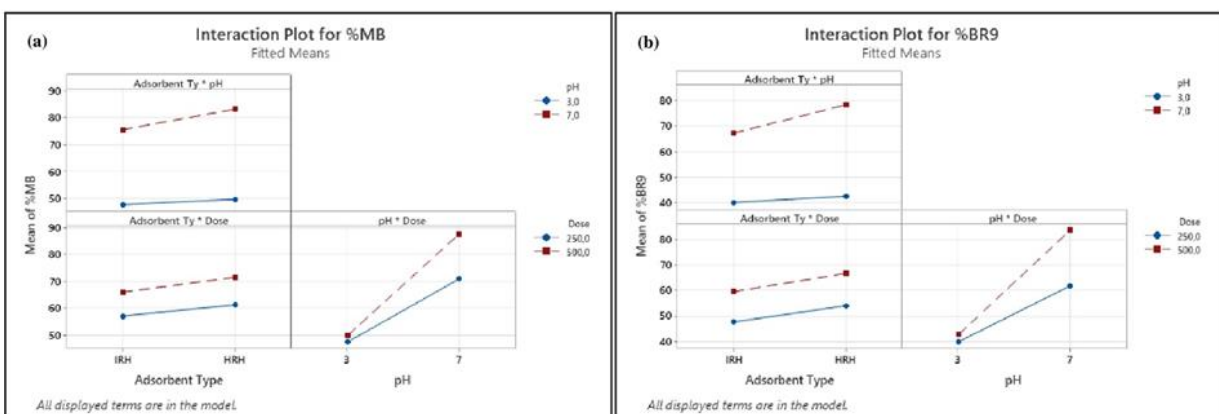


Figure 31. Interaction plots of dye removal for (a) MB (%) and (b) BR9 (%) during binary adsorption

Main factors (adsorbent type, pH, and dose) display positive values and are far from the red line (Figure 30a,b). Interactions between main factors show a similar result. However, interactions between adsorbent type*pH*dose for both dyes and adsorbent type*dose in BR9

present negative and insignificant impacts. Normal probability plots are consistent with Pareto charts (Figure 29).

Interaction plots for pH*dose, adsorbent type*dose, and adsorbent type*pH interactions were also considered (Figure 31a,b). When plot lines are not parallel, interactions between control factors are strong and vice versa [233]. Important interactions were observed between pH and dose for MB and BR9. Further, the interaction of adsorbent type and pH is less crucial, and the interaction between adsorbent type and dose can be characterized as minimal.

5.4 Adsorption of methylene blue using rice husk from model wastewater

5.4.1 Effect of pH

The pH of a solution is a crucial factor that affects adsorption efficiency, the surface properties of the adsorbent, and the ionization and structure of the adsorbate [257]. Figure 32 displays the percentages of MB removal at pH 4 to 12. HRH and IRH had a maximum MB removal of 92% and 88%, respectively, at pH 12. The zeta potentials of HRH and IRH at pH 12 support this result. These findings are consistent with the results of Sukmana et al. [258], which investigated the removal of MB under alkaline conditions. Our findings indicate that MB removal increases under alkali, but decreases under acidic conditions.

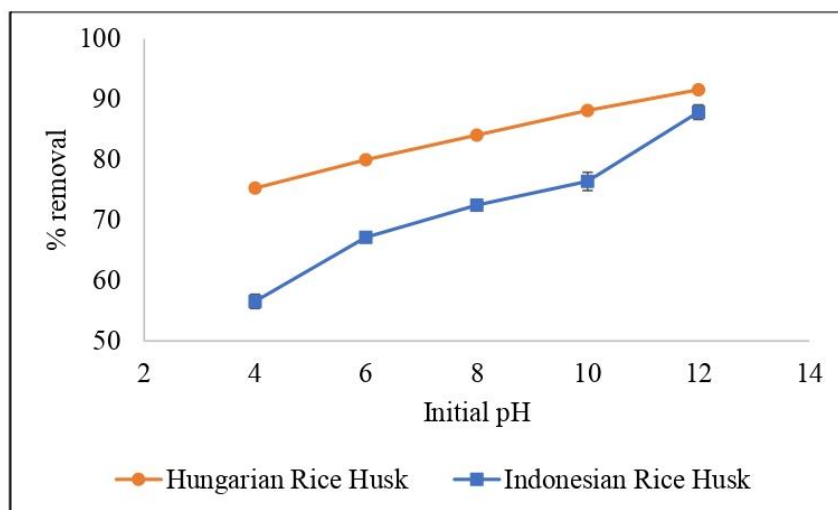


Figure 32. Effect of pH on MB removal by rice husks of different origin (adsorbent dose: 600 mg, initial concentration of dyes: 60 mg/L, temperature: 25 °C, time: 60 min)

This phenomenon occurs due to the deprotonation and protonation of the functional groups on the surface of the RH and MB. With decreasing pH, the concentration of hydrogen ions (H^+ or protons) in the solution rises, increasing the protonation of the functional groups on the RH surface. The presence of hydrogen ions in the solution competed with MB in the adsorption

process. Nevertheless, elevating the pH towards alkaline conditions decreases the concentration of hydrogen ions near the surface. Therefore, an increase in the deprotonation of functional groups located on the RH surface influences the charge density and increases the Coulomb interaction between the positive charge of the dye molecules and the negative charge of the adsorbent [166], [167], [259].

5.4.2 Effect of initial concentration

This study examined the impact of different initial dye concentrations (ranging from 60 to 300 mg/L) on the removal of MB using IRH and HRH, and the results are illustrated in Figure 33. The findings indicate that a higher initial concentration of MB decreases the efficiency of its removal. However, the adsorption of MB increases due to the increased driving force in the adsorption process. Additionally, as the number of available active sites decreases, the surface of the adsorbent becomes saturated. Thus, the mass transfer of dyes from the solutions to the RH surface decreases, decreasing the degree of adsorption [117], [168], [169], [260], [261].

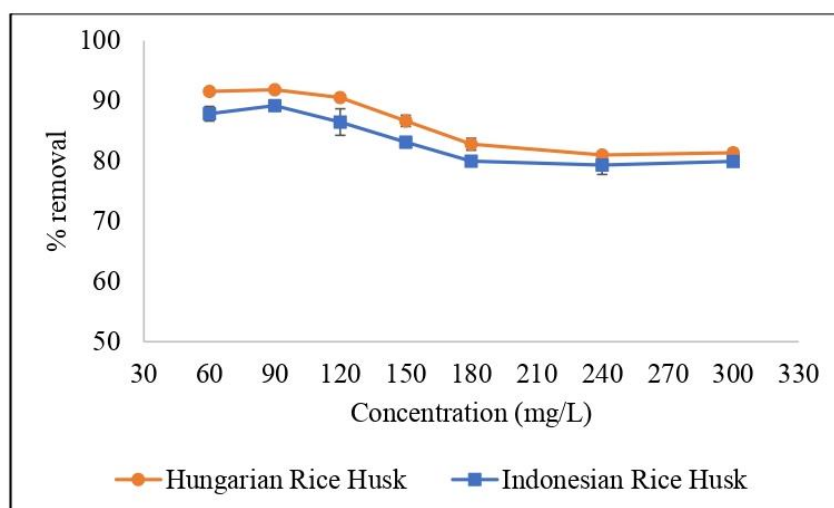


Figure 33. Effect of initial concentration on MB removal by rice husks of different origins (pH: 12, adsorbent dose: 600 mg, temperature: 25 °C, time: 60 min)

5.4.3 Effect of adsorbent dose

The impact of varying adsorbent doses (ranging from 200 to 1000 mg) on adsorption was investigated, using 250 mL of MB-containing wastewater. The adsorbate–adsorbent equilibrium is significantly influenced by the quantity of adsorbent used during adsorption [262]. At a dose of 600 mg, the highest removal percentages for HRH and IRH were 92% and 88%, respectively. The effects of the doses of the two adsorbents are shown in Figure 34. Increasing the quantity of adsorbent from 200 mg to 600 mg enhances the removal percentage.

However, when the adsorbent dose was increased from 800 mg to 1000 mg, the removal percentage decreased slightly due to the saturation of the surface by MB molecules. Therefore, the number of unbound MB molecules in the solution was higher, even after applying a bigger adsorbent dose [263]. Increasing the adsorbent dose results in higher MB removal percentages due to the increased surface area and active sites [264], [265]. Consequently, this results in more accessible active sites, favoring adsorption. Hence, an adsorbent dose of 600 mg was selected as the optimal dose for subsequent investigations.

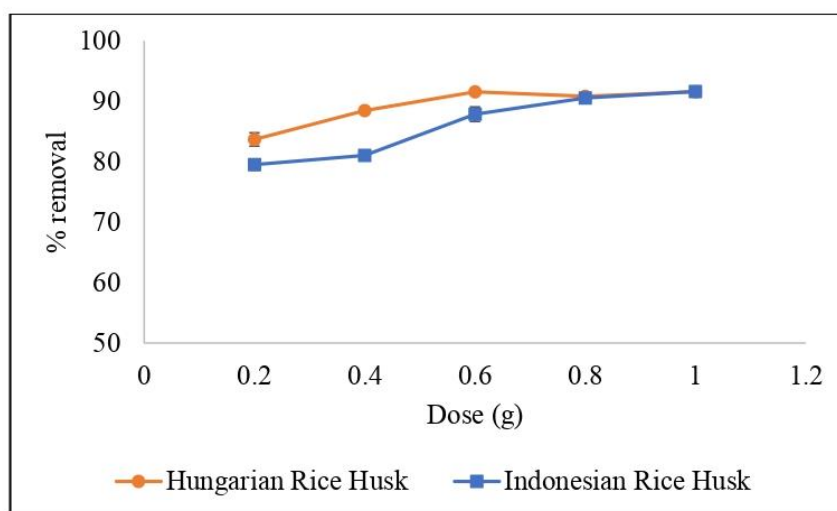


Figure 34. Effect of adsorbent dose on MB removal by rice husks of different origins (pH: 12, initial concentration of dyes: 60 mg/L, temperature: 25 °C, time: 60 min)

5.4.4 Effect of particle size

Adsorption capacity is significantly influenced by the size of adsorbent particles, and there is a direct relationship between adsorbent particle size and the diffusion of adsorbates into pores [194]. Hence, we investigated the influence of particle size (ranging from 0.25 to 2 mm) on the adsorption process. Figure 35 demonstrates that the removal percentages of MB declined from 92% to 64% for HRH and from 88% to 61% for IRH as the particle sizes increased from 0.25 to 2 mm. With an increase in particle size, diffusion became restricted, resulting in inadequate access of dye molecules to the internal surface of the adsorbent [266]. Simultaneously, as the particle size reduced, the specific surface area of the particles increased. Consequently, the adsorbent particles possessed a greater number of active sites available for MB molecules, resulting in larger removal percentages [267], [268], [269].

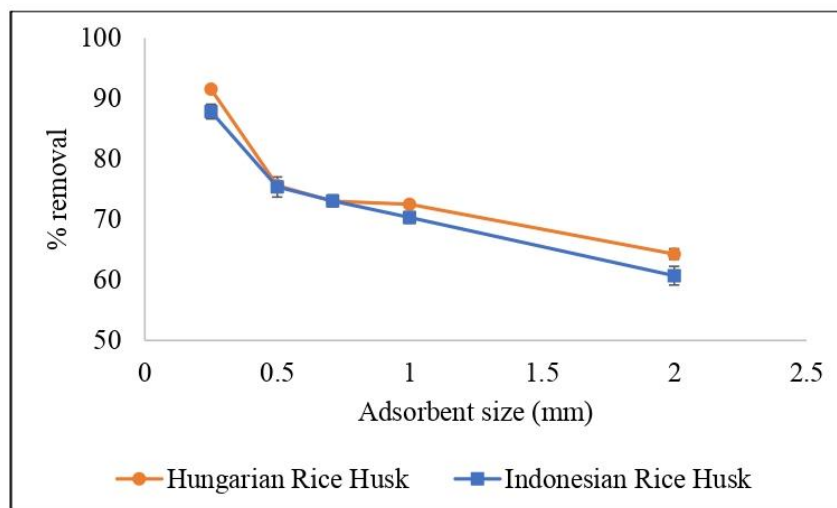


Figure 35. Effect of particle size on MB removal by rice husks of different origins (pH: 12, adsorbent dose: 600 mg, initial concentration of dyes: 60 mg/L, temperature: 25 °C, time: 60 min)

5.4.5 Effect of contact time and comparison with hydrochar

To understand the equilibrium time and reactions between the adsorbents and adsorbates, it is crucial to investigate the effect of contact time on the adsorption process (Shrinath Bhat). For this purpose, the adsorption process was carried out for 60 min and samples were collected every 5 min. Figure 36a,b demonstrates the impact of contact time on the removal percentages for both the raw and hydrochar adsorbents. Adsorption processes comprise an initial, an intermediate, and an equilibrium phase [172], [173]. An adsorption process begins in the initial phase, characterized by rapid kinetics and significant removal efficiency. HRH and IRH hydrochar removal percentages were 88% and 93% within 5 min, respectively. Similarly, IRH and HRH hydrochar removal percentages are 76% and 89%, respectively.

During the intermediate phase, as the contact time increases, both the number of adsorption sites and the driving force of the concentration gradient reduce, decreasing the percentage and rate of adsorption [270]. For our samples, after 60 min, the removal percentages stabilized, reaching a constant value during the equilibrium phase. At this point, the MB removal percentage for HRH, HRH hydrochar, IRH, and IRH hydrochar were 92%, 94%, 88%, and 92%, respectively. MB adsorption onto hydrochar surfaces is attributed to a combination of interactions, including electrostatic attractions, π - π stacking, hydrogen bonding, and van der Waals forces [271]. The removal percentage for hydrochar RH was slightly greater than that for raw RH; however, the difference was insignificant. Consequently, raw RH is cheaper and more effective for MB removal from wastewater than RH hydrochar.

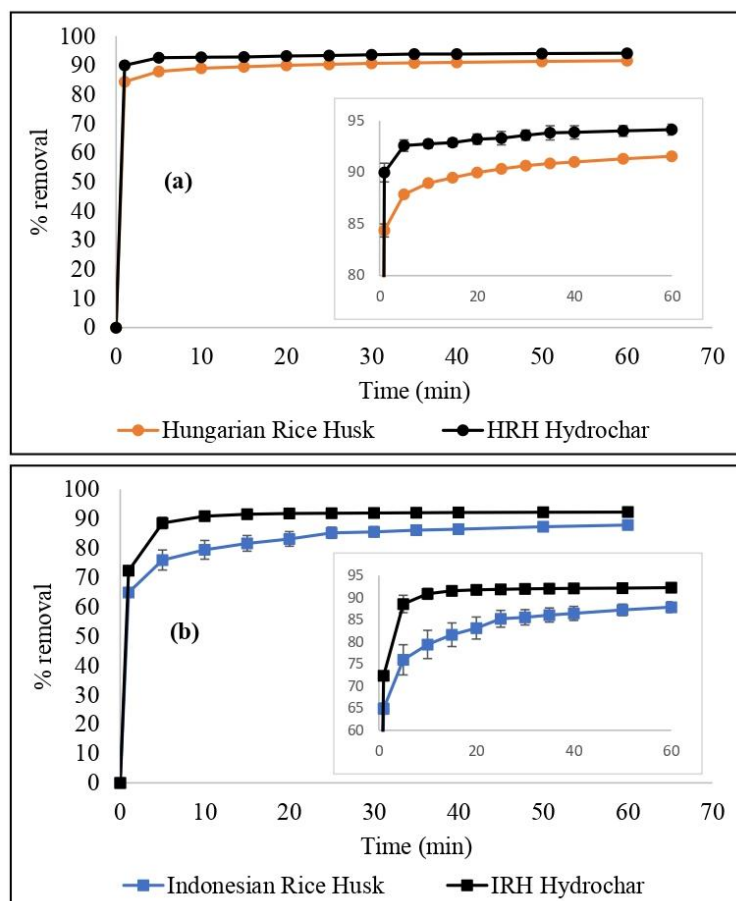


Figure 36. Effect of contact time on MB removal by (a) HRH and HRH hydrochar, (b) IRH and IRH hydrochar (pH: 12, adsorbent dose: 600 mg, initial concentration of dyes: 60 mg/L, temperature: 25 °C)

5.4.6 Adsorption isotherm modelling in model wastewater

Adsorption isotherms quantify the correlation between the quantity of adsorbate absorbed by the adsorbent (q_e) and the equilibrium concentration of adsorbate (C_e) at constant temperature. The adsorption capacity of RH for MB was examined by batch adsorption experiments. Different initial concentrations and constant doses of RH were used at a room temperature. The adsorption equilibrium of MB was investigated using multilayer isotherm models such as the HJ, AD, and BET models. The experimental data and isotherm models were compared, as shown in Figure 37a,b.

The isotherm model exhibited a sigmoidal form (S-shape) with a pronounced rise in the adsorbed quantity beyond a particular dye concentration in the liquid phase. This phenomenon can be attributed to dye aggregation at higher concentrations, resulting in several molecules attaching to each adsorption site instead of a single molecule. Thus, the amount of dye adsorbed increases after a specific initial dye concentration in the liquid phase [229]. This result strongly supports the idea of multilayer adsorption due to self-aggregation, which is the primary

consideration in the BET multilayer isotherm model. Depending on the concentration, organic dyes in aqueous solutions often self-aggregate, known as dimers, trimers, and higher-order aggregates [180].

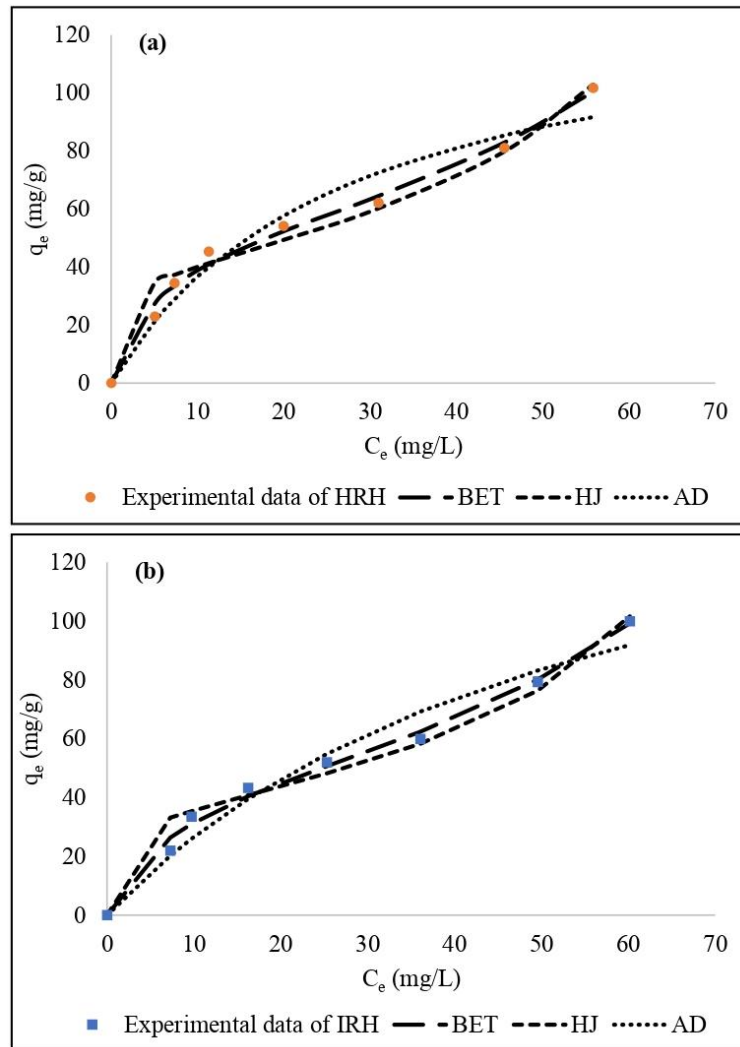


Figure 37. Comparison of experimental data and nonlinear isotherm models for (a) Hungarian rice husk and (b) Indonesian rice husk

The self-aggregation of MB dyes in aqueous solutions has been investigated in some previous studies [181], [183], [184], [185]. According to Sukmana et al. [258], the concentration of MB at 2.8×10^{-5} M (~ 9 mg/L) tends to increase indefinitely due to noticeable aggregation in both the aqueous solution and the surface. Furthermore, in our current study, the concentration of MB undergoes self-aggregation starting at 6.2×10^{-5} M (~ 20 mg/L) for HRH and 7.8×10^{-5} M (~ 25 mg/L) for IRH. Our result is in good accordance with the findings of Karimi Goftar et al. [182], who reported that the concentration range at which a monomer-dimer can exist is between 10^{-3} – 10^{-6} M.

Based on the examination of the multilayer isotherm models, it was noted that monolayer adsorption occurred at concentrations up to 20 and 25 mg/L for HRH and IRH, respectively. In turn, multilayer adsorption occurred at concentrations above 20 and 25 mg/L, due to the aggregation of dye molecules.

Table 22. The multilayer isotherm model parameters for the adsorption of MB

Model	Parameter	Adsorbents	
		Hungarian Rice Husk	Indonesian Rice Husk
Harkins–Jura (HJ)	A	37.60	33.57
	B	1.88	1.89
	R ²	0.47	0.42
	χ ²	0.96	0.97
Aranovich–Donohue (AD)	Q _m (mg/g)	136.87	179.85
	K ₁	0.04	0.02
	K ₂	0.0001	0.003
	n ²	0.0001	0.0001
	R ²	0.94	0.95
	χ ²	0.76	0.64
Brunauer–Emmett–Teller (BET)	Q _m (mg/g)	52.23	47.92
	K _L	0.009	0.009
	K _S	0.19	0.14
	R ²	0.99	0.99
	χ ²	0.14	0.11

The parameters of the HJ, AD, and BET multilayer models, acquired by a nonlinear fitting approach, are presented in Table 21. Based on the correlation coefficient (R²) and nonlinear Chi-square (χ²) values presented in Table 21, it can be concluded that the BET multilayer adsorption isotherm is the most suitable model for fitting the experimental adsorption data. The HJ Equation [187], calculates the isotherm parameter by Equation 8. The HJ adsorption isotherm characterizes heterogeneous pore distribution and the adsorption of multilayer molecules [188].

Aranovich and Donohue [226] have proposed an effective empirical approach for fitting multilayer adsorption isotherms. Their model, designed for adsorption in the liquid phase, is expressed as Equation 20:

$$q_e = \left(\frac{Q_m K_1 C_e}{1 + K_1 C_e} \right) \left(\frac{1}{(1 - K_2 C_e)^{n_2}} \right) \quad (20)$$

where Q_m is the monolayer adsorption capacity, K_1 and K_2 are the Aranovich–Donohue equilibrium constants, and n_2 is the modified form of the second term on the right side of the BET Equation.

The BET multilayer isotherm is a theoretical model frequently employed in gas–solid equilibrium systems [101], [189]. The conventional BET Equation can be adapted for adsorption in the liquid phase and involves three independent variables (Q_m , K_s , K_L) [190]. The BET Equation for adsorption in the liquid phase, as proposed by Ebadi et al. [190], can be calculated by Equation 9.

According to the BET multilayer isotherm model, the maximum adsorption capacity has no limit, and there is a potential to approach infinite [190]. The isotherm modeling carried out in this study shows similarity to our prior findings regarding RH usage for MB removal, as reported by Sukmana et al. [258].

The adsorption isotherm experiment shows that the isotherm model refers to multilayer adsorption because the curve reaches saturation indicating the completion of the first monolayer, which continues with the formation of another layer [272]. Therefore, the Langmuir and Freundlich isotherm models were fitted to the experimental data to investigate the adsorption mechanism where monolayer adsorption occurred. The estimated parameter values of the models are presented in Table 22, while the simulations can be observed in Figure 38a,b.

The result is shown in Table 22; the Langmuir isotherm fits the experimental adsorption data the best. The adsorption of MB using HRH and IRH had a higher R^2 of >0.96 . The Langmuir isotherm model indicates that adsorption occurs on a homogeneous surface. In this process, adsorbed molecules create a saturated layer on the adsorbent, so monolayer adsorption and maximum adsorption occur. Meanwhile, the Freundlich isotherm describes adsorption that occurs on a heterogeneous surface [103], [104].

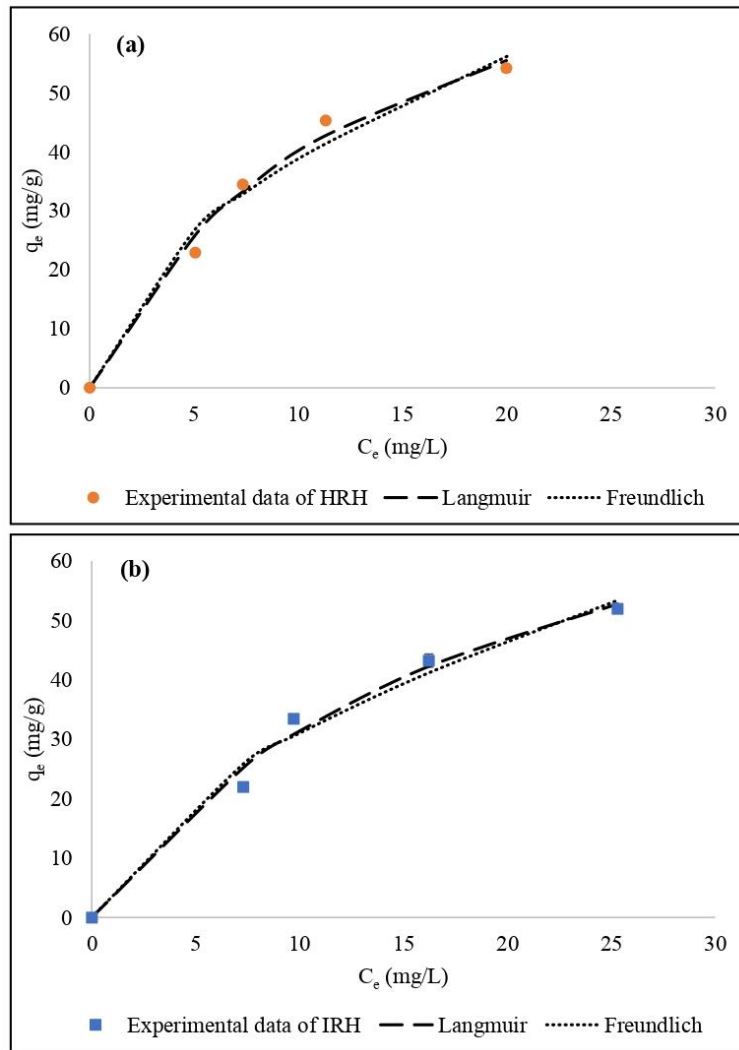


Figure 38. Simulation of the Langmuir and Freundlich isotherm models for monolayer adsorption using (a) Hungarian rice husk and (b) Indonesian rice husk

Table 23. Monolayer isotherm model parameters for the adsorption of MB

Model	Parameter	Adsorbents	
		Hungarian Rice Husk	Indonesian Rice Husk
Langmuir	Q_{\max} (mg/g)	90.66	94.80
	K_L	0.08	0.05
	R_L	0.17	0.25
	R^2	0.97	0.96
	χ^2	0.12	0.12
Freundlich	n	1.86	1.71
	K_F	11.26	8.10
	R^2	0.93	0.94
	χ^2	0.24	0.20

To determine the isotherm parameter, Equation 12 presents the Langmuir Equation in nonlinear form [273]. Table 22 shows that the low K_L value for MB adsorption showed a low affinity of MB molecules to the RH adsorbent [66]. The dimensionless constant separation factor (R_L) is represented by Equation 21:

$$R_L = \frac{1}{1 + K_L C_i} \quad (21)$$

where C_i is the initial concentration of dyes, and K_L is the Langmuir isotherm constant. The parameter states isotherm to be irreversible ($R_L = 0$), favorable ($0 < R_L < 1$), linear ($R_L = 1$), and unfavorable ($R_L > 1$) [274]. Table 22 shows that the R_L values for all adsorptions are < 1 , indicating the favorable adsorption process.

The Freundlich isotherm in nonlinear form [275] can be expressed by Equation 22:

$$q_e = K_f C_e^n \quad (22)$$

where K_f is the Freundlich isotherm constant, an approximate indicator of adsorption capacity, while n is the adsorption intensity/heterogeneity parameter indicating the extent of the adsorption driving force or surface heterogeneity [276]. Table 22 displays the n values for all adsorption processes, all of which were > 1 . This indicates favorable adsorption since the values fall within the range of $1 < n < 10$ [277]. By comparing the R^2 values presented in Table 22, it is evident that the adsorption process is more accurately described by the Langmuir isotherm model rather than the Freundlich model.

5.4.7 Adsorption kinetic modelling in model wastewater

Kinetic models are employed to mathematically elucidate the adsorption mechanism of molecules as they traverse the bulk solution toward the adsorbent surface [278]. Figure 39a,b displays the experimental data and adsorption kinetic models by plotting time (min) as a function of q_e (mg/g). The q_e experimental measurements closely correspond to the estimated q_e data obtained from the Elovich kinetic model.

According to the correlation coefficient (R^2) and the nonlinear chi-square (χ^2) values presented in Table 23, it can be concluded that all the experimental data agree with the Elovich kinetic model. Hence, chemisorption governs the MB adsorption processes [279]. The kinetic modeling used in this work showed relevance to our prior findings as reported by Sukmana et al. [280], which was also used to describe MB elimination via binary adsorption.

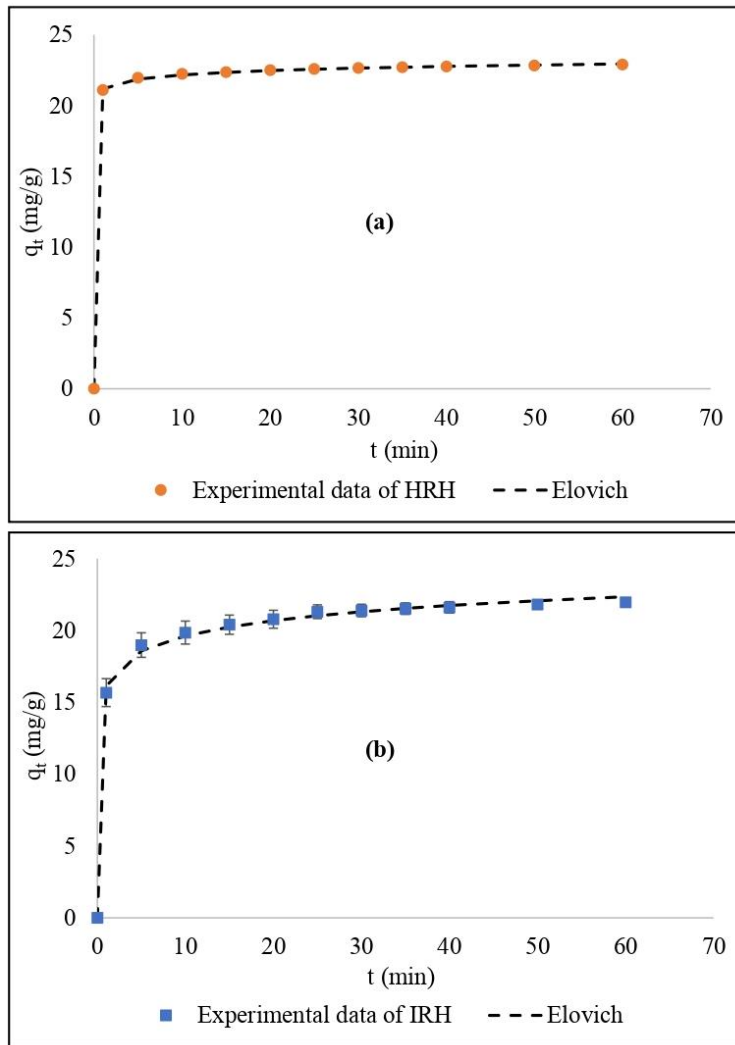


Figure 39. Comparison of the experimental data and the Elovich model for (a) Hungarian rice husk and (b) Indonesian rice husk

The adsorption kinetics of MB were examined by using the pseudo-first-order (PFO), pseudo-second-order (PSO), and Elovich models. The PFO kinetic model explains that reaction rate depends on the number of vacant adsorption sites (Hülya Koyuncu). The nonlinear PFO [206] form is expressed by Equation 10. The PFO model is typically the most suitable when the number of active sites is not a limiting factor [281].

The PSO kinetic model considers that adsorption is influenced by the characteristics of the adsorbent and the solute molecules [282]. The nonlinear PSO [207] form is represented by Equation 11. The PSO reaction rate k_2 for HRH adsorbent (0.55 g/mg/h) is greater than the PSO reaction rate k_2 for IRH adsorbent (0.11 g/mg/h). The result indicates the formation of covalent bonds between the MB molecules and the RH surface [258]. The PSO kinetic model

demonstrates superior fitting at relatively low initial concentrations and undergoes high variations throughout adsorption [213].

Table 24. The kinetic parameters for the adsorption of MB

Model	Parameter	Adsorbents	
		Hungarian Rice Husk	Indonesian Rice Husk
Pseudo first order	q_e (mg/g)	22.55	20.97
	k_1	2.74	1.37
	R^2	0.72	0.89
	$\chi^2(10^{-4})$	30	362
Pseudo second order	q_e (mg/g)	22.67	21.50
	k_2	0.55	0.11
	R^2	0.87	0.96
	$\chi^2(10^{-4})$	15	124
Elovich	α	1.03.E+21	6.45.E+04
	β	2.32	0.66
	R^2	0.99	0.99
	$\chi^2(10^{-4})$	1	35

The Elovich model considers heterogeneous adsorbent surfaces, assuming that adsorption occurs through chemical interactions [283]. The nonlinear Elovich [236] form can be expressed by the Equation 16. The values of α were much greater than those of β . The findings suggest that the adsorption rate of MB is greater than its desorption rate [284].

In our case, the PFO and PSO models were inadequate in explaining the diffusion mechanism involved in the adsorption of MB. Thus, the intraparticle model was utilized to identify the factor limiting the adsorption of MB onto the RHs. The intraparticle diffusion model considers that adsorption is influenced by the rate at which adsorbate molecules move from the solution to the surface of the adsorbent. This movement is governed by various steps, such as film or external diffusion, pore diffusion, and surface diffusion [285]. The intraparticle diffusion model [242] form can be expressed by Equation 17.

The linearized intraparticle diffusion kinetic model was utilized to represent the relationship between q_t and $t^{1/2}$ (Figure 40). If the line of best fit passes through the origin (0, 0), it signifies that intraparticle diffusion is the sole governing factor in the adsorption process. Nevertheless, the regression lines did not intersect with the origin (0, 0), and intraparticle diffusion was not

the sole rate-controlling step in the adsorption process. Therefore, this observation suggests that adsorption occurred in three distinct phases [286].

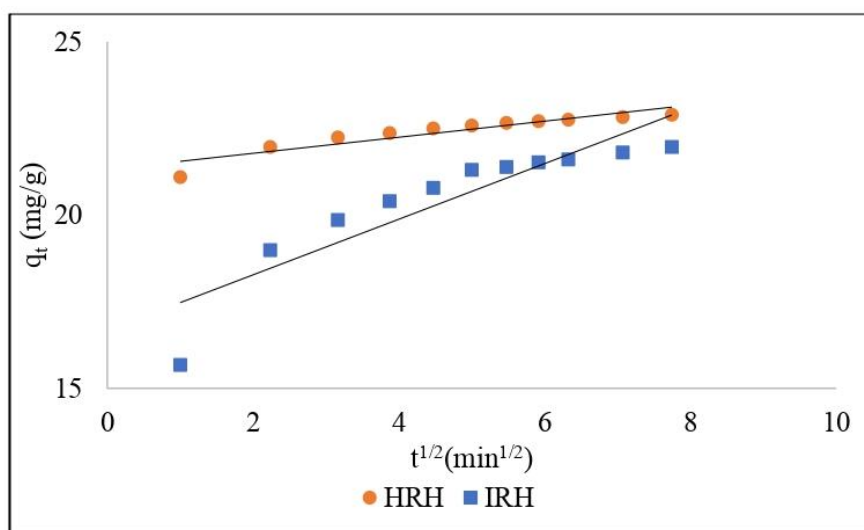


Figure 40. Intraparticle diffusion model

The initial phase involves the movement of molecules from the surrounding solution to the external surface of the solid (known as film diffusion) [286]. Subsequently, during the second phase, the dye particles present on the external surface were transferred and adsorbed onto the pores of the adsorbent through intraparticle diffusion [287]. The adsorption intensity varied between values typical of monolayer and multilayer adsorption at this stage. The adsorption intensity was greater for adsorption monolayer due to the facile adsorption of MB onto the surface of the RHs [244]. This statement can be verified by analyzing the BET isotherm model, which showed a greater value for the first layer constant (K_S) in comparison to the constants of the subsequent layers (K_L). The third step signifies the equilibrium phase. The C value (Table 24) for MB adsorption indicates that the intraparticle diffusion mechanism is not the sole limiting factor in the overall adsorption process [288].

Table 25. Intraparticle diffusion parameters for MB adsorption on RHs

Model	Parameter	Adsorbents	
		Hungarian Rice Husk	Indonesian Rice Husk
Intraparticle diffusion	k_{id}	0.23	0.80
	C	21.32	16.67

5.5 Desorption and regeneration of rice husk

Regeneration of adsorbents is essential to ensure the economic viability and scalability of the adsorption process [219]. It is a requirement for the environmentally friendly utilization of adsorbents. For a successful regeneration, it is crucial to choose appropriate eluents. The selection of eluents depends on the specific mechanism and type of dye removal [231]. After we investigated the applicability of HCl and NaOH as regenerating solutions, we found that the 1.0 M HCl solution produced the best result for the desorption of MB, as shown in Figure 41.

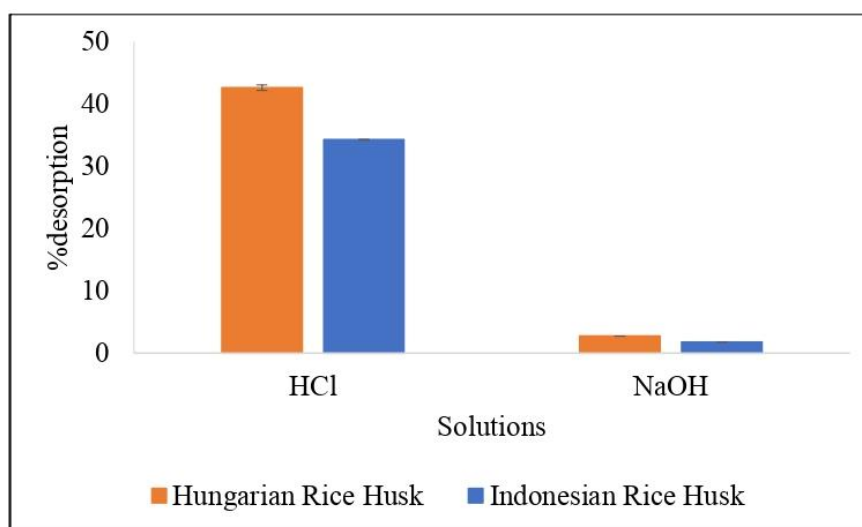


Figure 41. Desorption of RH with HCl and NaOH solutions

Since MB adsorption is favored at alkaline pH ranges, desorption is favored at acidic pH ranges. The ionization constant of HCl is greater than that of NaOH, increasing the number of positive charges on the surface of the adsorbent in an acidic environment. This ultimately enhances the desorption of MB. The desorption of MB can be attributed to the electrostatic repulsion between MB molecules and the surface of the RHs. Cationic dye molecules exhibit an affinity for the negative charge present on the surface of the adsorbent [289].

After carrying out four adsorption–desorption cycles (Figure 42), we found that the adsorption and desorption efficiencies of MB by HRH and IRH decreased from 92% to 87% and from 88% to 83%, respectively. These decreases can be attributed to the gradual buildup of MB molecules on the surface of the adsorbent. These molecules cannot be eliminated during the desorption process, leading to reduced adsorption capacity in subsequent experiments [290] from 22.9 mg/g to 21.7 mg/g (HRH) and from 22 mg/g to 20.8 mg/g (Figure 43). Moreover, the RHs were effectively recycled for four consecutive adsorption/desorption cycles,

demonstrating their exceptional reusability. Thus, it has been demonstrated that RH is both environmentally friendly and cost-effective as an adsorbent.

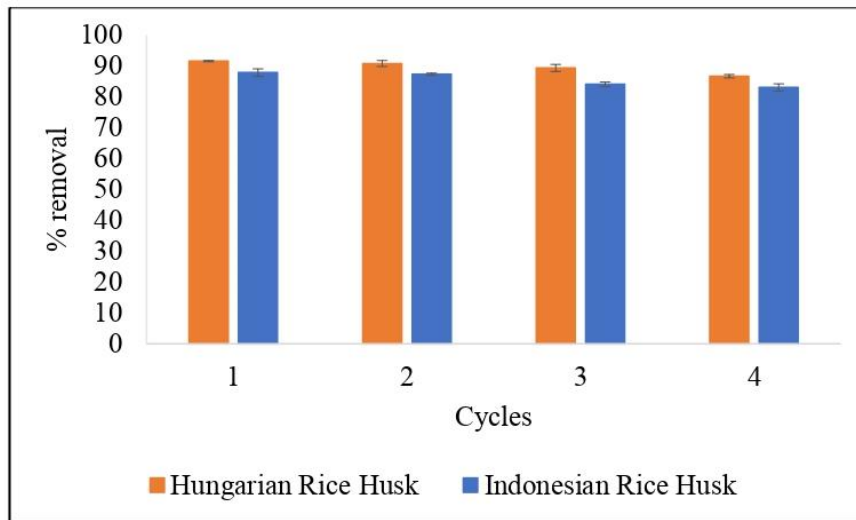


Figure 42. Regeneration of RH adsorbent

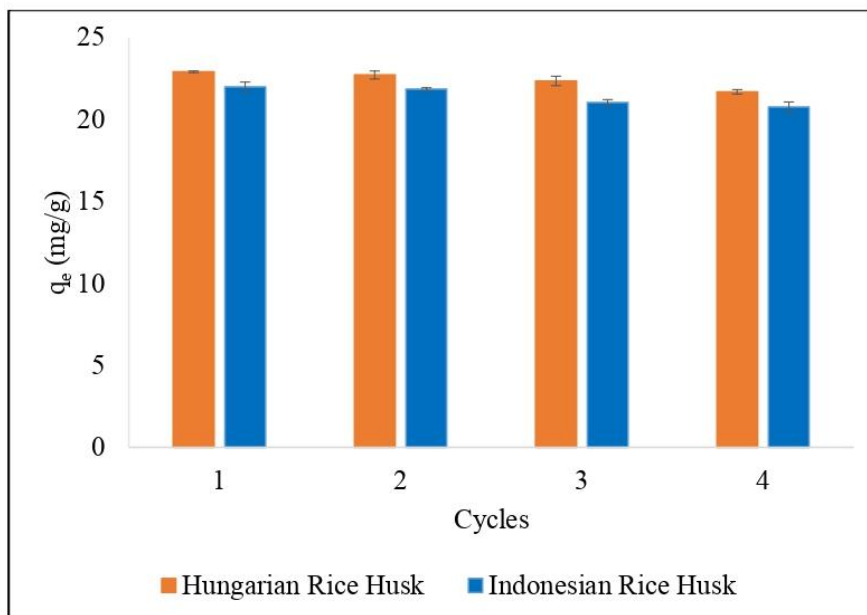


Figure 43. Adsorption capacity of RH adsorbent

The raw material costs for HRH and IRH are approximately 0.032 and 0.393 USD/kg, respectively. The price differential between HRH and IRH is primarily attributable to technological and human resource allocation. Typically, IRH is cultivated by local farmers employing conventional agricultural methods. Given rice's pivotal role as a staple food for the majority of Indonesians and resulting in heightened demand. Therefore, prompting government intervention to regulate dry grain prices and stabilize local markets. Conversely, HRH is

sourced from a Hungarian company and uses modern rice milling techniques tailored to the Hungarian market. Given rice's less prominent dietary role in Hungary, pricing remains comparatively moderate. Thus, the observed price variance underscores the influence of technology adoption, agricultural practices, and socio-economic contexts on global food commodity markets. The adsorption and desorption of MB were compared also with different adsorbents, as presented in Table 25.

Table 26. Adsorption and desorption of MB for different adsorbents

No	Adsorbent	Desorbing solution	Cycles	References
1	Modified corn stalks	1 M HCl	4	[291]
2	<i>Salvinia minima</i> biomass	0.1 M HCl	3	[292]
3	Carbonized mandarin peel	1 M HCl	3	[293]
4	<i>Ipomoea carnea</i> wood	0.1 M HCl	5	[294]
5	<i>Dialium guineense</i> fruit shells	1 M HCl	5	[295]
6	Hungarian Rice Husk	1 M HCl	4	This study
7	Indonesian Rice Husk	1 M HCl	4	This study

5.6 Reusing dye for cotton fabrics

After desorption, the MB was recovered, and the solutions were used for dyeing cotton fabrics. After four cycles, the recovered MB was still capable of dyeing the cotton fabrics, as shown in Figure 43a,b. The CIE L*a*b* coordinates were used to quantitatively measure the dyeing efficiency. The CIE L*a*b* coordinates are commonly employed to quantify color differences (Δ values) between samples [146].

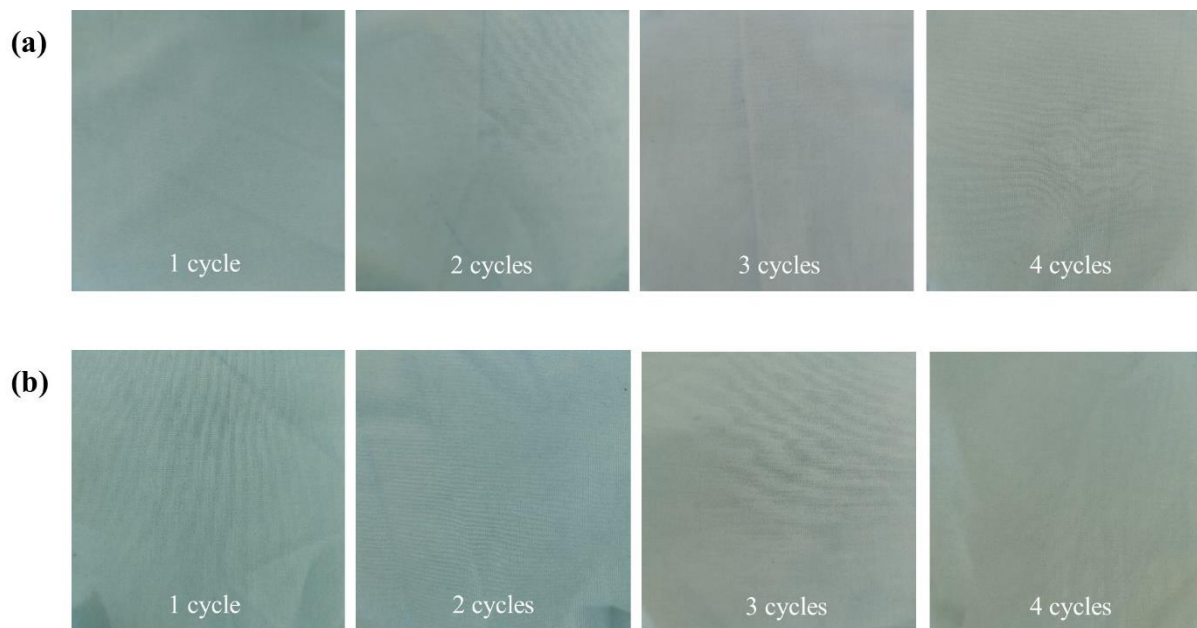


Figure 44. Cotton fabrics dyed with MB after its desorption from (a) HRH, and (b) IRH adsorbents

Accordingly, the ΔL^* , Δa^* , and Δb^* coordinates [146] were obtained using Equations 23–25.

$$\Delta L^* = \Delta L^*_{reference} - \Delta L^*_{sample} \quad (23)$$

$$\Delta a^* = \Delta a^*_{reference} - \Delta a^*_{sample} \quad (24)$$

$$\Delta b^* = \Delta b^*_{reference} - \Delta b^*_{sample} \quad (25)$$

The L^* coordinate represents the brightness level, with a scale from 0 to 100. Higher values indicate lighter shades, while lower values indicate darker shades. The a^* coordinate represents the degree of redness or greenness, where positive values indicate redness and negative values indicate greenness. Similarly, the b^* coordinate represents yellowness or blueness, with positive values indicating the former and negative values indicating the latter [296]. The ΔE^* value represents the color difference between the reference and the cotton fabric sample in the three-dimensional CIE $L^*a^*b^*$ color space. The ΔE^* form [146] can be expressed by Equation 26.

$$\Delta E^* = \sqrt{\Delta L^{*2} + \Delta a^{*2} + \Delta b^{*2}} \quad (26)$$

The ΔE^* values can vary from 0 to 100. Within this interval, a zero value indicates no distinction between the two images. Whereas, a value of 100 signifies that the sample image completely contrasts the reference image in color [142]. Based on the results shown in Table 26, the acceptable tolerance for this investigation was considered $\Delta E^* < 5$. Based on the literature, the acceptable range for ΔE^* tolerance is between 2 and 6, beyond which differences are highly discernible [143].

Table 27. CIE $L^*a^*b^*$ value between cotton fabric from HRH and IRH recycling

No	Adsorbent	L^*	a^*	b^*	ΔL^*	Δa^*	Δb^*	ΔE^*
1	HRH 1 cycle (standard)	84.38	-10.58	-18.52	-	-	-	-
2	HRH 2 cycles	83.48	-11.07	-19.14	-0.90	-0.49	-0.62	0.71
3	HRH 3 cycles	81.44	-11.08	-19.44	-2.94	-0.50	-0.91	4.86
4	HRH 4 cycles	83.19	-10.57	-19.03	-1.19	0.00	-0.50	0.83
5	IRH 1 cycle (standard)	82.65	-12.90	-19.93	-	-	-	-
6	IRH 2 cycles	81.44	-11.73	-20.45	-1.21	1.17	-0.52	1.54
7	IRH 3 cycles	80.07	-11.59	-18.99	-2.58	1.31	0.94	4.62
8	IRH 4 cycles	83.60	-11.46	-18.69	0.95	1.44	1.24	2.26

6 Conclusion

The present study explores a novel approach to addressing environmental challenges by focusing on the adsorption and recovery of dyes from rice husk (RH). This investigation aims to contribute to mitigating dye-related pollutants, water reuse, and sustainable dyeing practices. Specifically, this Ph.D. thesis systematically examines the utilization of RH as a bioadsorbent for removing and recovering dyes from aqueous solutions.

The study used raw Indonesian rice husk (IRH) and Hungarian rice husk (HRH) as bioadsorbents to remove MB and BR9 from aqueous solutions. Findings showed that pH, adsorbent dose, initial dye concentration, and contact time significantly affected adsorption, but temperature did not. The MB removal percentage of IRH and HRH at pH 10 was 96%, while BR9 removal percentages at pH 7 were 82% and 87%, respectively. The optimal adsorbent dose for adsorbing MB and BR9 using IRH and HRH from a 250 mL aqueous solution was 500 mg. The isotherm data agreed with the BET multilayer adsorption isotherm model. The kinetic data indicated that MB and BR9 adsorption follow the pseudo-second order kinetic model. IRH and HRH exhibited different MB and BR9 adsorption capacities because of their different chemical compositions. Moreover, the chemical composition of RH depended on the RH location, farm climate, and crop technology, among others.

Removal of MB and BR9 in binary adsorption was investigated also. Maximum removal percentages for MB and BR9 using HRH were 91.7% and 88.8%, respectively, and 83.8% and 78.2% using IRH, respectively. A BET multilayer isotherm best fit experimental data for binary adsorption. Binary adsorption of dyes followed the Elovich Equation based on kinetic data. A factorial design analysis indicated that interactions among adsorbent type*pH*dose for both dyes were insignificant. Interactions between main factors (adsorbent type, pH, and dose) were significant for MB and BR9, except for two-way interactions (adsorbent type*dose) for BR9.

This study examines the effectiveness of using raw RHs as bioadsorbents to remove MB from model wastewater. The impact of pH, adsorbent dose, initial dye concentration, particle size, and contact time on adsorption was investigated. The removal percentages of MB by HRH, IRH, HRH hydrochar, and IRH hydrochar at pH 12 were 92%, 88%, 94%, and 92%, respectively. MB removal was most effective at an adsorbent dose of 600 mg, achieved within a contact time of 60 minutes. In addition, the BET multilayer adsorption model characterized the isotherm data well, whereas the kinetic results were in good agreement with the Elovich model. Following the regeneration procedure, RH could be reused with only a 5% reduction in

adsorption percentages, even after four adsorption–desorption cycles. Reusing the desorbed MB for dyeing cotton fabrics demonstrated an acceptable ΔE^* tolerance range.

7 Summary

In this Ph.D. thesis, I have undertaken a comprehensive investigation into removing the dye from aqueous solutions, employing rice husk (RH) as the adsorbent material. Following this examination, emphasis was placed on the recovery of dyes through an exploration of the regeneration process of rice husk and its application in the coloring of cotton fabrics. The research endeavors encompassed a rigorous analysis of the adsorption isotherm and kinetics phenomena governing the interaction between dyes and RH, as well as an exploration of regeneration methodologies aimed at facilitating the reuse of RH for sustainable cotton fabric dyeing practices.

In the introduction, I have given an overview of the dye industry, which contributes to the global economy and poses significant environmental challenges due to its pollution footprint. I have emphasized that wastewater from dyeing processes contains harmful compounds that threaten both human health and aquatic ecosystems. Meanwhile, various wastewater treatment technologies exist, with adsorption emerging as a cost-effective and efficient dye removal and recovery method. Further, natural adsorbents, particularly agricultural waste like rice husk, show promise for sustainable dye removal. Therefore, Indonesia, a major rice producer, generates substantial rice husk waste, which could mitigate environmental pollution if repurposed as a bioadsorbent. Studies on utilizing rice husk for dye removal emphasize its effectiveness, especially against common cationic dyes like MB and BR9. However, research gaps exist regarding the influence of rice husk origin on adsorption capacity. To address these issues, studies are underway focusing on the principles of reduce-reuse-recycle, aiming for environmental sustainability through dye pollutant reduction, water and rice husk reuse, and dye recycling. Evaluation of adsorption-desorption cycles and sustainability considerations are crucial in assessing rice husk's viability as a bioadsorbent in a circular economy framework.

In the literature review, I have discussed dyes in detail, such as the categorization of dyes and the identification of hazardous dyes. Also, I have focused on MB and BR9. I have presented wastewater treatment, including an emphasis on adsorption as a method, an explanation of the adsorption mechanism, a discussion on adsorption modeling and an exploration of different adsorbents. I have discussed the utilization of rice husk and its modification as a bioadsorbent for dye removal. Further, the implementation of color evaluation is used to assess dye reuse for cotton fabrics.

According to the main aim of this Ph.D. research, I have started my experimental work by comparing the performance of Indonesian rice husk (IRH) and Hungarian rice husk (HRH) as bioadsorbents for removing MB and BR9 from aqueous solutions. Chemical content, zeta potential, and Fourier-transform infrared spectroscopy analyses were used to characterize the rice husks (RHs). Adsorption studies were performed through batch experiments involving several parameters, namely, pH, adsorbent dose, initial dye concentration, contact time, and temperature to observe the self-association (aggregation) of MB and BR9. Adsorption kinetic studies showed that maximum dye removal was achieved at a contact time of 120 min. MB and BR9 adsorption followed a pseudo-second order kinetic model, and the BET multilayer isotherm model provided a better fit to the experimental data of MB and BR9 adsorption. The IRH adsorption capacities were 15.0 mg/g for MB and 7.2 mg/g for BR9, whereas those of HRH were 24.4 mg/g for MB and 8.3 mg/g for BR9.

The adsorption of MB and BR9 using a simple solution could help elucidate the general aspects of the adsorption process. Binary solutions should be used in further studies to get a better understanding of the interaction between adsorbent and adsorbate. Therefore, I have investigated the removal of MB and BR9 dyes by Hungarian rice husk (HRH) and Indonesian rice husk (IRH) using binary adsorption from aqueous solutions. Adsorbents were characterized by zeta potential, Fourier-transform infrared spectroscopy, and scanning electron microscopy. Batch adsorption evaluated the influence of different variables, including pH, adsorbent dose, contact time, and initial concentrations. Several factors that influence the adsorption of MB and BR9 onto rice husk were assessed using main effect, Pareto charts, normal probability plots, and interaction effect in a factorial design. The optimum contact time was 60 min. Isotherm and kinetic models of MB and BR9 in binary adsorption fitted to the Brunauer–Emmett–Teller multilayer and the Elovich equation based on correlation coefficients and nonlinear chi-square. Results showed that the adsorption capacity of HRH was 10.4 mg/g for MB and 10 mg/g for BR9; values for IRH were 9.3 mg/g and 9.6 mg/g, respectively.

HRH and IRH are inexpensive and environmentally friendly materials that can be successfully utilized as adsorbents for removing MB and BR9. These adsorbents should be further studied for dye removal from wastewater to evaluate practical applicability and considered the regeneration–reusability of adsorbent. Therefore, I have investigated the efficacy of Hungarian and Indonesian raw rice husks (RHs) as bioadsorbents for removing MB from wastewater. Characterization of the RHs was conducted through zeta potential measurements, Fourier-transform infrared spectroscopy, and scanning electron microscopy. Batch adsorption

experiments were carried out to evaluate the influence of various parameters, including pH, adsorbent dose, initial dye concentration, particle size, and contact time on adsorption. The results indicate that the maximum dye removal was achieved at a contact time of 60 minutes. Adsorption kinetics followed the Elovich model, while the BET multilayer isotherm model provided a superior fit to the experimental data for MB adsorption. The adsorption capacities of Hungarian and Indonesian RHs were 52.23 mg/g and 47.92 mg/g. The regeneration of RHs after adsorption–desorption cycles required using hydrochloric acid as a desorbing solution in four cycles. Reusing the dye for cotton fabrics demonstrated tolerable ΔE^* color values. These findings suggest that RHs possess considerable potential as bioadsorbents for removing MB from wastewater.

The use of rice husk (RH) in the extended technological framework for removing and recovering dyes represents a successful strategy that combines water conservation and agricultural by-product valuation. Although the current study effectively addresses all the research objectives described, some aspects need to be considered in the future investigations, mainly:

- a. Further study of using rice husks from other subspecies could provide valuable insights into the potential variations in adsorption capacity.
- b. The investigation of anionic dye adsorption onto rice husks could lead to the development of more efficient and environmentally friendly wastewater treatment methods.
- c. Further investigation of rice husk hydrochar using batch experiments is crucial for understanding its adsorption properties under various conditions.
- d. Further study to improve the regeneration of adsorbents using a wider range of desorbing solutions could enhance the sustainability and cost-effectiveness of the adsorption process.
- e. Investigating the cost analysis of the original and modified rice husk could provide valuable insights into economic feasibility.
- f. Further investigation of the fixed bed column method's scalability for industrial purposes is essential to assess its feasibility for large-scale wastewater treatment applications.

- g. Further improvement of the cotton fabric coloring method could lead to developing more sustainable and efficient dyeing processes, reducing environmental impact and enhancing product quality in the textile industry.

8 Összefoglalás

Ph.D. tézisemben átfogó vizsgálatot végeztem festékanyagok vizes oldatokból adszorpcióval történő eltávolítására rizshéjat/rizspelyvát (RH) alkalmazva. Az adszorpciót követően a festékanyagok deszorpcióját is megvizsgáltam, a bioadszorbensek valamint a leoldott festékek újbóli, színezőanyagként történő felhasználhatóságára helyezve a hangsúlyt. A kutatásaim kiterjedtek a festékek és az RH közötti kölcsönhatást szabályozó adszorpciós folyamatok, az adszorpciós izoterma és kinetikai jelenségek összefüggéseinek elemzésére, valamint a regenerációs módszerek feltárására, amelyek célja az RH újrafelhasználásának elősegítése a fenntartható pamutszövetfestési gyakorlatokban.

A bevezetőben áttekintést adtam a festékiparról, amely ugyan jelentősen hozzájárul a világgazdasághoz, de környezetszennyezési lábnyoma miatt jelentős környezeti kihívást jelent. Hangsúlyoztam, hogy a festési folyamatokból származó szennyvíz olyan káros vegyületeket tartalmaz, amelyek az emberi egészséget és a vízi ökoszisztémákat egyaránt veszélyeztetik. Természetesen a különféle szennyvízkezelési technológiák alkalmazásával ezt a rizikót jelentősen csökkenthetjük, különösen olyan műveleti lépések beiktatásával, mint az adszorpció/bioadszorpció, mely nem csak eltávolítás szempontjából hatékony hanem, költségek szempontjából is figyelemre méltó, sőt megfelelő körülmények között hatékonyan visszaforgatható a rendszerbe. Ezenkívül a természetes adszorbensek, különösen a mezőgazdasági hulladékok, például a rizshéj, ígéretesek a fenntartható festék kinyerés/visszaforgatásban. Indonézia, mint egy jelentős rizstermelő ország, jelentős mennyiségű rizshéjhulladékot termel, melynek környezetszennyező hatását mérsékelhetjük, ha bioadszorbensként hasznosítjuk. A rizshéj színezék eltávolítására való felhasználásával kapcsolatos tanulmányok hangsúlyozzák annak hatékonyságát, különösen az olyan általános kationos színezékekkel szemben, mint a metilénkék (MB) és az alapvörös 9 (BR9). A rizs származásának, a termelési és feldolgozási módszereinek a rizspelyve adszorpciós kapacitásra gyakorolt hatását illetően azonban kutatási hiányosságok vannak. Ezért is terjesztettem ki vizsgálataimat az indonéz rizspelyva (IRH) mellett a magyarországi rizspelyvára (HRH) is.

Mind a rizspelyva, mind pedig a festékanyagok környezetszennyező problémájának megoldása érdekében folyó kutatásokhoz kapcsolódik disszertációm, amelyben a redukálás-újrahasználat-újrahasznosítás elveire történik az összpontosítás. A környezeti fenntarthatóságot a festékszennyező anyagok csökkentésén, a víz és a rizshéj újrahasználatán, valamint a festék-újrahasznosításon keresztül kívánjuk biztosítani. Az adszorpciós-deszorpciós

ciklusok és a fenntarthatósági szempontok értékelése kulcsfontosságú a rizshéj bioadszorbensként való életképességének felmérésében a körkörös gazdaság keretein belül.

A szakirodalmi áttekintésben részletesen tárgyaltam a színezékeket, így a festékek kategorizálását és a veszélyes színezékek azonosítását. Nagy hangsúlyt fektettem a metilénkékre és a alapvörösre is. Bemutattam a szennyvízkezelés általános technológiáját, külön hangsúlyozva az adszorpciót, az adszorpciós mechanizmusát, az adszorpciós modellezést és a különböző adszorbenseket. Szóba került a rizshéj és annak módosított (aktív szénre alakított) változatának bioadszorbensként történő felhasználási lehetőségei. Ezenkívül a színmérés gyakorlati módszerét is ismertettem, hogy objektív módszerrel vizsgálhatóvá váljon a visszanyert festékanyag újrafelhasználásának értékelése.

Ph.D. disszertációm alapvető céljának megfelelően a kísérleti munkám első lépéseként összehasonlítottam az indonéz rizshéj (IRH) és a magyar rizshéj (HRH) bioadszorbens kapacitását az MB és BR9 festékanyagok vizes oldatokból történő eltávolítására. A rizshéjak (RH-k) jellemzésére kémiai összetétel, zéta potenciál és Fourier-transzformációs infravörös spektroszkópiás elemzéseket használtam. Az adszorpciós vizsgálatokat szakaszos kísérletek sorozatával végeztem, amelyek során vizsgáltam a pH, az adszorbens dózis, a kezdeti festékkoncentráci, érintkezési idő és a hőmérséklet befolyásoló szerepét. Az adszorpciós kinetikai vizsgálatok azt mutatták, hogy a maximális festékeltávolítás 120 perces érintkezési idővel érhető el. Az MB és BR9 adszorpciója pszeudo-másodrendű kinetikai modellt követett, és a BET többrétegű izoterma modell jobban illeszkedett az MB és BR9 adszorpció kísérleti adataihoz. Az IRH adszorpciós kapacitása MB esetében 15,0 mg/g és BR9 esetében 7,2 mg/g volt, míg a HRH adszorpciós kapacitása 24,4 mg/g MB és 8,3 mg/g BR9 esetében.

Bináris megoldásokat kell használni további vizsgálatok során, hogy jobban megértsük az adszorbens és az adszorbátum közötti kölcsönhatást. Ezért megvizsgáltam a metilénkék (MB) és a bázikus vörös 9 (BR9) színezékek eltávolítását magyar rizshéj (HRH) és indonéz rizshéj (IRH) által vizes oldatokból bináris bioszorpcióval. Az adszorbenseket zéta potenciállal, Fourier-transzformációs infravörös spektroszkópiával és pásztázó elektronmikroszkópiával jellemeztük. A szakaszos bioszorpció során is a meghatározó változók a pH, az adszorbens dózisa, az érintkezési idő és a kezdeti koncentráció hatását értékeltük, beleértve. A hatások matematikai/statisztikai elemzésének eredményeit Pareto diagramok, normál valószínűségi diagramok és kölcsönhatások ábrozolásának segítségével mutatom be, mindezt egy faktoriális tervezésű kísérlettervre alapozva. Az optimális érintkezési idő 60 percre adódott, az MB és BR9 izoterma és kinetikai modelljei bináris bioszorpcióban a legjobb illeszkedést a Brunauer–

Emmett–Teller többrétegű rendszerre és az Elovich-egyenletre illesztve adta a korrelációs együtthatók és nemlineáris khi-négyzet alapján. Az eredmények azt mutatták, hogy a HRH bioszorpció kapacitása 10,4 mg/g MB és 10 mg/g BR9 esetében; az IRH értéke 9,3 mg/g és 9,6 mg/g volt.

A HRH és az IRH olcsó és környezetbarát anyagok, amelyek sikeresen használhatók adszorbensként az MB és BR9 eltávolítására, ám gyakorlati alkalmazhatóság szempontjából a méréseket ki kell terjeszteni a valós szennyvízből történő festékeltávolításra is, valamint figyelembe kell venni az adszorbens regenerálhatóságát-újrafelhasználhatóságát. Ezért megvizsgáltam a magyar és indonéz rizshéj (RH) bioadszorbens hatékonyságát a metilénkék (MB) szennyvízből történő eltávolítására. Batch adszorpció kísérleteket végeztünk a különböző paraméterek, köztük a pH, az adszorbens dózis, a kezdeti festékkoncentráció, a részecskeméret és az érintkezési idő adszorpcióra gyakorolt hatásának értékelésére. Az eredmények azt mutatják, hogy a maximális festékeltávolítást 60 perces érintkezési idővel érték el. Az adszorpció kinetika az Elovich-modellt követte, míg a BET többrétegű izoterma modell kiváló illeszkedést biztosított az MB adszorpció kísérleti adataihoz. A magyar és indonéz RH adszorpció kapacitása 52,23 mg/g és 47,92 mg/g volt. Az adszorpció-deszorpció ciklusok után az RH-ek regenerálása sósav deszorpció oldatának felhasználásával négy ciklusban is lehetséges. A festék pamutszövetekhez való újrafelhasználása elfogadható ΔE^* színértékeket mutatott. Ezek az eredmények arra utalnak, hogy az RH-k jelentős bioadszorbens potenciállal rendelkeznek az MB szennyvízből történő eltávolítására.

A rizshéj (RH) alkalmazása a festékek eltávolítására és visszanyerésére keretben sikeres stratégia, amely egyesíti a vízmegőrzést és a mezőgazdasági melléktermékek hasznosítását. Bár a jelenlegi tanulmány hatékonyan foglalkozik az összes leírt kutatási céllal, néhány szempontot figyelembe kell venni a jövőbeni vizsgálatok során, elsősorban:

- a. A más alfajokból származó rizshéj felhasználásának további tanulmányozása értékes betekintést nyújthat az adszorpció kapacitás lehetséges változásaiba.
- b. Az anionos festék adszorpciójának vizsgálata a rizshéjon hatékonyabb és környezetbarátabb szennyvízkezelési módszerek kidolgozását eredményezheti.
- c. A rizshéjből készített aktív szén további vizsgálata kulcsfontosságú az adszorpció tulajdonságok megértésében.
- d. Az adszorbensek regenerációjának javítására irányuló további vizsgálatok a deszorbeáló megoldások szélesebb skálájával javíthatják az adszorpció folyamat fenntarthatóságát és költséghatékonyságát.

- e. Az eredeti és módosított rizshéj költségelemzésének vizsgálata értékes betekintést nyújthat a gazdasági megvalósíthatóságba.
- f. A fix ágyas oszlopos módszer ipari célú méretnövelésének további vizsgálata elengedhetetlen az ipari szennyvízkezelési alkalmazásokban történő megvalósíthatósághoz.
- g. A pamutszövet színezési módszerének további fejlesztése fenntarthatóbb és hatékonyabb festési eljárások kifejlesztéséhez, a környezeti hatások csökkentéséhez és a termékminőség javításához vezethet a textiliparban.

9 New scientific results

1. Rice Husk (RH) is proven to be a bioadsorbent for MB and BR9 removal from aqueous solution:

- a. Removal percentages for MB using HRH and IRH were 96%, respectively, and for BR9 using HRH and IRH were 83.8% and 78.2%, respectively.
- b. The optimal condition for MB and BR9 removal was achieved at a contact time of 120 min using concentration value is 2 g/L, initial dye concentration of 30 mg/L at pH 10 (MB) and pH 7 (BR9) and a stirring rate of 100 rpm.
- c. MB concentrations of 2.8×10^{-5} M (~9 mg/L) and BR9 concentrations of 4.1×10^{-5} (~12 mg/L) tend to increase to infinity, since the aggregation is perceptible in the aqueous solution and on the surface.
- d. The adsorption of MB and BR9 is governed by chemisorption, a process characterized by the sharing or exchange of electrons between the negatively charged functional groups on the RH bioadsorbent and the positively charged cationic dye molecules.

2. HRH and IRH exhibited different MB and BR9 adsorption capacities because of their different chemical compositions. The HRH adsorption capacities were 24.4 mg/g for MB and 8.3 mg/g for BR9, whereas those of IRH were 15.0 mg/g for MB and 7.2 mg/g for BR9.

3. Rice husk can be considered as bioadsorbent for binary adsorption of tested cationic dyes from aqueous solution as well:

- a. Removal percentages for MB and BR9 using HRH were 91.7% and 88.8%, respectively, and 83.8% and 78.2% using IRH, respectively.
- b. The adsorption capacity of HRH was 10.4 mg/g for MB and 10 mg/g for BR9; values for IRH were 9.3 mg/g and 9.6 mg/g, respectively.
- c. Adsorption is controlled by chemisorption, as evidenced by the application of the Elovich equation in describing the adsorption kinetics of MB and BR9.
- d. A factorial design analysis indicated that interactions among adsorbent type*pH*dose for both dyes were insignificant. Interactions between main factors (adsorbent type, pH, and dose) were significant for MB and BR9, except for two-way interactions (adsorbent type*dose) for BR9.

4. Rice husk was an effective bioadsorbent for Methylene Blue removal from model wastewater:

- a. Removal percentages for MB using HRH and IRH were 92% and 88%, respectively.
- b. The optimal condition for MB removal was achieved at a contact time of 60 min using 600 mg of adsorbent dose in 250 mL aqueous solution, initial dye concentration of 60 mg/L at pH 12 and a stirring rate of 100 rpm.
- c. The HRH and IRH adsorption capacities were 52.23 mg/g and 47.92 mg/g.
- d. The chemisorption took place during the adsorption process, as indicated by the Elovich model. This model assumes that adsorption involves chemical interactions between the MB and the RH biosorbent.

5. Rice husk was successfully modified by hydrothermal carbonization method for efficient Methylene Blue adsorption:

- a. The hydrothermal carbonization changed the previously smooth surface of the raw RH, the RH is transformed into smaller particles with rough surfaces and porous structures.
- b. The removal percentage for hydrochar RH was slightly greater than that for raw RH; however, the difference was insignificant. Consequently, raw RH is cheaper and more effective for MB removal from wastewater than RH hydrochar.

6. Rice husk was successfully utilized for desorption and regeneration processes, aligning with the principles of the circular economy to evaluate the environmental sustainability of this bioadsorbent:

- a. 1.0 M HCl was the most effective desorbing solution in the desorption of MB from model wastewater.
- b. The RH was effectively recycled for four consecutive adsorption-desorption cycles and can be reused with a 5% reduction in adsorption percentages.

7. The MB solution recovered by desorption can be used for dyeing cotton fabrics:

- a. After four processing cycles, the recovered MB was still capable of dyeing the cotton fabrics.
- b. Reusing dye for cotton fabrics after the adsorption-desorption process demonstrated an acceptable range for ΔE^* value of 0 to 5 or below.

10 Publications

MTMT Author ID: 10081549

1. **Sukmana, H.**, Bellahsen, N., Pantoja, F., & Hodur, C. (2021). Adsorption and coagulation in wastewater treatment–Review. *Progress in Agricultural Engineering Sciences*, 17(1), 49-68. <https://doi.org/10.1556/446.2021.00029> (**Q3, 70 Citations**)
2. **Sukmana, H.**, Ballai, G., Gyulavári, T., Illés, E., Kozma, G., Kónya, Z., & Hodúr, C. (2023). Hungarian and Indonesian rice husk as bioadsorbents for binary biosorption of cationic dyes from aqueous solutions: A factorial design analysis. *Heliyon*, 9(6). <https://doi.org/10.1016/j.heliyon.2023.e17154> (**Q1, IF:3.4, 3 Citations**)
3. **Sukmana, H.**, Tombácz, E., Ballai, G., Kozma, G., Kónya, Z., & Hodúr, C. (2023). Comparative Study of Adsorption of Methylene Blue and Basic Red 9 Using Rice Husks of Different Origins. *Recycling*, 8(5), 1–20. <https://doi.org/10.3390/recycling8050074> (**Q1, IF:4.6, 2 Citations**)
4. **Sukmana, H.**, Radojčin, M., Gyulavári, T., Kozma, G., Kónya, Z., & Hodúr, C. (2023). Utilization of Rice Husks as Effective Bioadsorbents for Methylene Blue Removal from Wastewater: Characterization, Adsorption Performance, and Regeneration Studies. (**under review in Applied Water Science Journal, Q1, IF:5.7**)

11 Presentation in conferences

1. **Sukmana, H.**, Tombácz, E., Ballai, G., Kozma, G., Kónya, Z., & Hodúr, C. Comparative Study of Different Subspecies of *Oryza Sativa* for Cationic Dyes Removal from Aqueous Solution: 3rd EUGLOH Plant Science Meeting, Portugal, Porto, 20-22 November 2023.
2. **Sukmana, H.**, Ballai, G., Gyulavári, T., Illés, E., Kozma, G., Kónya, Z., & Hodúr, C. Binary Adsorption by Bio-adsorbents: 8th International Conference Sustainable Postharvest and Food Technologies, Serbia, Subotica-Palic, 23-28 April 2023.
3. **Sukmana, H.**, Tombácz, E., Ballai, G., Kozma, G., Kónya, Z., & Hodúr, C. The Adsorption of Cationic Dyes from Aqueous Solution Using Hungarian and Indonesian Rice Husk: 2nd International Conference on Advanced Production and Processing, Serbia, Novi Sad, 20-22 October 2022.

4. **Sukmana, H.**, Ballai, G., Gyulavári, T., Illés, E., Kozma, G., Kónya, Z., & Hodúr, C. Adsorption of Methylene Blue (MB) and Basic Red 9 (BR9) in Binary Solutions Using Rice Husk: Factorial Design Analysis: 6th International Conference on Chemical Engineering, Romania, Lasi, 5-7 October 2022.
5. **Sukmana, H.**, & Hodúr, C. The Adsorption Isotherm of Cationic Dyes from Aqueous Solution Using Various Rice Husk: 50th Chemical Engineering Days, Hungary, Veszprem, 26-28 April 2022.
6. **Sukmana, H.**, & Hodúr, C. Rice Husk as a Bio-adsorbent for Ammonium Removal: 4th International Conference on Biosystems and Food Engineering, Hungary, Budapest, 4 June 2021.
7. **Sukmana, H.**, & Hodúr, C. Grain/Rice Husk and Grain/Rice Husk Ash Utilization in The Wastewater Treatment: The IV. Sustainable Raw Materials Management International Project Week. Hungary, Miskolc, 25 November 2020.

12 References

- [1] K. Bing, M. Vakili, B. Amini, P. Eong, A. Zuhairi, and B. Salamatinia, "Adsorption of dyes by nanomaterials : Recent developments and adsorption mechanisms," *Sep. Purif. Technol.*, vol. 150, pp. 229–242, 2015, doi: 10.1016/j.seppur.2015.07.009.
- [2] D. Bhatia, N. R. Sharma, J. Singh, and R. S. Kanwar, "Biological methods for textile dye removal from wastewater: A review," *Crit. Rev. Environ. Sci. Technol.*, vol. 47, no. 19, pp. 1836–1876, 2017, doi: 10.1080/10643389.2017.1393263.
- [3] S. C. Bhatia and S. Devraj, *Pollution control in textile industry*. WPI Publishing, 2017.
- [4] P. S. Kumar *et al.*, "A critical review on recent developments in the low-cost adsorption of dyes from wastewater," *Desalin. Water Treat.*, vol. 172, pp. 395–416, 2019, doi: 10.5004/dwt.2019.24613.
- [5] M. Bellaj *et al.*, "Cationic and anionic dyes adsorption from wastewater by clay-chitosan composite : An integrated experimental and modeling study," *Chem. Eng. Sci.*, vol. 285, no. November 2023, p. 119615, 2024, doi: 10.1016/j.ces.2023.119615.
- [6] H. Sukmana, N. Bellahsen, F. Pantoja, and C. Hodur, "Adsorption and coagulation in wastewater treatment – Review," *Prog. Agric. Eng. Sci.*, vol. 17, no. 1, pp. 49–68, Dec. 2021, doi: 10.1556/446.2021.00029.
- [7] J. Fito *et al.*, "Adsorption of methylene blue from textile industrial wastewater using activated carbon developed from Rumex abyssinicus plant," *Sci. Rep.*, pp. 1–17, 2023, doi: 10.1038/s41598-023-32341-w.
- [8] N. Kumar, A. Pandey, and Y. C. Sharma, "Journal of Water Process Engineering A review on sustainable mesoporous activated carbon as adsorbent for efficient removal of hazardous dyes from industrial wastewater," *J. Water Process Eng.*, vol. 54, no. June, p. 104054, 2023, doi: 10.1016/j.jwpe.2023.104054.
- [9] S. Singh, A. Kumar, P. Jyoti, P. Chakraborty, and M. Kumar, "Adsorption potential of biochar obtained from pyrolysis of raw and torrefied Acacia nilotica towards removal of methylene blue dye from synthetic wastewater," *Biomass Convers. Biorefinery*, pp. 6083–6104, 2023, doi: 10.1007/s13399-021-01645-0.
- [10] L. Cai *et al.*, "Effective Adsorption of Diesel Oil by Crab-Shell-Derived Biochar Nanomaterials," *Materials (Basel)*, vol. 12, no. 2, p. 236, Jan. 2019, doi: 10.3390/ma12020236.
- [11] N. S. Ali, N. M. Jabbar, S. M. Alardhi, H. S. Majdi, and T. M. Albayati, "Adsorption of methyl violet dye onto a prepared bio-adsorbent from date seeds: isotherm, kinetics, and thermodynamic studies," *Heliyon*, vol. 8, no. 8, p. e10276, 2022, doi: 10.1016/j.heliyon.2022.e10276.
- [12] B. Thomas, E. P. Shilpa, and L. K. Alexander, "Role of functional groups and morphology on the pH-dependent adsorption of a cationic dye using banana peel, orange peel, and neem leaf bio-adsorbents," *Emergent Mater.*, vol. 4, no. 5, pp. 1479–1487, 2021, doi: 10.1007/s42247-021-00237-y.
- [13] R. Mallampati, L. Xuanjun, A. Adin, and S. Valiyaveetil, "Fruit peels as efficient renewable adsorbents for removal of dissolved heavy metals and dyes from water," *ACS Sustain. Chem. Eng.*, vol. 3, no. 6, pp. 1117–1124, 2015, doi: 10.1021/acssuschemeng.5b00207.
- [14] J. Wu *et al.*, "Spent substrate of Ganodorma lucidum as a new bio-adsorbent for adsorption of three typical dyes," *Bioresour. Technol.*, vol. 266, no. June, pp. 134–138, 2018, doi: 10.1016/j.biortech.2018.06.078.
- [15] M. A. Hossain and M. L. Hossain, "Kinetic study of Malachite Green adsorption on used black tea leaves from aqueous solution," *Int. J. Adv. Res.*

- Journalwww.journalijar.com Int. J. Adv. Res.*, vol. 2, no. 4, pp. 360–374, 2014.
- [16] S. Jain and R. V. Jayaram, “Removal of basic dyes from aqueous solution by low-cost adsorbent: Wood apple shell (*Feronia acidissima*),” *Desalination*, vol. 250, no. 3, pp. 921–927, 2010, doi: 10.1016/j.desal.2009.04.005.
- [17] W. Li, B. Mu, and Y. Yang, “Bioresource Technology Feasibility of industrial-scale treatment of dye wastewater via bio- adsorption technology,” *Bioresour. Technol.*, vol. 277, no. December 2018, pp. 157–170, 2019, doi: 10.1016/j.biortech.2019.01.002.
- [18] M. Kadhom, N. Albayati, H. Alalwan, and M. Al-Furaiji, “Removal of dyes by agricultural waste,” *Sustain. Chem. Pharm.*, vol. 16, no. April, p. 100259, 2020, doi: 10.1016/j.scp.2020.100259.
- [19] M. Ahmaruzzaman and V. K. Gupta, “Rice Husk and Its Ash as Low-Cost Adsorbents in Water and Wastewater Treatment,” *Ind. Eng. Chem. Res.*, vol. 50, no. 24, pp. 13589–13613, Dec. 2011, doi: 10.1021/ie201477c.
- [20] A. H. Matin, S. S. Khaloo, A. Akbarzadeh, and M. Riahi, “Comparison of surface functional groups and metal uptake efficiency of rice husk harvested from different climatic zones,” *Water Sci. Technol.*, vol. 65, no. 10, pp. 1738–1744, 2012, doi: 10.2166/wst.2012.066.
- [21] BPS-STATISTICS INDONESIA, “Harvested Area and Rice Production in Indonesia 2023,” Jakarta, Indonesia, 2023.
- [22] I. N. Khasanah and K. Astuti, *Harvest Area and Rice Production in Indonesia 2021*. Jakarta, Indonesia: Indonesian Central Bureau of Statistics, 2022.
- [23] B. Noroozi, G. A. Sorial, H. Bahrami, and M. Arami, “Adsorption of binary mixtures of cationic dyes,” *Dye. Pigment.*, vol. 76, no. 3, pp. 784–791, 2008, doi: 10.1016/j.dyepig.2007.02.003.
- [24] L. Liu, Z. Y. Gao, X. P. Su, X. Chen, L. Jiang, and J. M. Yao, “Adsorption removal of dyes from single and binary solutions using a cellulose-based bioadsorbent,” *ACS Sustain. Chem. Eng.*, vol. 3, no. 3, pp. 432–442, 2015, doi: 10.1021/sc500848m.
- [25] H. Bai, J. Chen, X. Zhou, and C. Hu, “Single and binary adsorption of dyes from aqueous solutions using functionalized microcrystalline cellulose from cotton fiber,” *Korean J. Chem. Eng.*, vol. 37, no. 11, pp. 1926–1932, 2020, doi: 10.1007/s11814-020-0621-3.
- [26] N. M. Mahmoodi, M. Taghizadeh, and A. Taghizadeh, “Mesoporous activated carbons of low-cost agricultural bio-wastes with high adsorption capacity: Preparation and artificial neural network modeling of dye removal from single and multicomponent (binary and ternary) systems,” *J. Mol. Liq.*, vol. 269, pp. 217–228, 2018, doi: 10.1016/j.molliq.2018.07.108.
- [27] Z. Liu, T. A. Khan, M. A. Islam, and U. Tabrez, “A review on the treatment of dyes in printing and dyeing wastewater by plant biomass carbon,” *Bioresour. Technol.*, vol. 354, no. March, p. 127168, 2022, doi: 10.1016/j.biortech.2022.127168.
- [28] A. Aichour and H. Zaghouane-Boudiaf, “Single and competitive adsorption studies of two cationic dyes from aqueous mediums onto cellulose-based modified citrus peels/calcium alginate composite,” *Int. J. Biol. Macromol.*, vol. 154, pp. 1227–1236, 2020, doi: 10.1016/j.ijbiomac.2019.10.277.
- [29] C. Vîrlan, R. G. Ciocârlan, T. Roman, D. Gherca, N. Cornei, and A. Pui, “Studies on adsorption capacity of cationic dyes on several magnetic nanoparticles,” *Acta Chem. Iasi*, vol. 21, no. 1, pp. 19–30, 2013, doi: 10.2478/achi-2013-0003.
- [30] G. O. El-Sayed, “Removal of methylene blue and crystal violet from aqueous solutions by palm kernel fiber,” *Desalination*, vol. 272, no. 1–3, pp. 225–232, 2011, doi: 10.1016/j.desal.2011.01.025.
- [31] L. R. S. Pinheiro, D. G. Gradíssimo, L. P. Xavier, and A. V. Santos, “Degradation of

- Azo Dyes: Bacterial Potential for Bioremediation,” *Sustain.*, vol. 14, no. 3, pp. 1–23, 2022, doi: 10.3390/su14031510.
- [32] S. Dutta, B. Gupta, S. K. Srivastava, and A. K. Gupta, “Recent advances on the removal of dyes from wastewater using various adsorbents: A critical review,” *Mater. Adv.*, vol. 2, no. 14, pp. 4497–4531, 2021, doi: 10.1039/d1ma00354b.
- [33] R. Bushra, S. Mohamad, Y. Alias, Y. Jin, and M. Ahmad, “Current approaches and methodologies to explore the perceptive adsorption mechanism of dyes on low-cost agricultural waste: A review,” *Microporous Mesoporous Mater.*, vol. 319, no. February, p. 111040, 2021, doi: 10.1016/j.micromeso.2021.111040.
- [34] G. Sriram *et al.*, “Recent trends in the application of metal-organic frameworks (MOFs) for the removal of toxic dyes and their removal mechanism-a review,” *Sustain. Mater. Technol.*, vol. 31, no. December 2021, p. e00378, 2022, doi: 10.1016/j.susmat.2021.e00378.
- [35] N. Tara, S. I. Siddiqui, G. Rathi, S. A. Chaudhry, Inamuddin, and A. M. Asiri, “Nano-engineered Adsorbent for the Removal of Dyes from Water: A Review,” *Curr. Anal. Chem.*, vol. 16, no. 1, pp. 14–40, 2019, doi: 10.2174/1573411015666190117124344.
- [36] S. Varjani, P. Rakholiya, H. Y. Ng, S. You, and J. A. Teixeira, “Microbial degradation of dyes: An overview,” *Bioresour. Technol.*, vol. 314, no. June, 2020, doi: 10.1016/j.biortech.2020.123728.
- [37] M. F. Chowdhury, S. Khandaker, F. Sarker, A. Islam, M. T. Rahman, and M. R. Awual, “Current treatment technologies and mechanisms for removal of indigo carmine dyes from wastewater: A review,” *J. Mol. Liq.*, vol. 318, p. 114061, 2020, doi: 10.1016/j.molliq.2020.114061.
- [38] K. Piaskowski, R. Świdarska-Dąbrowska, and P. K. Zarzycki, “Dye removal from water and wastewater using various physical, chemical, and biological processes,” *J. AOAC Int.*, vol. 101, no. 5, pp. 1371–1384, 2018, doi: 10.5740/jaoacint.18-0051.
- [39] S. Rodriguez Couto, “Dye removal by immobilised fungi,” *Biotechnol. Adv.*, vol. 27, no. 3, pp. 227–235, 2009, doi: 10.1016/j.biotechadv.2008.12.001.
- [40] E. Errais *et al.*, “Efficient anionic dye adsorption on natural untreated clay: Kinetic study and thermodynamic parameters,” *Desalination*, vol. 275, no. 1–3, pp. 74–81, 2011, doi: 10.1016/j.desal.2011.02.031.
- [41] A. Islam *et al.*, “Step towards the sustainable toxic dyes and heavy metals removal and recycling from aqueous solution- A comprehensive review,” *Resour. Conserv. Recycl.*, vol. 175, no. August, p. 105849, 2021, doi: 10.1016/j.resconrec.2021.105849.
- [42] I. Khan, K. Saeed, N. Ali, I. Khan, B. Zhang, and M. Sadiq, “Heterogeneous photodegradation of industrial dyes: An insight to different mechanisms and rate affecting parameters,” *J. Environ. Chem. Eng.*, vol. 8, no. 5, 2020, doi: 10.1016/j.jece.2020.104364.
- [43] E. Routoula and S. V. Patwardhan, “Degradation of Anthraquinone Dyes from Effluents: A Review Focusing on Enzymatic Dye Degradation with Industrial Potential,” *Environ. Sci. Technol.*, vol. 54, no. 2, pp. 647–664, 2020, doi: 10.1021/acs.est.9b03737.
- [44] D. Lan *et al.*, “Adsorptive removal of organic dyes via porous materials for wastewater treatment in recent decades: A review on species, mechanisms and perspectives,” *Chemosphere*, vol. 293, no. December 2021, p. 133464, 2022, doi: 10.1016/j.chemosphere.2021.133464.
- [45] D. A. Yaseen and M. Scholz, *Textile dye wastewater characteristics and constituents of synthetic effluents: a critical review*, vol. 16, no. 2. Springer Berlin Heidelberg, 2019. doi: 10.1007/s13762-018-2130-z.
- [46] M. F. Abid, M. A. Zablouk, and A. M. Abid-Alameer, “Experimental study of dye

- removal from industrial wastewater by membrane technologies of reverse osmosis and nanofiltration,” *J. Environ. Heal. Sci. Eng.*, vol. 9, no. 1, pp. 1–9, 2012.
- [47] D. Sivakumar, “Role of *Lemna minor* Lin. in treating the textile industry wastewater,” *Int. J. Mater. Text. Eng.*, vol. 8, no. 3, pp. 208–212, 2014.
- [48] A. Ghaly, R. Ananthashankar, M. Alhattab, and V. Ramakrishnan, “Production, Characterization and Treatment of Textile Effluents: A Critical Review,” *J. Chem. Eng. Process Technol.*, vol. 05, no. 01, 2013, doi: 10.4172/2157-7048.1000182.
- [49] I. Ihsanullah, A. Jamal, M. Ilyas, M. Zubair, G. Khan, and M. A. Atieh, “Bioremediation of dyes: Current status and prospects,” *J. Water Process Eng.*, vol. 38, no. October, p. 101680, 2020, doi: 10.1016/j.jwpe.2020.101680.
- [50] A. Tkaczyk, K. Mitrowska, and A. Posyniak, “Synthetic organic dyes as contaminants of the aquatic environment and their implications for ecosystems: A review,” *Sci. Total Environ.*, vol. 717, p. 137222, 2020, doi: 10.1016/j.scitotenv.2020.137222.
- [51] C. Osagie, A. Othmani, S. Ghosh, A. Malloum, Z. Kashitarash Esfahani, and S. Ahmadi, “Dyes adsorption from aqueous media through the nanotechnology: A review,” *J. Mater. Res. Technol.*, vol. 14, pp. 2195–2218, 2021, doi: 10.1016/j.jmrt.2021.07.085.
- [52] M. J. Uddin, R. E. Ampiauw, and W. Lee, “Adsorptive removal of dyes from wastewater using a metal-organic framework: A review,” *Chemosphere*, vol. 284, no. January, p. 131314, 2021, doi: 10.1016/j.chemosphere.2021.131314.
- [53] S. S. Affat, “Classifications, Advantages, Disadvantages, Toxicity Effects of Natural and Synthetic Dyes: A review,” *Classif. advantages, disadvantages, Toxic. Eff. Nat. Synth. Dye. A Rev. Univ. Thi-Qar J. Sci.*, vol. 8, no. 1, pp. 130–135, 2021, [Online]. Available: <http://doi.org/10.32792/utq/utjsoci/v8/1/21>
- [54] K. Hunger, *Industrial dyes: chemistry, properties, applications*. John Wiley & Sons, 2007.
- [55] S. Sutar, P. Patil, and J. Jadhav, “Recent advances in biochar technology for textile dyes wastewater remediation: A review,” *Environ. Res.*, vol. 209, no. October 2021, p. 112841, 2022, doi: 10.1016/j.envres.2022.112841.
- [56] A. K. D. Alsukaibi, “Various Approaches for the Detoxification of Toxic Dyes in Wastewater,” *Processes*, vol. 10, no. 10, 2022, doi: 10.3390/pr10101968.
- [57] E. F. D. Januário *et al.*, “Advanced graphene oxide-based membranes as a potential alternative for dyes removal: A review,” *Sci. Total Environ.*, vol. 789, 2021, doi: 10.1016/j.scitotenv.2021.147957.
- [58] G. A. Ismail and H. Sakai, “Review on effect of different type of dyes on advanced oxidation processes (AOPs) for textile color removal,” *Chemosphere*, vol. 291, no. P3, p. 132906, 2022, doi: 10.1016/j.chemosphere.2021.132906.
- [59] J. Sharma, S. Sharma, and V. Soni, “Classification and impact of synthetic textile dyes on Aquatic Flora: A review,” *Reg. Stud. Mar. Sci.*, vol. 45, 2021, doi: 10.1016/j.rsma.2021.101802.
- [60] H. Ben Slama *et al.*, “Diversity of synthetic dyes from textile industries, discharge impacts and treatment methods,” *Appl. Sci.*, vol. 11, no. 14, pp. 1–21, 2021, doi: 10.3390/app11146255.
- [61] A. M. Elgarahy, K. Z. Elwakeel, S. H. Mohammad, and G. A. Elshoubaky, “A critical review of biosorption of dyes, heavy metals and metalloids from wastewater as an efficient and green process,” *Clean. Eng. Technol.*, vol. 4, no. June, p. 100209, 2021, doi: 10.1016/j.clet.2021.100209.
- [62] H. Wang *et al.*, “Colloids and Surfaces A : Physicochemical and Engineering Aspects Highly effective removal of methylene blue from wastewater by modified hydroxyl groups materials : Adsorption performance and mechanisms,” *Colloids Surfaces A*

- Physicochem. Eng. Asp.*, vol. 656, no. PA, p. 130290, 2023, doi: 10.1016/j.colsurfa.2022.130290.
- [63] E. Alver, A. Ü. Metin, and F. Brouers, “Methylene blue adsorption on magnetic alginate/rice husk bio-composite,” *Int. J. Biol. Macromol.*, vol. 154, pp. 104–113, 2020, doi: 10.1016/j.ijbiomac.2020.02.330.
- [64] M. A. Mohammed, A. Shitu, and A. Ibrahim, “Removal of Methylene Blue Using Low Cost Adsorbent: A Review,” *Res. J. Chem. Sci.*, vol. 4, no. 1, pp. 91–102, 2014.
- [65] C. Alex, A. Kamoru, T. Chinedu, J. Ifeanyichukwu, I. Jacinta, and S. Mustapha, “Results in Engineering Green synthesis of iron oxide nanoparticles by Taguchi design of experiment method for effective adsorption of methylene blue and methyl orange from textile wastewater,” *Results Eng.*, vol. 19, no. June, p. 101198, 2023, doi: 10.1016/j.rineng.2023.101198.
- [66] E. Alver, A. Ü. Metin, and F. Brouers, “Methylene blue adsorption on magnetic alginate/rice husk bio-composite,” *Int. J. Biol. Macromol.*, vol. 154, pp. 104–113, Jul. 2020, doi: 10.1016/j.ijbiomac.2020.02.330.
- [67] D. Pihusut and M. Chantharat, “Removal of methylene blue using agricultural waste: A case study of rice husk and rice husk ash from Chaipattana rice mill demonstration center,” *Environ. Nat. Resour. J.*, vol. 15, no. 2, p. 30, 2017, doi: 10.14456/ennrj.2017.10.
- [68] O. Duman, S. Tunç, and T. Gürkan Polat, “Adsorptive removal of triarylmethane dye (Basic Red 9) from aqueous solution by sepiolite as effective and low-cost adsorbent,” *Microporous Mesoporous Mater.*, vol. 210, no. February, pp. 176–184, 2015, doi: 10.1016/j.micromeso.2015.02.040.
- [69] B. Lellis, C. Z. Fávaro-Polonio, J. A. Pamphile, and J. C. Polonio, “Effects of textile dyes on health and the environment and bioremediation potential of living organisms,” *Biotechnol. Res. Innov.*, vol. 3, no. 2, pp. 275–290, 2019, doi: 10.1016/j.biori.2019.09.001.
- [70] N. Sivarajasekar and R. Baskar, “Adsorption of basic red 9 on activated waste Gossypium hirsutum seeds: Process modeling, analysis and optimization using statistical design,” *J. Ind. Eng. Chem.*, vol. 20, no. 5, pp. 2699–2709, 2014, doi: 10.1016/j.jiec.2013.10.058.
- [71] Y. Zhou, S. Yao, Y. Ma, G. Li, Q. Huo, and Y. Liu, “An anionic single-walled metal-organic nanotube with an armchair (3,3) topology as an extremely smart adsorbent for the effective and selective adsorption of cationic carcinogenic dyes,” *Chem. Commun.*, vol. 54, no. 24, pp. 3006–3009, 2018, doi: 10.1039/c8cc00542g.
- [72] A. Mills, “An overview of the methylene blue ISO test for assessing the activities of photocatalytic films,” *Appl. Catal. B Environ.*, vol. 128, pp. 144–149, 2012, doi: 10.1016/j.apcatb.2012.01.019.
- [73] N. Ramanathan, K. I. Priyadarsini, S. N. Guha, and H. Mohan, “Spectral, Kinetic, and Redox Properties of Basic Fuchsin in Homogeneous Aqueous and Sodium Dodecyl Sulfate Micellar Media,” *Int. J. Chem. Kinet.*, vol. 35, no. 12, pp. 629–636, 2003, doi: 10.1002/kin.10164.
- [74] A. Tiri, L. Belkhir, and L. Mouni, “Evaluation of surface water quality for drinking purposes using fuzzy inference system,” *Groundw. Sustain. Dev.*, vol. 6, pp. 235–244, Mar. 2018, doi: 10.1016/j.gsd.2018.01.006.
- [75] S. M. Abdelbasir and A. E. Shalan, “An overview of nanomaterials for industrial wastewater treatment,” *Korean J. Chem. Eng.*, vol. 36, no. 8, pp. 1209–1225, 2019.
- [76] WWAP (United Nations World Water Assessment Programme), *The United Nations world water development report, 2017*. Paris: UNESCO, 2017.
- [77] A. F. Mohd Udaiyappan, H. Abu Hasan, M. S. Takriff, and S. R. Sheikh Abdullah, “A

- review of the potentials, challenges and current status of microalgae biomass applications in industrial wastewater treatment,” *J. Water Process Eng.*, vol. 20, pp. 8–21, Dec. 2017, doi: 10.1016/j.jwpe.2017.09.006.
- [78] S. S. Kontos, P. G. Koutsoukos, and C. A. Paraskeva, “Removal and recovery of phenolic compounds from olive mill wastewater by cooling crystallization,” *Chem. Eng. J.*, vol. 251, pp. 319–328, Sep. 2014, doi: 10.1016/j.cej.2014.04.047.
- [79] G. Crini and E. Lichtfouse, “Advantages and disadvantages of techniques used for wastewater treatment,” *Environ. Chem. Lett.*, vol. 17, no. 1, pp. 145–155, Mar. 2019, doi: 10.1007/s10311-018-0785-9.
- [80] M. Ahmaruzzaman, “Role of Fly Ash in the Removal of Organic Pollutants from Wastewater,” *Energy & Fuels*, vol. 23, no. 3, pp. 1494–1511, Mar. 2009, doi: 10.1021/ef8002697.
- [81] Y. W. Cheng, M. R. Khan, K. H. Ng, S. Wongsakulphasatch, and C. K. Cheng, “Harnessing renewable hydrogen-rich syngas from valorization of palm oil mill effluent (POME) using steam reforming technique,” *Renew. Energy*, vol. 138, pp. 1114–1126, Aug. 2019, doi: 10.1016/j.renene.2019.02.040.
- [82] T. A. Saleh and V. K. Gupta, *Nanomaterial and polymer membranes: synthesis, characterization, and applications*. Elsevier, 2016.
- [83] F. Zhang, S. Gao, Y. Zhu, and J. Jin, “Alkaline-induced superhydrophilic/underwater superoleophobic polyacrylonitrile membranes with ultralow oil-adhesion for high-efficient oil/water separation,” *J. Memb. Sci.*, vol. 513, pp. 67–73, Sep. 2016, doi: 10.1016/j.memsci.2016.04.020.
- [84] P. M. Budiman and T. Y. Wu, “Ultrasonication pre-treatment of combined effluents from palm oil, pulp and paper mills for improving photofermentative biohydrogen production,” *Energy Convers. Manag.*, vol. 119, pp. 142–150, Jul. 2016, doi: 10.1016/j.enconman.2016.03.060.
- [85] A. H. Mahvi, “Application of ultrasonic technology for water and wastewater treatment,” *Iran. J. Public Health*, vol. 38, no. 2, pp. 1–17, 2009.
- [86] N. Ariffin *et al.*, “Review on Adsorption of Heavy Metal in Wastewater by Using Geopolymer,” *MATEC Web Conf.*, vol. 97, p. 01023, Feb. 2017, doi: 10.1051/mateconf/20179701023.
- [87] E. Bazrafshan, P. Amirian, A. H. Mahvi, and A. Ansari-Moghaddam, “Application of adsorption process for phenolic compounds removal from aqueous environments: a systematic review,” *Glob. NEST J.*, vol. 18, no. 1, pp. 146–163, 2016.
- [88] J. L. Diaz de Tuesta, A. M. T. Silva, J. L. Faria, and H. T. Gomes, “Removal of Sudan IV from a simulated biphasic oily wastewater by using lipophilic carbon adsorbents,” *Chem. Eng. J.*, vol. 347, pp. 963–971, Sep. 2018, doi: 10.1016/j.cej.2018.04.105.
- [89] W. L. Ang and A. W. Mohammad, “State of the art and sustainability of natural coagulants in water and wastewater treatment,” *J. Clean. Prod.*, vol. 262, p. 121267, Jul. 2020, doi: 10.1016/j.jclepro.2020.121267.
- [90] M. Chethana, L. G. Sorokhaibam, V. M. Bhandari, S. Raja, and V. V. Ranade, “Green Approach to Dye Wastewater Treatment Using Biocoagulants,” *ACS Sustain. Chem. Eng.*, vol. 4, no. 5, pp. 2495–2507, May 2016, doi: 10.1021/acssuschemeng.5b01553.
- [91] A. Dąbrowski, “Adsorption — from theory to practice,” *Adv. Colloid Interface Sci.*, vol. 93, no. 1–3, pp. 135–224, Oct. 2001, doi: 10.1016/S0001-8686(00)00082-8.
- [92] W. Huang and Z. Liu, “Biosorption of Cd(II)/Pb(II) from aqueous solution by biosurfactant-producing bacteria: Isotherm kinetic characteristic and mechanism studies,” *Colloids Surfaces B Biointerfaces*, vol. 105, pp. 113–119, May 2013, doi: 10.1016/j.colsurfb.2012.12.040.
- [93] S. Afroze, T. K. Sen, and H. M. Ang, “Adsorption removal of zinc (II) from aqueous

- phase by raw and base modified Eucalyptus sheathiana bark: Kinetics, mechanism and equilibrium study,” *Process Saf. Environ. Prot.*, vol. 102, pp. 336–352, Jul. 2016, doi: 10.1016/j.psep.2016.04.009.
- [94] A. Kumar, S. Singha, B. Sengupta, D. Dasgupta, S. Datta, and T. Mandal, “Intensive insight into the enhanced utilization of rice husk ash: Abatement of rice mill wastewater and recovery of silica as a value added product,” *Ecol. Eng.*, vol. 91, pp. 270–281, Jun. 2016, doi: 10.1016/j.ecoleng.2016.02.034.
- [95] J. Xu *et al.*, “A review of functionalized carbon nanotubes and graphene for heavy metal adsorption from water: Preparation, application, and mechanism,” *Chemosphere*, vol. 195, pp. 351–364, Mar. 2018, doi: 10.1016/j.chemosphere.2017.12.061.
- [96] B. Naoufal, K. Szabolcs, P. Zoltán, and H. Cecilia, “Adsorption of nutrients using low-cost adsorbents from agricultural waste and by-products – review,” *Prog. Agric. Eng. Sci.*, vol. 14, no. 1, pp. 1–30, Dec. 2018, doi: 10.1556/446.14.2018.1.1.
- [97] J. L. Sotelo, G. Ovejero, A. Rodríguez, S. Álvarez, and J. García, “Study of Natural Clay Adsorbent Sepiolite for the Removal of Caffeine from Aqueous Solutions: Batch and Fixed-Bed Column Operation,” *Water, Air, Soil Pollut.*, vol. 224, no. 3, p. 1466, Mar. 2013, doi: 10.1007/s11270-013-1466-8.
- [98] J. Rouquerol, F. Rouquerol, P. Llewellyn, G. Maurin, and K. S. W. Sing, *Adsorption by powders and porous solids: principles, methodology and applications*. Academic press, 2013.
- [99] K. L. Tan and B. H. Hameed, “Insight into the adsorption kinetics models for the removal of contaminants from aqueous solutions,” *J. Taiwan Inst. Chem. Eng.*, vol. 74, pp. 25–48, May 2017, doi: 10.1016/j.jtice.2017.01.024.
- [100] N. B. Singh, G. Nagpal, S. Agrawal, and Rachna, “Water purification by using Adsorbents: A Review,” *Environ. Technol. Innov.*, vol. 11, pp. 187–240, Aug. 2018, doi: 10.1016/j.eti.2018.05.006.
- [101] K. Y. Foo and B. H. Hameed, “Insights into the modeling of adsorption isotherm systems,” *Chem. Eng. J.*, vol. 156, no. 1, pp. 2–10, Jan. 2010, doi: 10.1016/j.cej.2009.09.013.
- [102] A. B. Das, “separation, purification and application bioactive compounds from pigmented rice bran,” 2020, *Department of Chemical Engineering, Indian Institute of Technology Guwahati*. [Online]. Available: <http://gyan.iitg.ernet.in/handle/123456789/1787>
- [103] M. D. Alves, F. M. Aracri, É. C. Cren, and A. A. Mendes, “Isotherm, kinetic, mechanism and thermodynamic studies of adsorption of a microbial lipase on a mesoporous and hydrophobic resin,” *Chem. Eng. J.*, vol. 311, pp. 1–12, Mar. 2017, doi: 10.1016/j.cej.2016.11.069.
- [104] S. A. Sadeek, N. A. Negm, H. H. H. Hefni, and M. M. A. Wahab, “Metal adsorption by agricultural biosorbents: Adsorption isotherm, kinetic and biosorbents chemical structures,” *Int. J. Biol. Macromol.*, vol. 81, pp. 400–409, Nov. 2015, doi: 10.1016/j.ijbiomac.2015.08.031.
- [105] I. Anastopoulos, M. Karamesouti, A. C. Mitropoulos, and G. Z. Kyzas, “A review for coffee adsorbents,” *J. Mol. Liq.*, vol. 229, pp. 555–565, Mar. 2017, doi: 10.1016/j.molliq.2016.12.096.
- [106] G. K. Sarma, S. Sen Gupta, and K. G. Bhattacharyya, “Nanomaterials as versatile adsorbents for heavy metal ions in water: a review,” *Environ. Sci. Pollut. Res.*, vol. 26, no. 7, pp. 6245–6278, Mar. 2019, doi: 10.1007/s11356-018-04093-y.
- [107] J. Abdi, M. Vossoughi, N. M. Mahmoodi, and I. Alemzadeh, “Synthesis of metal-organic framework hybrid nanocomposites based on GO and CNT with high adsorption capacity for dye removal,” *Chem. Eng. J.*, vol. 326, pp. 1145–1158, Oct.

- 2017, doi: 10.1016/j.cej.2017.06.054.
- [108] V. Katheresan, J. Kansedo, and S. Y. Lau, "Efficiency of various recent wastewater dye removal methods: A review," *J. Environ. Chem. Eng.*, vol. 6, no. 4, pp. 4676–4697, Aug. 2018, doi: 10.1016/j.jece.2018.06.060.
- [109] N. Ballav, R. Das, S. Giri, A. M. Muliwa, K. Pillay, and A. Maity, "l-cysteine doped polypyrrole (PPy@L-Cyst): A super adsorbent for the rapid removal of Hg²⁺ and efficient catalytic activity of the spent adsorbent for reuse," *Chem. Eng. J.*, vol. 345, pp. 621–630, Aug. 2018, doi: 10.1016/j.cej.2018.01.093.
- [110] G. Crini, E. Lichtfouse, L. D. Wilson, and N. Morin-Crini, "Conventional and non-conventional adsorbents for wastewater treatment," *Environ. Chem. Lett.*, vol. 17, no. 1, pp. 195–213, Mar. 2019, doi: 10.1007/s10311-018-0786-8.
- [111] V. K. Gupta and Suhas, "Application of low-cost adsorbents for dye removal – A review," *J. Environ. Manage.*, vol. 90, no. 8, pp. 2313–2342, Jun. 2009, doi: 10.1016/j.jenvman.2008.11.017.
- [112] K. A. Adegoke and O. S. Bello, "Dye sequestration using agricultural wastes as adsorbents," *Water Resour. Ind.*, vol. 12, pp. 8–24, Dec. 2015, doi: 10.1016/j.wri.2015.09.002.
- [113] H. D. da Rocha *et al.*, "Use of PMMA/(rice husk ash)/polypyrrole membranes for the removal of dyes and heavy metal ions," *J. Taiwan Inst. Chem. Eng.*, vol. 110, pp. 8–20, May 2020, doi: 10.1016/j.jtice.2020.03.003.
- [114] S. Martini, S. Afroze, and K. Ahmad Roni, "Modified eucalyptus bark as a sorbent for simultaneous removal of COD, oil, and Cr(III) from industrial wastewater," *Alexandria Eng. J.*, vol. 59, no. 3, pp. 1637–1648, Jun. 2020, doi: 10.1016/j.aej.2020.04.010.
- [115] L. Mathurasa and S. Damrongsiri, "Low cost and easy rice husk modification to efficiently enhance ammonium and nitrate adsorption," *Int. J. Recycl. Org. Waste Agric.*, vol. 7, no. 2, pp. 143–151, Jun. 2018, doi: 10.1007/s40093-018-0200-3.
- [116] J. Mo, Q. Yang, N. Zhang, W. Zhang, Y. Zheng, and Z. Zhang, "A review on agro-industrial waste (AIW) derived adsorbents for water and wastewater treatment," *J. Environ. Manage.*, vol. 227, pp. 395–405, Dec. 2018, doi: 10.1016/j.jenvman.2018.08.069.
- [117] N. Bellahsen, G. Varga, N. Halyag, S. Kertész, E. Tombácz, and C. Hodúr, "Pomegranate peel as a new low-cost adsorbent for ammonium removal," *Int. J. Environ. Sci. Technol.*, vol. 18, no. 3, pp. 711–722, Mar. 2021, doi: 10.1007/s13762-020-02863-1.
- [118] R. Baby, B. Saifullah, and M. Z. Hussein, "Palm Kernel Shell as an effective adsorbent for the treatment of heavy metal contaminated water," *Sci. Rep.*, vol. 9, no. 1, p. 18955, Dec. 2019, doi: 10.1038/s41598-019-55099-6.
- [119] A. Zulkania, M. Iqbal, and Syamsumarlin, "Characterization of Adsorbents Derived from Palm Fiber Waste and its Potential on Methylene Blue Adsorption," *Key Eng. Mater.*, vol. 841, pp. 273–277, May 2020, doi: 10.4028/www.scientific.net/KEM.841.273.
- [120] P. T. Phan, T. T. Nguyen, N. H. Nguyen, and S. Padunghon, "Triamine-bearing activated rice husk ash as an advanced functional material for nitrate removal from aqueous solution," *Water Sci. Technol.*, vol. 79, no. 5, pp. 850–856, Mar. 2019, doi: 10.2166/wst.2018.445.
- [121] S. Mor, K. Chhoden, and K. Ravindra, "Application of agro-waste rice husk ash for the removal of phosphate from the wastewater," *J. Clean. Prod.*, vol. 129, pp. 673–680, Aug. 2016, doi: 10.1016/j.jclepro.2016.03.088.
- [122] T. Nguyen Thi *et al.*, "Study On The Removal Of Ammonia In Wastewater Using

- Adsorbent Prepared From Rice Hull With Magnesium Oxide Modification,” *Vietnam J. Sci. Technol.*, vol. 58, no. 3A, p. 113, May 2020, doi: 10.15625/2525-2518/58/3A/14322.
- [123] T. Mitra, N. Bar, and S. K. Das, “Rice husk: green adsorbent for Pb(II) and Cr(VI) removal from aqueous solution—column study and GA–NN modeling,” *SN Appl. Sci.*, vol. 1, no. 5, p. 486, May 2019, doi: 10.1007/s42452-019-0513-5.
- [124] W. H. Kwan and Y. S. Wong, “Acid leached rice husk ash (ARHA) in concrete: A review,” *Mater. Sci. Energy Technol.*, vol. 3, pp. 501–507, 2020, doi: 10.1016/j.mset.2020.05.001.
- [125] S. K. Shukla, “Rice Husk Derived Adsorbents for Water Purification,” in *Green Materials for Wastewater Treatment*, Springer, 2020, pp. 131–148. doi: 10.1007/978-3-030-17724-9_6.
- [126] O. Olawale and F. A. Oyawale, “Characterization of rice husk via atomic absorption spectrophotometer for optimal silica production,” *Int. J. Sci. Technol.*, vol. 2, no. 4, pp. 210–213, 2012, [Online]. Available: <http://citeseerx.ist.psu.edu/viewdoc/download?doi=10.1.1.301.1849&rep=rep1&type=pdf>
- [127] L. N. Ludueña, D. P. Fasce, V. A. Alvarez, and P. M. Stefani, “Nanocellulose from rice husk following alkaline treatment to remove silica,” *Bioresources*, vol. 6, no. 2, pp. 1440–1453, 2011, [Online]. Available: http://ojs.cnr.ncsu.edu/index.php/BioRes/article/view/BioRes_06_2_1440_Luduenaf_FAS_Nanocellulose_Rice_Husk
- [128] S. Mirmohamadsadeghi and K. Karimi, “Recovery of silica from rice straw and husk,” in *Current Developments in Biotechnology and Bioengineering*, Elsevier, 2020, pp. 411–433.
- [129] B. A. Goodman, “Utilization of waste straw and husks from rice production: A review,” *J. Bioresour. Bioprod.*, vol. 5, no. 3, pp. 143–162, Aug. 2020, doi: 10.1016/j.jobab.2020.07.001.
- [130] P. Chen, W. Gu, W. Fang, X. Ji, and R. Bie, “Removal of metal impurities in rice husk and characterization of rice husk ash under simplified acid pretreatment process,” *Environ. Prog. Sustain. Energy*, vol. 36, no. 3, pp. 830–837, May 2017, doi: 10.1002/ep.12513.
- [131] H. R. Ong, W. M. E. Iskandar, and M. M. R. Khan, “Rice Husk Nanosilica Preparation and Its Potential Application as Nanofluids,” in *Silver Nanoparticles-Health and Safety*, IntechOpen, 2019.
- [132] P. Sharma, R. Kaur, C. Baskar, and W.-J. Chung, “Removal of methylene blue from aqueous waste using rice husk and rice husk ash,” *Desalination*, vol. 259, no. 1–3, pp. 249–257, Sep. 2010, doi: 10.1016/j.desal.2010.03.044.
- [133] J. O. Quansah *et al.*, “Nascent Rice Husk as an Adsorbent for Removing Cationic Dyes from Textile Wastewater,” *Appl. Sci.*, vol. 10, no. 10, p. 3437, May 2020, doi: 10.3390/app10103437.
- [134] Y. Yusmaniar, E. Erdawati, Y. F. Ghifari, and D. P. Ubit, “Synthesis of mesopore silica composite from rice husk with activated carbon from coconut shell as adsorbent methyl orange color adsorbent,” *IOP Conf. Ser. Mater. Sci. Eng.*, vol. 830, p. 032078, May 2020, doi: 10.1088/1757-899X/830/3/032078.
- [135] K. Moeinian and S. M. Mehdinia, “Removing Methylene Blue from Aqueous Solutions Using Rice Husk Silica Adsorbent,” *Polish J. Environ. Stud.*, vol. 28, no. 4, pp. 2281–2287, Mar. 2019, doi: 10.15244/pjoes/91044.
- [136] M. P. da Rosa *et al.*, “A new approach to convert rice husk waste in a quick and efficient adsorbent to remove cationic dye from water,” *J. Environ. Chem. Eng.*, vol. 7,

- no. 61. da Rosa, M.P.; Igansi, A.V.; Lütke, S.F.; Sant'Anna Cadaval, T.R.; do Santos, A.C.R.; de Oliveira Lopes Inacio, A.P.; Almeida Pinto, L.A.; Beck, P.H. A New Approach to Convert Rice Husk Waste in a Quick and Efficient Adsorbent to Remove Cationic Dy, p. 103504, Dec. 2019, doi: 10.1016/j.jece.2019.103504.
- [137] A. Malik, A. Khan, N. Anwar, and M. Naem, "A comparative study of the adsorption of congo red dye on rice husk, rice husk char and chemically modified rice husk char from aqueous media," *Bull. Chem. Soc. Ethiop.*, vol. 34, no. 1, pp. 41–54, Apr. 2020, doi: 10.4314/bcse.v34i1.4.
- [138] I. Dahlan, H. M. Zwain, M. A. O. Seman, N. H. Baharuddin, and M. R. Othman, "Adsorption of brilliant green dye in aqueous medium using magnetic adsorbents prepared from rice husk ash," AIP Publishing LLC, 2019, p. 020017. doi: 10.1063/1.5117077.
- [139] W. Zou, K. Li, H. Bai, X. Shi, and R. Han, "Enhanced cationic dyes removal from aqueous solution by oxalic acid modified rice husk," *J. Chem. Eng. Data*, vol. 56, no. 5, pp. 1882–1891, 2011, doi: 10.1021/je100893h.
- [140] E. BAYRAK TEZCAN, Z. CEYLAN, and F. N. ACAR, "Kinetics, Isotherm and Thermodynamic Studies of The Adsorption Behavior of Basic Yellow 51 Onto Rice Husk and Burned Rice Husk," *J. Inst. Sci. Technol.*, vol. 9, no. November 2011, pp. 1977–1988, 2019, doi: 10.21597/jist.608915.
- [141] E. M. Osman, A. A. El-Ebissy, and M. N. Michael, "Characterization and Evaluation of the Levelness Parameters of Natural Dyes on Natural Fabrics," *Res. J. Text. Appar.*, vol. 13, no. 2, pp. 61–68, 2009, doi: 10.1108/RJTA-13-02-2009-B007.
- [142] Z. Zehra and M. N. Bashir, "Color fastness grading system for textile industry using CIEL*a*b color space," *2019 4th MEC Int. Conf. Big Data Smart City, ICBDS 2019*, pp. 1–5, 2019, doi: 10.1109/ICBDS.2019.8645600.
- [143] Amanda J. Thompson and Marcy L. Koontz, "Determining the True Color Measurements of Historic Dress with a Mobile Spectrophotometer and an Adapted Zone Grid System," *Int. J. Incl. Museum*, vol. 15, no. 1, 2021, doi: <http://doi.org/10.18848/1835-2014/CGP>.
- [144] T. Paul, M. C. Mugdho, R. Mia, and S. Sultana, "Investigation of color yield & color space between different parts of a garments body," *North Am. Acad. Res.*, vol. 2, no. November, pp. 18–33, 2019, doi: 10.5281/zenodo.3529872.
- [145] B. Raluca, "Fascicle of Textiles , Leatherwork a Review of Color Measurements in the Textile Industry," *Ann. Univ. Oradea Fascicle Text. Leatherwork*, vol. 17, no. 1, pp. 19–24, 2016.
- [146] V. Malm, M. Strååt, and P. Walkenström, "Effects of surface structure and substrate color on color differences in textile coatings containing effect pigments," *Text. Res. J.*, vol. 84, no. 2, pp. 125–139, 2014, doi: 10.1177/0040517513485626.
- [147] S. Noonpui and P. Thiravetyan, "Treatment of reactive azo dye from textile wastewater by burhead (*Echinodorus cordifolius* L.) in constructed wetland: Effect of molecular size," *J. Environ. Sci. Heal. - Part A Toxic/Hazardous Subst. Environ. Eng.*, vol. 46, no. 7, pp. 709–714, 2011, doi: 10.1080/10934529.2011.571577.
- [148] Mahyati *et al.*, "Biodegradation Of Lignin From Corn Cob By Using A Mixture Of Phanerochaete Chrysosporium , Lentinus Edodes And Pleurotus Ostreatus," *Int. J. Sci. Technol.*, vol. 2, no. 11, pp. 3–7, 2013, [Online]. Available: www.ijstr.org
- [149] M. El Khomri *et al.*, "Modification of low-cost adsorbent prepared from agricultural solid waste for the adsorption and desorption of cationic dye," *Emergent Mater.*, vol. 5, no. 6, pp. 1679–1688, 2022, doi: 10.1007/s42247-022-00390-y.
- [150] S. Moon and Y. Chae, "Colorful graphene-based wearable e-textiles prepared by co-dyeing cotton fabrics with natural dyes and reduced graphene oxide," *Sci. Rep.*, vol.

- 14, no. 1, pp. 1–13, 2024, doi: 10.1038/s41598-024-52850-6.
- [151] L. Nazari, S. Sarathy, D. Santoro, D. Ho, M. B. Ray, and C. (Charles) Xu, *Recent advances in energy recovery from wastewater sludge*. 2017. doi: 10.1016/B978-0-08-101029-7.00011-4.
- [152] E. de Jong and R. J. A. Gosselink, *Lignocellulose-Based Chemical Products*. Elsevier, 2014. doi: 10.1016/B978-0-444-59561-4.00017-6.
- [153] A. Kumar and C. K. Dixit, “Methods for characterization of nanoparticles,” in *Advances in nanomedicine for the delivery of therapeutic nucleic acids*, Elsevier, 2017, pp. 43–58.
- [154] P. S. Kumar, K. G. Pavithra, and M. Naushad, “Characterization techniques for nanomaterials,” in *Nanomaterials for Solar Cell Applications*, Elsevier, 2019, pp. 97–124.
- [155] J. H. Yuan, R. K. Xu, and H. Zhang, “The forms of alkalis in the biochar produced from crop residues at different temperatures,” *Bioresour. Technol.*, vol. 102, no. 3, pp. 3488–3497, 2011, doi: 10.1016/j.biortech.2010.11.018.
- [156] S. H. Chang, H. T. V. Lin, G. J. Wu, and G. J. Tsai, “pH Effects on solubility, zeta potential, and correlation between antibacterial activity and molecular weight of chitosan,” *Carbohydr. Polym.*, vol. 134, pp. 74–81, 2015, doi: 10.1016/j.carbpol.2015.07.072.
- [157] G. C. Pathiraja, D. K. De Silva, L. Dhanapala, and N. Nanayakkara, “Investigating the surface characteristics of chemically modified and unmodified rice husk ash; bottom-up approach for adsorptive removal of water contaminants,” *Desalin. Water Treat.*, vol. 54, no. 2, pp. 547–556, Apr. 2015, doi: 10.1080/19443994.2014.883133.
- [158] M. Antil, S. Singh, M. Bhagat, V. Vilvas, and S. Sundaramurthy, “Column optimization of adsorption and evaluation of bed parameters-based on removal of arsenite ion using rice husk,” *Environ. Sci. Pollut. Res.*, pp. 72279–72293, 2022, doi: 10.1007/s11356-022-20580-9.
- [159] S. D. Genieva, S. C. Turmanova, A. S. Dimitrova, and L. T. Vlaev, “Characterization of rice husks and the products of its thermal degradation in air or nitrogen atmosphere,” *J. Therm. Anal. Calorim.*, vol. 93, no. 2, pp. 387–396, Aug. 2008, doi: 10.1007/s10973-007-8429-5.
- [160] O. V. Ovchinnikov, A. V. Evtukhova, T. S. Kondratenko, M. S. Smirnov, V. Y. Khokhlov, and O. V. Erina, “Manifestation of intermolecular interactions in FTIR spectra of methylene blue molecules,” *Vib. Spectrosc.*, vol. 86, pp. 181–189, 2016, doi: 10.1016/j.vibspec.2016.06.016.
- [161] K. A. Phan, D. Phihusut, and N. Tuntiwiwattanapun, “Preparation of rice husk hydrochar as an atrazine adsorbent: Optimization, characterization, and adsorption mechanisms,” *J. Environ. Chem. Eng.*, vol. 10, no. 3, p. 107575, 2022, doi: 10.1016/j.jece.2022.107575.
- [162] J. Naranjo *et al.*, “Preparation of Adsorbent Materials from Rice Husk via Hydrothermal Carbonization: Optimization of Operating Conditions and Alkali Activation,” *Resources*, vol. 12, no. 12, 2023, doi: 10.3390/resources12120145.
- [163] Y. Ding *et al.*, “Influence of process water recirculation on hydrothermal carbonization of rice husk at different temperatures,” *J. Environ. Chem. Eng.*, vol. 11, no. 2, p. 109364, 2023, doi: 10.1016/j.jece.2023.109364.
- [164] A. Ahmad, P. Tamunaidu, G. Masafumi, and U. Motoo, “Effects of Rice Husk and Rice Straw Hydrochar as Soil Amendment,” *Chem. Eng. Trans.*, vol. 106, pp. 1225–1230, 2023, doi: 10.3303/CET23106205.
- [165] A. N. Labaran, Z. U. Zango, U. Armaya’u, and Z. N. Garba, “Rice Husk as Biosorbent for the Adsorption of Methylene Blue,” *Sci. World J.*, vol. 14, no. 2, pp. 66–70, 2019.

- [166] X. Y. Huang, H. T. Bu, G. B. Jiang, and M. H. Zeng, "Cross-linked succinyl chitosan as an adsorbent for the removal of Methylene Blue from aqueous solution," *Int. J. Biol. Macromol.*, vol. 49, no. 4, pp. 643–651, 2011, doi: 10.1016/j.ijbiomac.2011.06.023.
- [167] H. M. A. Hassan *et al.*, "Sulfanilic acid-functionalized magnetic GO as a robust adsorbent for the efficient adsorption of methylene blue from aqueous solution," *J. Mol. Liq.*, vol. 361, p. 119603, 2022, doi: 10.1016/j.molliq.2022.119603.
- [168] S. Kizito *et al.*, "Evaluation of slow pyrolyzed wood and rice husks biochar for adsorption of ammonium nitrogen from piggery manure anaerobic digestate slurry," *Sci. Total Environ.*, vol. 505, pp. 102–112, 2015.
- [169] B. H. Hameed and A. A. Ahmad, "Batch adsorption of methylene blue from aqueous solution by garlic peel, an agricultural waste biomass," *J. Hazard. Mater.*, vol. 164, no. 2–3, pp. 870–875, 2009, doi: 10.1016/j.jhazmat.2008.08.084.
- [170] Z. Z. Ismail and B. B. Hameed, "Recycling of raw corn cob residues as an agricultural waste material for ammonium removal: kinetics, isotherms, and mechanisms," *Int. J. Environ. Waste Manag.*, vol. 13, no. 3, pp. 217–230, 2014.
- [171] M. A. Patil, P. J. K. Shinde, A. L. Jadhav, and S. R. Deshpande, "Adsorption of methylene blue in waste water by low cost adsorbent rice husk .," *Int. J. Eng. Res. Technol.*, vol. 10, no. 1, pp. 246–252, 2017.
- [172] É. C. Lima, M. A. Adebayo, and F. M. Machado, "Kinetic and equilibrium models of adsorption," in *Carbon nanomaterials as adsorbents for environmental and biological applications*, Springer, 2015, pp. 33–69.
- [173] M. Sulyman, J. Namiesnik, and A. Gierak, "Low-cost Adsorbents Derived from Agricultural By-products/Wastes for Enhancing Contaminant Uptakes from Wastewater: A Review.," *Polish J. Environ. Stud.*, vol. 26, no. 3, 2017.
- [174] M. Sh. Gohr, A. I. Abd-Elhamid, A. A. El-Shanshory, and H. M. A. Soliman, "Adsorption of cationic dyes onto chemically modified activated carbon: Kinetics and thermodynamic study," *J. Mol. Liq.*, vol. 346, p. 118227, 2022, doi: 10.1016/j.molliq.2021.118227.
- [175] E. Worch, *Adsorption Technology in Water Treatment*. 2012. doi: 10.1515/9783110240238.
- [176] Y. H. Zhao, J. T. Geng, J. C. Cai, Y. F. Cai, and C. Y. Cao, "Adsorption performance of basic fuchsin on alkali-activated diatomite," *Adsorpt. Sci. Technol.*, vol. 38, no. 5–6, pp. 151–167, 2020, doi: 10.1177/0263617420922084.
- [177] C. Hodúr, N. Bellahsen, E. Mikó, V. Nagypál, Z. Šereš, and S. Kertész, "The adsorption of ammonium nitrogen from milking parlor wastewater using pomegranate peel powder for sustainable water, resources, and waste management," *Sustain.*, vol. 12, no. 12, 2020, doi: 10.3390/SU12124880.
- [178] C. H. Giles and D. Smith, "A General Treatment and Classification of the Solute Adsorption Isotherm," *Dep. Math. Univ. Strat. Glas. G1, Scotl.*, vol. 47, no. 3, pp. 755–765, 1973.
- [179] A. K. Ghosh, P. Mukerjee, A. K. Ghosh, P. Mukerjee, A. K. Ghosh, and P. Mukerjee, "Multiple Association Equilibria in the Self-Association of Methylene Blue and Other Dyes," *J. Am. Chem. Soc.*, vol. 92, no. 22, pp. 6408–6412, 1970, doi: 10.1021/ja00725a003.
- [180] H. Li *et al.*, "Enhanced adsorptive removal of anionic and cationic dyes from single or mixed dye solutions using MOF PCN-222," *RSC Adv.*, vol. 7, no. 27, pp. 16273–16281, 2017, doi: 10.1039/c7ra01647f.
- [181] K. Fujita, K. Taniguchi, and H. Ohno, "Dynamic analysis of aggregation of methylene blue with polarized optical waveguide spectroscopy," *Talanta*, vol. 65, no. 5, pp. 1066–1070, 2005, doi: 10.1016/j.talanta.2004.04.044.

- [182] M. Karimi Goftar, K. Moradi, and N. M. Kor, "Spectroscopic studies on aggregation phenomena of dyes," *Eur. J. Exp. Biol.*, vol. 4, no. 2, pp. 72–81, 2014.
- [183] A. Fernández-Pérez, T. Valdés-Solís, and G. Marbán, "Visible light spectroscopic analysis of Methylene Blue in water; the resonance virtual equilibrium hypothesis," *Dye. Pigment.*, vol. 161, no. October 2018, pp. 448–456, 2019, doi: 10.1016/j.dyepig.2018.09.083.
- [184] A. Fernandez-Perez and G. Marban, "Visible light spectroscopic analysis of methylene blue in water; what comes after dimer?," *ACS Omega*, vol. 5, no. 46, pp. 29801–29815, 2020, doi: 10.1021/acsomega.0c03830.
- [185] E. Morgounova, Q. Shao, B. J. Hackel, D. D. Thomas, and S. Ashkenazi, "Photoacoustic lifetime contrast between methylene blue monomers and self-quenched dimers as a model for dual-labeled activatable probes," *J. Biomed. Opt.*, vol. 18, no. 5, p. 056004, 2013, doi: 10.1117/1.jbo.18.5.056004.
- [186] B. Pathrose, V. P. N. Nampoori, P. Radhakrishnan, and A. Mujeeb, "Measurement of absolute fluorescence quantum yield of basic fuchsin solution using a dual-beam thermal lens technique," *J. Fluoresc.*, vol. 24, no. 3, pp. 895–898, 2014, doi: 10.1007/s10895-014-1369-0.
- [187] W. D. Harkins and G. Jura, "Surfaces of Solids. XI. Determination of Decrease (π) of Free Surface Energy of a Solid by Adsorbed Film," *J. Am. Chem. Soc.*, vol. 66, pp. 1356–1362, 1944.
- [188] M. Hadi, M. R. Samarghandi, and G. McKay, "Equilibrium two-parameter isotherms of acid dyes sorption by activated carbons: Study of residual errors," *Chem. Eng. J.*, vol. 160, no. 2, pp. 408–416, 2010, doi: 10.1016/j.cej.2010.03.016.
- [189] M. A. Al-Ghouti and D. A. Da'ana, "Guidelines for the use and interpretation of adsorption isotherm models: A review," 2020. doi: 10.1016/j.jhazmat.2020.122383.
- [190] A. Ebadi, J. S. Soltan Mohammadzadeh, and A. Khudiev, "What is the correct form of BET isotherm for modeling liquid phase adsorption?," *Adsorption*, vol. 15, no. 1, pp. 65–73, 2009, doi: 10.1007/s10450-009-9151-3.
- [191] V. H. Vargas, R. R. Paveglio, P. de S. Pauletto, N. P. G. Salau, and L. G. Dotto, "Sisal fiber as an alternative and cost-effective adsorbent for the removal of methylene blue and reactive black 5 dyes from aqueous solutions," *Chem. Eng. Commun.*, vol. 207, no. 4, pp. 523–536, 2020, doi: 10.1080/00986445.2019.1605362.
- [192] L. N. Côrtes *et al.*, "Biochars from animal wastes as alternative materials to treat colored effluents containing basic red 9," *J. Environ. Chem. Eng.*, vol. 7, no. 6, p. 103446, 2019, doi: 10.1016/j.jece.2019.103446.
- [193] N. H. Razak, Hazmi F.A, and Tahrim A.A, "Comparative Adsorption Studies by Using Low Cost Adsorbents of Rice Husk and Rice Husk Ash on Methylene Blue Dye Removal," *J. Eng. Technol.*, vol. 4, no. 2, pp. 40–48, 2013, [Online]. Available: <http://journal.utem.edu.my/index.php/jet/article/view/248/163>
- [194] P. Suresh Kumar, L. Korving, K. J. Keesman, M. C. M. van Loosdrecht, and G. J. Witkamp, "Effect of pore size distribution and particle size of porous metal oxides on phosphate adsorption capacity and kinetics," *Chem. Eng. J.*, vol. 358, no. July 2018, pp. 160–169, 2019, doi: 10.1016/j.cej.2018.09.202.
- [195] F. Kazembeigi *et al.*, "Removal of Methylene Blue from Aqueous Solutions using Raw and Modified Rice Husk," *Veliger*, vol. 53, pp. 1–7, 2014, doi: 10.13140/RG.2.1.3726.3204.
- [196] D. S. P. Franco, E. H. Tanabe, D. A. Bertuol, G. S. Dos Reis, É. C. Lima, and G. L. Dotto, "Alternative treatments to improve the potential of rice husk as adsorbent for methylene blue," *Water Sci. Technol.*, vol. 75, no. 2, pp. 296–305, 2017, doi: 10.2166/wst.2016.504.

- [197] S. Chandrasekhar, K. G. Satyanarayana, P. N. Pramada, P. Raghavan, and T. N. Gupta, "Processing, properties and applications of reactive silica from rice husk - An overview," *J. Mater. Sci.*, vol. 38, no. 15, pp. 3159–3168, 2003, doi: 10.1023/A:1025157114800.
- [198] J. Kong, L. Huang, Q. Yue, and B. Gao, "Preparation of activated carbon derived from leather waste by H₃PO₄ activation and its application for basic fuchsin adsorption," *Desalin. Water Treat.*, vol. 52, no. 13–15, pp. 2440–2449, 2014, doi: 10.1080/19443994.2013.794713.
- [199] B. Kizilkaya, "Usage of Biogenic Apatite (Fish Bones) on Removal of Basic Fuchsin Dye from Aqueous Solution," *J. Dispers. Sci. Technol.*, vol. 33, no. 11, pp. 1596–1602, 2012, doi: 10.1080/01932691.2011.629497.
- [200] E. O. Oyelude, F. Frimpong, and D. Dawson, "Studies on the removal of basic fuchsin dye from aqueous solution by HCl treated malted sorghum mash," *J. Mater. Environ. Sci.*, vol. 6, no. 4, pp. 1126–1136, 2015.
- [201] C. Li *et al.*, "Fast adsorption of methylene blue, basic fuchsin, and malachite green by a novel sulfonic-grafted triptycene-based porous organic polymer," *RSC Adv.*, vol. 8, no. 73, pp. 41986–41993, 2018, doi: 10.1039/c8ra09012b.
- [202] X. Chen and C. J. M. Chin, "Adsorption and desorption of crystal violet and basic red 9 by multi-walled carbon nanotubes," *Water Sci. Technol.*, vol. 79, no. 8, pp. 1541–1549, 2019, doi: 10.2166/wst.2019.157.
- [203] M. El-Azazy, A. S. El-Shafie, A. Ashraf, and A. A. Issa, "Eco-structured biosorptive removal of basic fuchsin using pistachio nutshells: A definitive screening design-based approach," *Appl. Sci.*, vol. 9, no. 22, 2019, doi: 10.3390/app9224855.
- [204] W. Bessashia, Y. Berredjem, Z. Hattab, and M. Bououdina, "Removal of Basic Fuchsin from water by using mussel powdered eggshell membrane as novel bioadsorbent: Equilibrium, kinetics, and thermodynamic studies," *Environ. Res.*, vol. 186, no. February, p. 109484, 2020, doi: 10.1016/j.envres.2020.109484.
- [205] S. I. Naji and K. K. Jasim, "Adsorption study of basic fuchsin dye on the astragalus root surface in al-muthanna province," *Syst. Rev. Pharm.*, vol. 12, no. 1, pp. 850–857, 2021, doi: 10.31838/srp.2021.1.120.
- [206] S. Lagergren, "Zur theorie der sogenannten adsorption gelöster stoffe (Theory of adsorption substances from solution)," *K. Sven. Vetenskapsakademiens, Handl.*, vol. 24, pp. 1–39, 1898.
- [207] Y. S. Ho and G. McKay, "Pseudo-second order model for sorption processes," *Process Biochem.*, vol. 34, no. 5, pp. 451–465, 1999, doi: [https://doi.org/10.1016/S0032-9592\(98\)00112-5](https://doi.org/10.1016/S0032-9592(98)00112-5).
- [208] S. Liu, H. Ge, S. Cheng, and Y. Zou, "Green synthesis of magnetic 3D bio-adsorbent by corn straw core and chitosan for methylene blue removal," *Environ. Technol. (United Kingdom)*, vol. 41, no. 16, pp. 2109–2121, 2020, doi: 10.1080/09593330.2018.1556345.
- [209] H. Qiu, L. Lv, B. C. Pan, Q. J. Zhang, W. M. Zhang, and Q. X. Zhang, "Critical review in adsorption kinetic models," *J. Zhejiang Univ. Sci. A*, vol. 10, no. 5, pp. 716–724, 2009, doi: 10.1631/jzus.A0820524.
- [210] H. Guo *et al.*, "Camellia oleifera seed shell carbon as an efficient renewable bio-adsorbent for the adsorption removal of hexavalent chromium and methylene blue from aqueous solution," *J. Mol. Liq.*, vol. 249, pp. 629–636, 2018, doi: 10.1016/j.molliq.2017.11.096.
- [211] F. Olivito *et al.*, "Cellulose citrate: A convenient and reusable bio-adsorbent for effective removal of methylene blue dye from artificially contaminated water," *RSC Adv.*, vol. 11, no. 54, pp. 34309–34318, 2021, doi: 10.1039/d1ra05464c.

- [212] J. X. Yu, L. Y. Wang, R. A. Chi, Y. F. Zhang, Z. G. Xu, and J. Guo, "Removal of cationic dyes: Basic magenta and methylene blue from aqueous solution by adsorption on modified loofah," *Res. Chem. Intermed.*, vol. 39, no. 8, pp. 3775–3790, 2013, doi: 10.1007/s11164-012-0880-7.
- [213] M. A. Hubbe, S. Azizian, and S. Douven, "Implications of Apparent Pseudo-Second-Order Adsorption Kinetics onto Cellulosic Materials: Review," *BioResources*, vol. 14, no. 3, pp. 7582–7626, 2019.
- [214] F. Liu, K. C. Kollipara Venkata Sai, and W. Zhang, "Conversion of Spiky Sweetgum tree (*Liquidambar styraciflua*) Seeds as into Bio-adsorbent: Static and Dynamic Adsorption Assessment," *J. Hazard. Mater. Adv.*, vol. 1, no. May, p. 100001, 2021, doi: 10.1016/j.hazadv.2021.100001.
- [215] Z. M. Şenol, N. El Messaoudi, Y. Fernine, and Z. S. Keskin, "Bioremoval of rhodamine B dye from aqueous solution by using agricultural solid waste (almond shell): experimental and DFT modeling studies," *Biomass Convers. Biorefinery*, no. 0123456789, 2023, doi: 10.1007/s13399-023-03781-1.
- [216] S. Bentahar, A. Dbik, M. El Khomri, N. El Messaoudi, and A. Lacherai, "Adsorption of methylene blue, crystal violet and congo red from binary and ternary systems with natural clay: Kinetic, isotherm, and thermodynamic," *J. Environ. Chem. Eng.*, vol. 5, no. 6, pp. 5921–5932, 2017, doi: 10.1016/j.jece.2017.11.003.
- [217] A. Al Ashik, M. A. Rahman, D. Halder, and M. M. Hossain, "Removal of methylene blue from aqueous solution by coconut coir dust as a low-cost adsorbent," *Appl. Water Sci.*, vol. 13, no. 3, pp. 1–11, 2023, doi: 10.1007/s13201-023-01887-5.
- [218] M. A. Zayed, S. A. Abdel-Gawad, H. M. Abdel-Aziz, and Z. A. Abo-Ayad, "Green Synthesis of Nano-Zero-Valent Copper for the D-Blue 60 Textile Dye Removal from Aqueous Medium," *Int. J. Environ. Res.*, vol. 17, no. 1, pp. 1–14, 2023, doi: 10.1007/s41742-022-00499-2.
- [219] M. El Khomri *et al.*, "Optimization Based on Response Surface Methodology of Anionic Dye Desorption From Two Agricultural Solid Wastes," *Chem. Africa*, vol. 5, no. 4, pp. 1083–1095, 2022, doi: 10.1007/s42250-022-00395-4.
- [220] M. El-Kammah, E. Elkhatib, S. Gouveia, C. Cameselle, and E. Aboukila, "Enhanced removal of Indigo Carmine dye from textile effluent using green cost-efficient nanomaterial: Adsorption, kinetics, thermodynamics and mechanisms," *Sustain. Chem. Pharm.*, vol. 29, no. June, p. 100753, 2022, doi: 10.1016/j.scp.2022.100753.
- [221] R. K. Sharma, R. Kumar, and A. P. Singh, "Metal ions and organic dyes sorption applications of cellulose grafted with binary vinyl monomers," *Sep. Purif. Technol.*, vol. 209, no. August 2018, pp. 684–697, 2019, doi: 10.1016/j.seppur.2018.09.011.
- [222] S. M. Miraboutalebi, S. K. Nikouzad, M. Peydayesh, N. Allahgholi, L. Vafajoo, and G. McKay, "Methylene blue adsorption via maize silk powder: Kinetic, equilibrium, thermodynamic studies and residual error analysis," *Process Saf. Environ. Prot.*, vol. 106, pp. 191–202, 2017, doi: 10.1016/j.psep.2017.01.010.
- [223] F. B. Scheufele *et al.*, "Monolayer-multilayer adsorption phenomenological model: Kinetics, equilibrium and thermodynamics," *Chem. Eng. J.*, vol. 284, pp. 1328–1341, 2016, doi: 10.1016/j.cej.2015.09.085.
- [224] O. Aksakal and H. Ucu, "Equilibrium, kinetic and thermodynamic studies of the biosorption of textile dye (Reactive Red 195) onto *Pinus sylvestris* L.," *J. Hazard. Mater.*, vol. 181, no. 1–3, pp. 666–672, 2010, doi: 10.1016/j.jhazmat.2010.05.064.
- [225] A. Maleki *et al.*, "Amine functionalized multi-walled carbon nanotubes: Single and binary systems for high capacity dye removal," *Chem. Eng. J.*, vol. 313, pp. 826–835, 2017, doi: 10.1016/j.cej.2016.10.058.
- [226] G. de V. Brião, M. G. C. da Silva, M. G. A. Vieira, and K. H. Chu, "Correlation of

- type II adsorption isotherms of water contaminants using modified BET equations,” *Colloids Interface Sci. Commun.*, vol. 46, 2022, doi: 10.1016/j.colcom.2021.100557.
- [227] A. Ebadi, J. S. Soltan Mohammadzadeh, and A. Khudiev, “Adsorption of methyl tert-butyl ether on perfluorooctyl alumina adsorbents - High concentration range,” *Chem. Eng. Technol.*, vol. 30, no. 12, pp. 1666–1673, 2007, doi: 10.1002/ceat.200700201.
- [228] D. L. Rossatto, M. S. Netto, S. L. Jahn, E. S. Mallmann, G. L. Dotto, and E. L. Foletto, “Highly efficient adsorption performance of a novel magnetic geopolymer/Fe₃O₄ composite towards removal of aqueous acid green 16 dye,” *J. Environ. Chem. Eng.*, vol. 8, no. 3, p. 103804, 2020, doi: 10.1016/j.jece.2020.103804.
- [229] A. N. Módenes *et al.*, “A new alternative to use soybean hulls on the adsorptive removal of aqueous dyestuff,” *Bioresour. Technol. Reports*, vol. 6, no. March, pp. 175–182, 2019, doi: 10.1016/j.biteb.2019.03.004.
- [230] A. N. Módenes *et al.*, “Assessment of the banana pseudostem as a low-cost biosorbent for the removal of reactive blue 5G dye,” *Environ. Technol. (United Kingdom)*, vol. 36, no. 22, pp. 2892–2902, 2015, doi: 10.1080/09593330.2015.1051591.
- [231] N. El Messaoudi *et al.*, “Regeneration and reusability of non-conventional low-cost adsorbents to remove dyes from wastewaters in multiple consecutive adsorption–desorption cycles: a review,” *Biomass Convers. Biorefinery*, no. 0123456789, 2022, doi: 10.1007/s13399-022-03604-9.
- [232] A. Regti, H. B. El Ayouchia, M. R. Laamari, S. E. Stiriba, H. Anane, and M. El Haddad, “Experimental and theoretical study using DFT method for the competitive adsorption of two cationic dyes from wastewaters,” *Appl. Surf. Sci.*, vol. 390, pp. 311–319, 2016, doi: 10.1016/j.apsusc.2016.08.059.
- [233] A. Regti, A. El Kassimi, M. R. Laamari, and M. El Haddad, “Competitive adsorption and optimization of binary mixture of textile dyes: A factorial design analysis,” *J. Assoc. Arab Univ. Basic Appl. Sci.*, vol. 24, pp. 1–9, 2017, doi: 10.1016/j.jaubas.2016.07.005.
- [234] A. A. Nayl *et al.*, “A novel method for highly effective removal and determination of binary cationic dyes in aqueous media using a cotton-graphene oxide composite,” *RSC Adv.*, vol. 10, no. 13, pp. 7791–7802, 2020, doi: 10.1039/c9ra09872k.
- [235] Y. Achour and E. K. Aziz, “Simultaneous Removal of Binary Mixture of Cationic Dyes onto Bombax Buonopozense Bark: Plackett–Burman and Central Composite Design,” *Biointerface Res. Appl. Chem.*, vol. 12, no. 1, pp. 326–338, 2021, doi: 10.33263/briac121.326338.
- [236] R. L. Tseng, H. N. Tran, and R. S. Juang, “Revisiting temperature effect on the kinetics of liquid–phase adsorption by the Elovich equation: A simple tool for checking data reliability,” *J. Taiwan Inst. Chem. Eng.*, vol. 136, no. March, p. 104403, 2022, doi: 10.1016/j.jtice.2022.104403.
- [237] A. N. M. A. Haque, R. Remadevi, X. Wang, and M. Naebe, “Adsorption of anionic Acid Blue 25 on chitosan-modified cotton gin trash film,” *Cellulose*, vol. 27, no. 16, pp. 9437–9456, 2020, doi: 10.1007/s10570-020-03409-x.
- [238] E. T. Acar, “An experimental and theoretical investigation of cationic azine dye adsorption on natural sepiolite in single and multi-component systems,” *Chem. Eng. Res. Des.*, vol. 187, pp. 507–515, 2022, doi: 10.1016/j.cherd.2022.09.013.
- [239] T. Shahnaz, D. Bedadeep, and S. Narayanasamy, “Investigation of the adsorptive removal of methylene blue using modified nanocellulose,” *Int. J. Biol. Macromol.*, vol. 200, no. August 2021, pp. 162–171, 2022, doi: 10.1016/j.ijbiomac.2021.12.081.
- [240] A. S. Al-Wasidi, I. I. S. AlZahrani, H. I. Thawibaraka, A. M. Naglah, M. G. El-Desouky, and M. A. El-Bindary, “Adsorption studies of carbon dioxide and anionic dye on green adsorbent,” *J. Mol. Struct.*, vol. 1250, p. 131736, 2022, doi:

- 10.1016/j.molstruc.2021.131736.
- [241] C. Manera, A. P. Tonello, D. Perondi, and M. Godinho, “Adsorption of leather dyes on activated carbon from leather shaving wastes: kinetics, equilibrium and thermodynamics studies,” *Environ. Technol. (United Kingdom)*, vol. 40, no. 21, pp. 2756–2768, 2019, doi: 10.1080/09593330.2018.1452984.
- [242] M. Gheibi, M. Eftekhari, M. G. Tabrizi, A. M. Fathollahi-Fard, and G. Tian, “Mechanistic evaluation of cationic dyes adsorption onto low-cost calcinated aerated autoclaved concrete wastes,” *Int. J. Environ. Sci. Technol.*, vol. 19, no. 7, pp. 6429–6444, 2022, doi: 10.1007/s13762-021-03576-9.
- [243] L. Su *et al.*, “Activated biochar derived from spent *Auricularia auricula* substrate for the efficient adsorption of cationic azo dyes from single and binary adsorptive systems,” *Water Sci. Technol.*, vol. 84, no. 1, pp. 101–121, 2021, doi: 10.2166/wst.2021.222.
- [244] A. Mirzaei, Z. Chen, F. Haghghat, and L. Yerushalmi, “Enhanced adsorption of anionic dyes by surface fluorination of zinc oxide: A straightforward method for numerical solving of the ideal adsorbed solution theory (IAST),” *Chem. Eng. J.*, vol. 330, pp. 407–418, 2017, doi: 10.1016/j.cej.2017.07.035.
- [245] S. Sultana *et al.*, “Adsorption of crystal violet dye by coconut husk powder: Isotherm, kinetics and thermodynamics perspectives,” *Environ. Nanotechnology, Monit. Manag.*, vol. 17, no. May 2021, p. 100651, 2022, doi: 10.1016/j.enmm.2022.100651.
- [246] S. Sahu *et al.*, “Adsorption of methylene blue on chemically modified lychee seed biochar: Dynamic, equilibrium, and thermodynamic study,” *J. Mol. Liq.*, vol. 315, p. 113743, 2020, doi: 10.1016/j.molliq.2020.113743.
- [247] S. Chowdhury, R. Mishra, P. Saha, and P. Kushwaha, “Adsorption thermodynamics, kinetics and isosteric heat of adsorption of malachite green onto chemically modified rice husk,” *Desalination*, vol. 265, no. 1–3, pp. 159–168, 2011, doi: 10.1016/j.desal.2010.07.047.
- [248] A. Kausar *et al.*, “Cellulose-based materials and their adsorptive removal efficiency for dyes: A review,” *Int. J. Biol. Macromol.*, vol. 224, no. July 2022, pp. 1337–1355, 2023, doi: 10.1016/j.ijbiomac.2022.10.220.
- [249] T. Saeed *et al.*, “Synthesis of chitosan composite of metal-organic framework for the adsorption of dyes; kinetic and thermodynamic approach,” *J. Hazard. Mater.*, vol. 427, no. June 2021, p. 127902, 2022, doi: 10.1016/j.jhazmat.2021.127902.
- [250] S. Mtaallah, I. Marzouk, and B. Hamrouni, “Factorial experimental design applied to adsorption of cadmium on activated alumina,” *J. Water Reuse Desalin.*, vol. 8, no. 1, pp. 76–85, 2018, doi: 10.2166/wrd.2017.112.
- [251] N. Özbay, A. Ş. Yargıç, R. Z. Yarbay-Şahin, and E. Önal, “Full factorial experimental design analysis of reactive dye removal by carbon adsorption,” *J. Chem.*, vol. 2013, 2013, doi: 10.1155/2013/234904.
- [252] N. Bellahsen *et al.*, “Iron-loaded pomegranate peel as a bio-adsorbent for phosphate removal,” *Water (Switzerland)*, vol. 13, no. 19, 2021, doi: 10.3390/w13192709.
- [253] A. K. Hegazy, N. T. Abdel-Ghani, and G. A. El-Chaghaby, “Adsorption of phenol onto activated carbon from *Rhazya stricta*: determination of the optimal experimental parameters using factorial design,” *Appl. Water Sci.*, vol. 4, no. 3, pp. 273–281, 2014, doi: 10.1007/s13201-013-0143-9.
- [254] D. Hank, Z. Azi, S. Ait Hocine, O. Chaalal, and A. Hellal, “Optimization of phenol adsorption onto bentonite by factorial design methodology,” *J. Ind. Eng. Chem.*, vol. 20, no. 4, pp. 2256–2263, 2014, doi: 10.1016/j.jiec.2013.09.058.
- [255] F. Geyikçi and H. Büyükgüngör, “Factorial experimental design for adsorption silver ions from water onto montmorillonite,” *Acta Geodyn. Geomater.*, vol. 10, no. 3, pp.

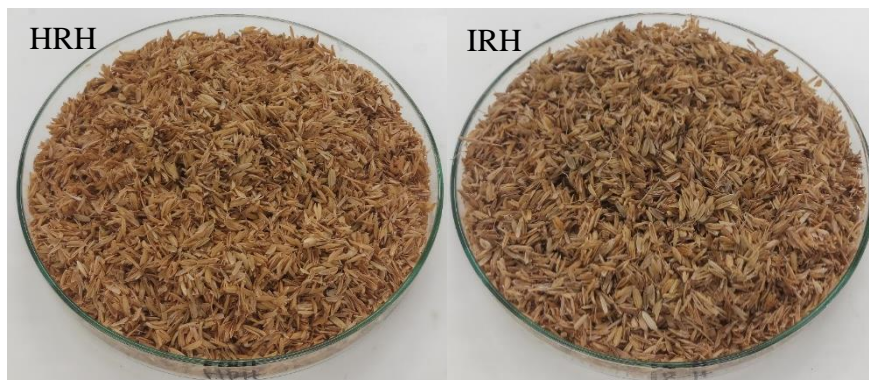
- 363–370, 2013, doi: 10.13168/AGG.2013.0035.
- [256] T. A. Saleh, M. Tuzen, and A. Sari, “Polyamide magnetic palygorskite for the simultaneous removal of Hg(II) and methyl mercury; with factorial design analysis,” *J. Environ. Manage.*, vol. 211, pp. 323–333, 2018, doi: 10.1016/j.jenvman.2018.01.050.
- [257] Y. Li, M. Wang, J. Liu, L. Han, Q. Qin, and X. Liu, “Adsorption/desorption behavior of ionic dyes on sintered bone char,” *Mater. Chem. Phys.*, vol. 297, no. January, p. 127405, 2023, doi: 10.1016/j.matchemphys.2023.127405.
- [258] H. Sukmana, E. Tombáč, G. Ballai, G. Kozma, Z. Kónya, and C. Hodúr, “Comparative Study of Adsorption of Methylene Blue and Basic Red 9 Using Rice Husks of Different Origins,” *Recycling*, vol. 8, no. 5, pp. 1–20, Sep. 2023, doi: 10.3390/recycling8050074.
- [259] Z. Lin *et al.*, “Nitrogen-doped hydrochar prepared by biomass and nitrogen-containing wastewater for dye adsorption: Effect of nitrogen source in wastewater on the adsorption performance of hydrochar,” *J. Environ. Manage.*, vol. 334, no. December 2022, p. 117503, 2023, doi: 10.1016/j.jenvman.2023.117503.
- [260] N. A. Rosli, M. A. Ahmad, and T. U. Noh, “Unleashing the potential of pineapple peel-based activated carbon: Response surface methodology optimization and regeneration for methylene blue and methyl red dyes adsorption,” *Inorg. Chem. Commun.*, vol. 155, no. July, p. 111041, 2023, doi: 10.1016/j.inoche.2023.111041.
- [261] S. Sudan, A. Khajuria, and J. Kaushal, “Adsorption potential of pristine biochar synthesized from rice husk waste for the removal of Eriochrome black azo dye,” *Mater. Today Proc.*, no. xxxx, 2023, doi: 10.1016/j.matpr.2023.01.258.
- [262] A. A. Hambisa, M. B. Regasa, H. G. Ejigu, and C. B. Senbeto, “Adsorption studies of methyl orange dye removal from aqueous solution using Anchote peel-based agricultural waste adsorbent,” *Appl. Water Sci.*, vol. 13, no. 1, pp. 1–11, 2023, doi: 10.1007/s13201-022-01832-y.
- [263] F. H. A. Mustafa, E. K. M. Gad ElRab, R. M. Kamel, and R. F. M. Elshaarawy, “Cost-effective removal of toxic methylene blue dye from textile effluents by new integrated crosslinked chitosan/aspartic acid hydrogels,” *Int. J. Biol. Macromol.*, vol. 248, no. July, p. 125986, 2023, doi: 10.1016/j.ijbiomac.2023.125986.
- [264] M. A. Dar, M. Anas, K. Kajal, S. Kumar, and G. Kaushik, “Adsorptive removal of crystal violet dye by *Azadirachta indica* (neem) sawdust: A low-cost bio-sorbent,” *Acta Ecol. Sin.*, vol. 43, no. 6, pp. 1049–1057, 2023, doi: 10.1016/j.chnaes.2023.02.011.
- [265] S. T. Nipa *et al.*, “Adsorption of methylene blue on papaya bark fiber: Equilibrium, isotherm and kinetic perspectives,” *Results Eng.*, vol. 17, no. December 2022, p. 100857, 2023, doi: 10.1016/j.rineng.2022.100857.
- [266] R. Zein, L. Hevira, Zilfa, Rahmayeni, S. Fauzia, and J. O. Ighalo, “The improvement of indigo carmine dye adsorption by *Terminalia catappa* shell modified with broiler egg white,” *Biomass Convers. Biorefinery*, vol. 13, no. 15, pp. 13795–13812, 2023, doi: 10.1007/s13399-021-02290-3.
- [267] P. Vairavel, N. Rampal, and G. Jeppu, “Adsorption of toxic Congo red dye from aqueous solution using untreated coffee husks: kinetics, equilibrium, thermodynamics and desorption study,” *Int. J. Environ. Anal. Chem.*, vol. 103, no. 12, pp. 2789–2808, 2023, doi: 10.1080/03067319.2021.1897982.
- [268] S. Wattanasiriwech, M. Naradisorn, and D. Wattanasiriwech, “Adsorption performance of macadamia husk-activated carbon from a household pyrolysis kiln,” *Green Mater.*, vol. 11, no. 3, pp. 137–144, 2023, doi: 10.1680/jgrma.22.00096.
- [269] G. Zhou, S. Li, Q. Meng, C. Niu, X. Zhang, and Q. Wang, “A new type of highly efficient fir sawdust-based super adsorbent: Remove cationic dyes from wastewater,”

- Surfaces and Interfaces*, vol. 36, no. January, p. 102637, 2023, doi: 10.1016/j.surfin.2023.102637.
- [270] B. Isik, S. Avci, F. Cakar, and O. Cankurtaran, “Adsorptive removal of hazardous dye (crystal violet) using bay leaves (*Laurus nobilis* L.): surface characterization, batch adsorption studies, and statistical analysis,” *Environ. Sci. Pollut. Res.*, vol. 30, no. 1, pp. 1333–1356, 2023, doi: 10.1007/s11356-022-22278-4.
- [271] T. H. Tran *et al.*, “Adsorption isotherms and kinetic modeling of methylene blue dye onto a carbonaceous hydrochar adsorbent derived from coffee husk waste,” *Sci. Total Environ.*, vol. 725, p. 138325, 2020, doi: 10.1016/j.scitotenv.2020.138325.
- [272] T. J. M. Fraga *et al.*, “Amino-Fe₃O₄-functionalized multi-layered graphene oxide as an ecofriendly and highly effective nanoscavenger of the reactive drimaren red,” *Environ. Sci. Pollut. Res.*, vol. 27, no. 9, pp. 9718–9732, 2020, doi: 10.1007/s11356-019-07539-z.
- [273] I. Langmuir, “The adsorption of gases on plane surfaces of glass, mica and platinum,” *J. Am. Chem. Soc.*, vol. 40, no. 9, pp. 1361–1403, 1918.
- [274] V. K. Gupta, R. Jain, T. A. Saleh, A. Nayak, S. Malathi, and S. Agarwal, “Equilibrium and Thermodynamic studies on the removal and recovery of Safranin-T dye from industrial effluents,” *Sep. Sci. Technol.*, vol. 46, no. 5, pp. 839–846, 2011, doi: 10.1080/01496395.2010.535591.
- [275] H. M. F. Freundlich, “Over the adsorption in solution,” *J. Phys. chem*, vol. 57, no. 385471, pp. 1100–1107, 1906.
- [276] A. Imessoudene *et al.*, “Adsorption Performance of Zeolite for the Removal of Congo Red Dye: Factorial Design Experiments, Kinetic, and Equilibrium Studies,” *Separations*, vol. 10, no. 1, 2023, doi: 10.3390/separations10010057.
- [277] Y. Bulut and H. Aydin, “A kinetics and thermodynamics study of methylene blue adsorption on wheat shells,” *Desalination*, vol. 194, no. 1–3, pp. 259–267, 2006, doi: 10.1016/j.desal.2005.10.032.
- [278] M. C. Holliday, D. R. Parsons, and S. H. Zein, “Agricultural Pea Waste as a Low-Cost Pollutant Biosorbent for Methylene Blue Removal: Adsorption Kinetics, Isotherm And Thermodynamic Studies,” *Biomass Convers. Biorefinery*, no. 0123456789, 2022, doi: 10.1007/s13399-022-02865-8.
- [279] A. H. Alabi, E. O. Oladele, A. J. O. Adeleke, F. C. Oni, and C. A. Olanrewaju, “Equilibrium, Kinetic and Thermodynamic Studies of Biosorption of Methylene Blue on Goethite Modified Baobab Fruit Pod (*Adansonia Digitata* L.),” *J. Appl. Sci. Environ. Manag.*, vol. 24, no. 7, pp. 1229–1243, 2020, doi: 10.4314/jasem.v24i7.16.
- [280] H. Sukmana *et al.*, “Hungarian and Indonesian rice husk as bioadsorbents for binary biosorption of cationic dyes from aqueous solutions: A factorial design analysis,” *Heliyon*, vol. 9, no. 6, pp. 1–19, 2023, doi: 10.1016/j.heliyon.2023.e17154.
- [281] J. O. Ighalo, K. O. Iwuzor, C. A. Igwegbe, and A. G. Adeniyi, “Verification of pore size effect on aqueous-phase adsorption kinetics: A case study of methylene blue,” *Colloids Surfaces A Physicochem. Eng. Asp.*, vol. 626, no. May, p. 127119, 2021, doi: 10.1016/j.colsurfa.2021.127119.
- [282] H. Koyuncu and A. R. Kul, “Removal of methylene blue dye from aqueous solution by nonliving lichen (*Pseudevernia furfuracea* (L.) Zopf.), as a novel biosorbent,” *Appl. Water Sci.*, vol. 10, no. 2, pp. 1–14, 2020, doi: 10.1007/s13201-020-1156-9.
- [283] T. Handayani, Emriadi, Deswati, P. Ramadhani, and R. Zein, “Modelling studies of methylene blue dye removal using activated corn husk waste: Isotherm, kinetic and thermodynamic evaluation,” *South African J. Chem. Eng.*, vol. 47, no. September 2023, pp. 15–27, 2024, doi: 10.1016/j.sajce.2023.10.003.
- [284] H. Koyuncu and A. R. Kul, “Biosorption study for removal of methylene blue dye

- from aqueous solution using a novel activated carbon obtained from nonliving lichen (*Pseudevernia furfuracea* (L.) Zopf.),” *Surfaces and Interfaces*, vol. 19, no. May, 2020, doi: 10.1016/j.surfin.2020.100527.
- [285] A. de F. A. Venceslau, A. C. Mendonça, L. B. Carvalho, G. M. D. Ferreira, S. S. Thomasi, and L. M. A. Pinto, “Removal of Methylene Blue from an Aqueous Medium Using Atemoya Peel as a Low-cost Adsorbent,” *Water. Air. Soil Pollut.*, vol. 232, no. 11, 2021, doi: 10.1007/s11270-021-05414-7.
- [286] A. N. M. A. Haque, R. Remadevi, O. J. Rojas, X. Wang, and M. Naebe, “Kinetics and equilibrium adsorption of methylene blue onto cotton gin trash bioadsorbents,” *Cellulose*, vol. 27, no. 11, pp. 6485–6504, 2020, doi: 10.1007/s10570-020-03238-y.
- [287] N. Somsesta, V. Sricharoenchaikul, and D. Aht-Ong, “Adsorption removal of methylene blue onto activated carbon/cellulose biocomposite films: Equilibrium and kinetic studies,” *Mater. Chem. Phys.*, vol. 240, no. June 2019, p. 122221, 2020, doi: 10.1016/j.matchemphys.2019.122221.
- [288] E. E. Jasper, V. O. Ajibola, and J. C. Onwuka, “Nonlinear regression analysis of the sorption of crystal violet and methylene blue from aqueous solutions onto an agro-waste derived activated carbon,” *Appl. Water Sci.*, vol. 10, no. 6, pp. 1–11, 2020, doi: 10.1007/s13201-020-01218-y.
- [289] Momina, S. Mohammad, and I. Suzylawati, “Study of the adsorption/desorption of MB dye solution using bentonite adsorbent coating,” *J. Water Process Eng.*, vol. 34, no. July 2019, 2020, doi: 10.1016/j.jwpe.2020.101155.
- [290] J. Bortoluz, F. Ferrarini, L. R. Bonetto, J. da Silva Crespo, and M. Giovanela, “Use of low-cost natural waste from the furniture industry for the removal of methylene blue by adsorption: isotherms, kinetics and thermodynamics,” *Cellulose*, vol. 27, no. 11, pp. 6445–6466, 2020, doi: 10.1007/s10570-020-03254-y.
- [291] Y. Tang, Y. Zhao, T. Lin, Y. Li, R. Zhou, and Y. Peng, “Adsorption performance and mechanism of methylene blue by H₃PO₄- modified corn stalks,” *J. Environ. Chem. Eng.*, vol. 7, no. 6, p. 103398, 2019, doi: 10.1016/j.jece.2019.103398.
- [292] J. M. Pérez-morales, G. Sánchez-galván, and E. J. Olguín, “Continuous dye adsorption and desorption on an invasive macrophyte (*Salvinia minima*),” *Environ. Sci. Pollut. Res.*, vol. 26, pp. 5955–5970, 2019.
- [293] T. Unugul and F. U. Nigiz, “Preparation and Characterization an Active Carbon Adsorbent from Waste Mandarin Peel and Determination of Adsorption Behavior on Removal of Synthetic Dye Solutions,” *Water. Air. Soil Pollut.*, vol. 231, no. 11, 2020, doi: 10.1007/s11270-020-04903-5.
- [294] M. Mathivanan, S. Syed Abdul Rahman, R. Vedachalam, A. Surya Pavan Kumar, G. SabareeshSabareesh, and S. Karuppiah, “Ipomoea carnea: a novel biosorbent for the removal of methylene blue (MB) from aqueous dye solution: kinetic, equilibrium and statistical approach,” *Int. J. Phytoremediation*, vol. 23, no. 9, pp. 982–1000, 2021, doi: 10.1080/15226514.2020.1871322.
- [295] M. A. Khoj and L. S. Almazroai, “Synthesis and characterization of treated and untreated Dialium guineense fruit shells as biosolid waste adsorbent : adsorption studies of methylene blue,” *Biomass Convers. Biorefinery*, no. 0123456789, 2023, doi: 10.1007/s13399-023-04419-y.
- [296] M. Safi, F. Gheisar, F. Najafi, and B. S. Hadavand, “Investigation of Shade Darkening Property of Polydimethylsiloxane and Poly (Dimethyl/Diphenyl Siloxane) Modified with Amino Groups on Dyed Textiles,” *Fibers Polym.*, vol. 24, no. 12, pp. 4213–4227, 2023, doi: 10.1007/s12221-023-00395-2.

13 Appendices

Appendix 1: Raw rice husk



Appendix 2: Batch adsorption experiment

Single solution (MB)



Single solution (BR9)



Binary solutions (MB+BR9)



MB model wastewater



Appendix 3: Rice husk adsorbent after adsorption

